8-2012

LOW REACTIVE OXYGEN SPECIES AND HIGH GLYCOLYSIS IN GLIOBLASTOMA STEM CELLS:MECHANISMS AND THERAPEUTIC IMPLICATIONS

Feng Wang

LOW REACTIVE OXYGEN SPECIES AND HIGH GLYCOLYSIS IN GLIOBLASTOMA STEM CELLS: MECHANISMS AND THERAPEUTIC IMPLICATIONS

By

Feng Wang, M.D., M.S.

APPROVED:

_____
Peng Huang, M.D., Ph.D., Supervisory Professor

_____
Zahid H. Siddik, Ph.D.

_____
Xiao-nan Li, M.D., Ph.D.

_____
Ju-Seog Lee Ph.D.

_____
Anthony Lucci, M.D.

APPROVED:

_____
George M. Stancel, Ph.D.
Dean, The University of Texas
Graduate School of Biomedical Sciences at Houston

LOW REACTIVE OXYGEN SPECIES AND HIGH GLYCOLYSIS IN GLIOBLASTOMA STEM CELLS: MECHANISMS AND THERAPEUTIC IMPLICATIONS

A

DISSERTATION

Presented to the faculty of

The University of Texas

Health Science Center at Houston

And

The University of Texas

M.D. Anderson Cancer Center

Graduate School of Biomedical Sciences

In partial fulfillment of the Requirements for the Degree of

DOCTOR OF PHILOSOPHY

By

Feng Wang, M.D, M.S.

Houston, Texas

August, 2012

Dedicated to my beloved grandpa Meiying Wang

ACKNOWLEDGEMENT

I would first like to express my gratitude and appreciation to my compassionate and wonderful husband Shuqiang Yuan. Your love, support and sacrifice have enabled me to concentrate on following my passion and helped me in getting through the toughest time in my life. I would like to express my gratitude to my 8 month daughter Elina, who came to this world during my graduate training and whose birth gave me a new perspective on life. My wonderful parents Xiaoou Wang and Jianguo Wang receive my deepest gratitude for their constant love and the many years of dedication that provided the foundation for this work. I have furthermore to thank my parents-in-law Lanying Lin and Hongwen Yuan whose support and care during the last year made this dissertation possible.

I would like to thank my mentor, Dr. Peng Huang for his guidance, support and patience. Although sometimes we don't see eye to eye on things, I will always appreciate your diligence and devotion to science. Thanks for taking me as a new graduate student who knew little about basic research. I would like to thank Dr. Zahid H. Siddik for giving me encouragement, and treating me with respect and timely advice during my graduate studies. I would like to thank Dr. Ju-Seog Lee for microarray experiments and good suggestions. I would also like to thank Dr. Xiao-nan Li for animal studies and valuable comments. I would like to thank Dr. Anthony Lucci for treating me as a friend and giving continuous support.

My thanks also go to the members of my advisory committee, Dr. Howard Colman and Dr. Hector Martinez-Valdez for providing many valuable suggestions.

I would like to thank all members of the Dr. Huang lab: Gang and Li for guiding me as a new student; Weiqin and Hui for inspired discussions; Marcia, Jinyun and Helene for help in some experiments; Celia, Kausar, Naima for providing a friendly environment. During my graduate study I received much help from many staff in the Department of Molecular Pathology: I wish to thank Dr. Arlinghaus, Alice, Linda, Susan, Pete, Barbara, Xiaohong, Wenjing, Yan, Wen-bin, Warapen and Yvette. I would also like to thank Sangbae Kim and Zhigang Liu for help in microarray and animal experiments.

Special thanks are owed to the Rosalie B. Hite Fellowship for providing two years of financial support that enabled me to concentrate on my work. I am grateful for receiving such a prestigious award and would like to thank the dean Dr. Michael J. Ahearn, the manager Frances A. Franco and all faculties in the Rosalie B. Hite Fellowship committee.

Being far away from homeland and family, I had gone through a difficult time. But I was fortunate to have Marcia, Sayano and Jinyun, I always think you are the angels sent to me by god. I am also grateful to having a lot of friends who give me tremendous help and support: Jing, Le, Yan Yang, Xuefei, Yalin, Tingting, Yumin, Zhao, Dunya and Yan Zhou. Additionally, I would like to thank my former mentor Dr. Rui-hua Xu for teaching me “Never try, never know”. I would also like to thank my former dean Dr. Wenqi Jiang and former president Dr. Yixin Zheng for encouragement and support.

Last but not least, I would like to express my gratitude to GSBS faculties Dr. Knutson, Dr. Stancel, Dr. Goka, Lourdes and all other members for their support.

LOW REACTIVE OXYGEN SPECIES AND HIGH GLYCOLYSIS IN GLIOBLASTOMA STEM CELLS: MECHANISMS AND THERAPEUTIC IMPLICATIONS

Publication No. _____

Feng Wang, M.D., M.S.

Supervisory Professor: Peng Huang, M.D., Ph.D.

Glioblastoma multiforme (GBM) is the most common and aggressive primary brain tumor with poor prognosis due in part to drug resistance and high incidence of tumor recurrence. The drug resistant and cancer recurrence phenotype may be ascribed to the presence of glioblastoma stem cells (GSCs), which seem to reside in special stem-cell niches in vivo and require special culture conditions including certain growth factors and serum-free medium to maintain their stemness in vitro. Exposure of GSCs to fetal bovine serum (FBS) can cause their differentiation, the underlying mechanism of which remains unknown. Reactive oxygen species (ROS) play an important role in normal stem cell differentiation, but their role in affecting cancer stem cell fate remains unclear. Whether the metabolic characteristics of GSCs are different from other glioblastoma cells and can be targeted are also unknown.

In this study, we used several stem-like glioblastoma cell lines derived from clinical tissues by typical neurosphere culture system or orthotopic xenografts, and showed that addition of fetal bovine serum to the medium induced an increase of ROS, leading to aberrant differentiation and decreases of stem cell markers such as CD133. We found that exposure of GSCs to serum induced their differentiation through activation of mitochondrial respiration, leading to an increase in superoxide (O_2^-) generation and a profound ROS stress response manifested by upregulation of oxidative stress response pathway. This increase in mitochondrial ROS led to a down-regulation of molecules including SOX2, and Olig2, and Notch1 that are important for stem cell function and an upregulation of mitochondrial superoxide dismutase SOD2 that converts O_2^- to H_2O_2. Neutralization of ROS by antioxidant N-acetyl-cysteine in the serum-treated GSCs suppressed the increase of superoxide and partially rescued the expression of SOX2, Olig2, and Notch1, and prevented the serum-induced differentiation phenotype. Additionally, GSCs showed high dependence on glycolysis for energy production. The combination of a glycolytic inhibitor 3-BrOP and a chemotherapeutic agent BCNU depleted cellular ATP and inhibited the repair of BCNU-induced DNA damage, achieving strikingly synergistic killing effects in drug resistant GSCs.

This study uncovers the metabolic properties of glioblastoma stem cells and suggests that mitochondrial function and cellular redox status may profoundly affect the fates of glioblastoma stem cells via a ROS-mediated mechanism, and that the active glycolytic metabolism in cancer stem cells may provide a biochemical basis for developing novel therapeutic strategies to effectively eliminate GSCs.

TABLE OF CONTENTS

LIST OF ILLUSTRATIONS

LIST OF TABLES

ABBREVIATIONS

8-OHdG	guanine in the 8-position
ABC	ATP-binding cassette
ALDH1	aldehyde dehydrogenase 1
AML	acute myeloid leukemia
ARE	antioxidant response element
ATRA	all-trans-retinoic acid
BDNF	brain-derived neurotrophic factor
CSCs	cancer stem cells
EMT	epithelial–mesenchymal transition
ER	endoplasmic reticulum
ESA	epithelial-specific antigen
ETC	electron transporter chain
FBS	fetal bovine serum
FoxO	forkhead box class O
GBM	glioblastoma multiforme
GCL	glutamate cysteine ligase
GPX	glutathione peroxidase

GRX	glutaredoxins
GSCs	glioblastoma stem cells
GSH	glutathione
GST	glutathione S-transferase
GSK3β	glycogen synthase kinase 3 beta
HSCs	hematopoietic stem cells
HIF	hypoxia-inducible factor
JNK	Jun N-terminal kinase
LSCs	leukemia stem cells
MAPK	mitogen-activated protein kinases
NAC	*N*-acetylcysteine
NADPH	nicotinamide adenine dinucleotide phosphate
NF-κB	nuclear factor-κB
NOD	nonobese diabetic
Nrf-2	Nuclear factor E2-related factor 2
NSC	neural stem cells
NQO	NAD(P)H: quinone oxidoreductase
PDH	pyruvate dehydrogenase
PDK	pyruvate dehydrogenase kinase
PKM	pyruvate kinase M
PRX	peroxiredoxins
Redox	oxidation-reduction reactions
γ-GCS	γ-glutamylcysteine synthetase
ROS	reactive oxygen species

SCID	severe combined immune-deficient
SOD	superoxide dismutase
TCA	tricarboxylic acid
TRX	thioredoxin
TrxR	thioredoxin reductase
VEGF	vascular endothelial growth factor

CHAPTER 1

INTRODUCTION

1. CANCER STEM CELL

Cancer stem cells (CSCs) are a sub-population of rare malignant cells which have a capability for indefinite proliferation, continuous self-renewal and multi-lineage differentiation (1). Although the existence of CSCs was first proposed over fifty years ago (2), only in the last two decades have these cells been discovered in hematological malignancies. Leukemia stem cells (LSCs) have been identified in both mice and patients with acute myeloid leukemia (AML) (3, 4). $CD34^+$ $CD38^-$ AML cells can engraft severe combined immune-deficient (SCID) mice to produce large numbers of colony-forming progenitors; however, CD34+ CD38+ and CD34- AML cells don't have this property (5). Since then, $CD34^+CD38^-$ have been utilized as markers for enriching LSCs (3). Other stem cell markers including $CD123^+$ (6) and $Hoechst33342^{low}$ (7) are also identified in AML. Additionally, CSCs have been identified in solid tumors of breast and brain. $CD44^+CD24^{-/low}Lineage^-$ breast cancer cells and CD133+ brain tumor cells can self-renew and differentiate to produce a phenotype identical to the initial tumor (8, 9). A large quantity of recent studies have also indicated the existence of CSCs in different types of solid tumors (10, 11) such as colon (12), pancreatic (13), prostate (14), and liver cancer (15). A number of cell surface markers including prominin-1 (CD133), CD44, aldehyde dehydrogenase 1 (ALDH1), epithelial-specific antigen (ESA) and a fluorescent dye Hoechst33342 have been proven useful for isolating CSCs (Table 1) (11).

Table 1. Cancer stem cell markers in different tumors.

Cancer Type	Markers	References
Brain Tumor	$CD133^+$, $Nestin^+$, Hoechst33342 exclusion	(9, 16, 17)
Breast Cancer	$CD44^+CD24^{-/low}$, $Oct4^+$, $CX43^-$, $ALDH1^+$	(8, 18-20)
Acute Myeloid Leukemia	$CD34^+CD38^-$, $CD123^+$, Hoechst33342 exclusion	(3, 6, 7)
Multiple Myeloma	$CD138^-$,$CD19^+$	(21, 22)
Colon Cancer	$CD133^+$, $ESA^{hi}/CD44^+$, $ALDH1^+$	(12, 23, 24)
Prostate Cancer	$CD133^+$	(25)
Hepatic Cancer	$CD133^+$, $CD90^+$	(26)
Lung Cancer	$CD133^+$, Hoechst33342 exclusion	(27, 28)
Head & Neck Cancer	$CD44^+$	(29)
Pancreatic Cancer	$CD44^+CD24^+$ ESA^+, $CD133^+CXCR4^+$	(13, 17, 30)
Melanoma	$ABCB5^+$	(31)
Ovarian Cancer	$CD44^+CD177^+$, Hoechst33342 exclusion	(32, 33)

There is growing evidence indicating that CSCs are crucial to tumor initiation and maintenance, while the origin of CSCs remains elusive. Since CSCs display normal stem cell features: the ability to self-renew and differentiate, either tissue stem cells or bone marrow stem cells have been identified as the cells of origin for cancer. Barker et al have shown that Apc deletion in long-lived intestinal stem cells ($Lgr5^+$) led to malignant transformation (34). Oncogenic K-ras transformation or p53 mutation can stimulate bronchioalveolar stem cell expansion, which is related to lung adenocarcinoma initiation (35, 36). In addition, bone marrow stem cells can be recruited into stomach and give rise to gastric cancer under chronic infection of Helicobacter pylori (37). However, a number of studies suggest that malignant tumors can be initiated in differentiated cells. Not only neural stem cells (NSCs) but also astrocytes can be induced into glioma by combined loss of p16 (INK4a) and p19 (ARF) (38, 39). But neurofibromin deficiency only cause tumor in differentiated glia cells instead of neural crest stem cells (40). It remains controversial whether CSCs origin from normal stems cells or differentiated cells. They may rise from normal stem cells or progenitor cells through mutations or they may be derived from differentiated cells through dedifferentiation (41, 42).

Although CSCs may constitute a small fraction of the total cancer cells in the tumor bulk, this special subpopulation is thought to play a major role in cancer resistance to chemotherapy and radiotherapy, leading to persistence of residual disease and cancer recurrence (43). This phenomenon is due in part to the unique biological properties of CSCs including high capacity of DNA repair, high expression of certain ATP-dependent drug exporting pumps, high levels of glutathione synthesis, and high expression of cell survival factors (44-46). On one hand, CSCs preferentially activate the DNA damage checkpoint

response after radiation that can repair radiation induced DNA damage more efficiently than non-CSCs (47). On the other hand, CSCs can pump out many chemotherapeutic agents through ATP-binding cassette (ABC) transporters, which contribute to their chemotherapy resistance (48). Additionally, compared to non-CSCs, CSCs show a significant overexpression of glutathione synthesis enzymes that might be responsible for chemotherapy and radiation resistance (46, 49).

A detailed understanding of the factors that affect the ability of CSCs to maintain their stemness is important for the development of new strategies to effectively eliminate cancer stem cells or to induce their differentiation. Nevertheless, there are very limited therapeutic strategies that are effective in eliminating CSCs currently, keeping CSCs a major challenge in cancer treatment.

GLIOBLASTOMA STEM CELL

Glioblastoma multiforme (GBM), a WHO grade IV astrocytoma, is the most common and aggressive primary brain tumor in adults. Although maximal surgical resection, radiotherapy, and chemotherapy are performed in patients with this brain cancer, the treatment outcomes are still unsatisfactory, with median survival durations of only 12-15 months and the 5-year survival rates of less than 10% (50, 51). Previous studies demonstrated that glioblastoma stem cells (GSCs) promote chemoresistance and radioresistance, which are likely responsible for the recurrence of GBM (47, 52-54). Several markers have been identified for isolating GSCs, among which CD133 is the most widely used one. CD133, a cell surface glycoprotein containing five trans-membrane domains and two glycosylated extracellular loops, was first identified in hematopoietic stem cells (55). High levels of CD133 expression have been found in various stem and progenitor cell populations including GBM. $CD133^+$ subpopulation of brain tumor cells have CSC properties (9) and only these cells but not the $CD133^-$ cells are capable of tumor initiation when inoculated into nonobese diabetic/severe combined immunodeficiency (NOD/SCID) mouse brains (56). Another CSC marker Hoechst 33342, a fluorescent DNA binding dye, was also applied to GBM (57, 58). The GSCs are isolated as the side population based on the ability of cells to pump out Hoechst 33342 through the verapamil-sensitive ATP binding cassette transporter (59). However, all of these GSC markers were challenged by some studies. CD133-negative glioblastoma cells are also able to initiate tumors (60, 61) and side population is not necessary for identifying GSCs (62).

Long-term expansion of GSCs has been possible in neural sphere culture which was previously established for isolating neural stem cells and progenitor cells (63). The neural

sphere culture contains no serum and is supplemented with growth factors EGF and FGF2, and additional mitogens or antioxidants. This serum-free culture system is successful to isolate GSCs with long term self-renewal and tumorigenic potential (64, 65), and it closely mimics the phenotype and genotype of parental GBM than serum-containing culture (66). However, adding serum into the neural sphere culture can cause irreversible differentiation of neural stem cells (67, 68).

Like other CSCs, GSCs have been found to be resistant to all kinds of treatments. GSCs display a marked resistance to commonly used chemotherapeutic agents and are able to recover and proliferate after drug treatment (69). GSCs can also be enriched after radiation or in recurrent GBM when compared with primary GBM, which might be attributed to GSCs' efficient activation of the DNA damage response (70, 71). Additionally, recent studies have suggested that hypoxic environment play critical roles in the maintenance of GSC population (72-74). The hypoxic niches may further promote drug resistance, which makes targeting GSCs more difficult. Some novel compounds have been found to be effective to kill GSCs including debromohymenialdisine, an inhibitor of checkpoint kinases, which can reverse the radioresistance of GSCs (70) and cyclopamine, a Hedgehog pathway inhibitor, which can decrease GSCs and block tumor formation (75).

MICROENVERIONMENT

Normal stem cells reside in some physiologically limited and specialized microenvironment, which is named stem cell niche (76). The stem cell niche is the sum of all cell-cell and cell-extracellular matrix interactions and controls normal asymmetrical division of stem cells by maintaining a balance between self-renewal and differentiation. Brain stem cells reside in the vascular rich subventricular zone and subgranular layer (77). It's likely that vascular-derived factors including brain-derived neurotrophic factor (BDNF), vascular endothelial growth factor C (VEGFC) and pigment epithelium-derived factor can regulate neural stem cell function (78). Other cell types such as ependymal and transit progenitor cells are also likely to regulate NSCs. The interaction of NSCs and their niche is not unidirectional. NSCs may modulate the stem cell niche and induce angiogenesis by increasing the expression of VEGF and BDNF in endothelial cells (79).

Recently, a CSC niche that has a similar role as normal stem cell niche has been proposed (80) and supported by emerging evidence. Like normal stem cells, CSCs depend on a permissive microenvironment to retain their self-renewal abilities and give rise to more differentiated cells (81). CSCs seem to reside in a hypoxic niche due to aberrant blood vessel formation and rapid cell growth (82). Hypoxia has been found to functionally promote the self-renewal ability of GSCs (73) and increase the expression of CD133 (83) and side population signature genes in glioblastoma cell lines (84, 85). These effects of hypoxia are likely mediated by HIF-1α or HIF-2 (84, 85). Knocking down HIF1α or HIF2α can not only lead to reduced cell growth and survival in GSCs in vitro but also result in decreased tumorigenic capacity and increased survival of mice in vivo (86).

Stem cells of brain tumors including GBM have been found within vascular niches and the relationship between CSCs and endothelial cell is reciprocal (Figure 1). On one hand, the vascular endothelial cells can maintain brain tumor cells in a stem-like state and accelerate the tumor initiation and growth when co-transplanted in mice brain (87). Endothelial cells directly provide Notch ligands (88) or release nitric oxide to neighboring CSCs (89), activating the Notch pathway in CSCs. On the other hand, CSC can promote the endothelial cell growth and vessel formation. $CD133^+$ glioma stem cells, but not $CD133^-$ glioma cells, cause highly proliferative and angiogenic tumors when implanted into mice brains, and they also secret 10 to 20 folds more VEGF than $CD133^-$ glioma cells in vitro (70). Treating $CD133^+$ glioblastoma cells with a VEGF antibody, bevacizumab which binds to VEGF-A ligand to prevent endothelial cell receptor activation, can inhibit their proangiogenic effects on endothelial cell (migration and tube formation) and initiate tumors in xenografts (70).

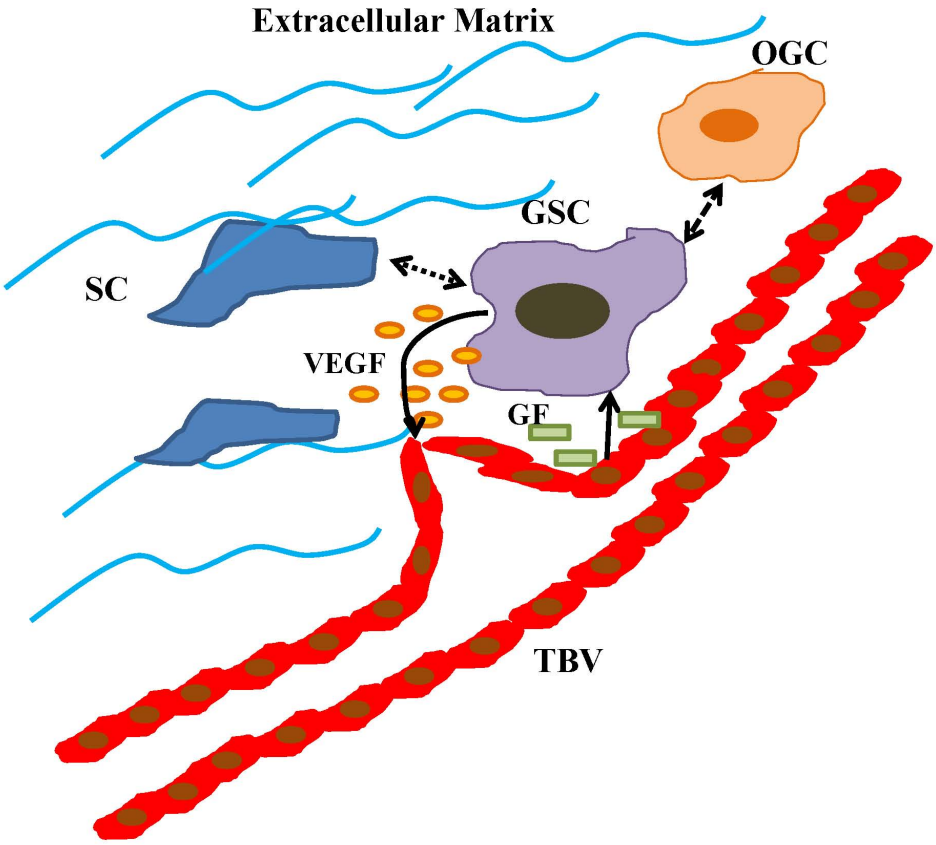

Figure 1. Glioblastoma stem cells reside within a hypoxia and perivascular niche. The GSC niche is composed of tumor blood vessels, stromal cells and extracellular matrix. GSCs remain quiescent in hypoxic niches, but create vascular niches in order to proliferate. On one hand, GSCs stimulate the growth of neovasculature by expressing growth factors such as VEGF. On the other hand, tumor blood vessels create a vascular niche to help maintain GSCs. GF: growth factors; GSC: glioblastoma stem cell; OGC: other glioblastoma cell; SC: stromal cell; TBV: tumor blood vessels.

ABERRANT DIFFERENTIATION

Glioblastoma grown from cancer stem cells contains mixed populations of cancer stem cell, progenitor cell and heterogeneous cell types. Besides self-renewal, GSCs can be induced to differentiate into all neuronal lineages expressing the markers of neuronal, astroglial or oligodendroglial cells (90). GSCs are also able to differentiate into functional endothelial cells in vivo (91). Since the differentiation of GSCs is not tightly regulated like in NSCs, it's difficult to categorize glioblastoma cells according to the hierarchical pyramid of normal development (90). However, most of studies have applied the markers based differentiation criteria of NSCs to GSCs.

Fetal bovine serum (FBS) or all-trans-retinoic acid (ATRA) treatment can rapidly cause GSC morphology change, dramatically decrease NSC markers and induce lineage-specific differentiation markers (92, 93). Culturing under serum condition results in a loss of NSC markers, a gain of glial or neuronal markers, and a decrease of tumorigenicity (94). ATRA which has been proven to be a powerful antitumor agent in acute promyelocytic leukemia can induce differentiation and cell death in GSCs (94, 95). It can also inhibit the tumor growth in xenograft mice, which is likely mediated by Notch pathway (92). Interference with other molecules or pathways is also able to induce differentiation. For instance, inhibition of Bmi1 and glycogen synthase kinase 3 beta (GSK3β) activity increases differentiation markers and reduces colony formation in glioblastoma cells (96).

2. REACTIVE OXYGEN SPECIES

Reactive oxygen species (ROS) are a group of highly reactive oxygen-containing species that include superoxide (O_2^-), singlet oxygen ($^1O_2$), hydrogen peroxide (H_2O_2) and the hydroxyl free radical ($^{\cdot}OH$) (97). ROS production is a cascade of reactions that usually begins with the generation of superoxide (98). Mitochondrial electron transport chain (ETC), the nicotinamide adenine dinucleotide phosphate (NADPH) oxidase (NOX) complex, and the endoplasmic reticulum (ER) system have been recognized as major generators of cellular ROS (Figure 2). Mitochondrial ETC produces O_2^- as a by-product of cellular metabolic pathway through passing electrons to O_2 (99). Among the five components of ETC, complex I and complex III are the major sites for ROS formation (99). Another major source of cellular ROS is the NOX, a membrane-bound enzyme complex, that generates superoxide by transferring electrons from NADPH to O_2 (100). The other primary generator for ROS is the ER, which is overcrowded with a number of enzymes (NOX, flavin monooxygenases, gulonolactone oxidase and cytochrome P450 isoenzymes) that can produce superoxide or hydrogen peroxide as by-products of the reactions (101-104).

Because ROS interact non-specifically with lipids, proteins and nucleic acids, causing lipid peroxidation, protein oxidation and DNA mutations, respectively (105), they were initially considered to be harmful. Later studies found that ROS also play an important role in cell proliferation, apoptosis and signaling (Figure 3) (100). ROS have a multitude of effects on cell cycle progression, of which depends upon the amount of ROS, the type of ROS, and the duration of exposure of the cells to ROS (106). A short exposure of non-proliferating cells to moderate ROS may stimulate proliferation. Prolonged exposure to low ROS results in differentiation. For instance, ROS generated from complex III is required to

initiate the differentiation of human mesencymal stem cells into adipocytes. Disruption of a bHLH transcription factor, UPB1, which directly regulates the expression of a set of antioxidant enzymes peroxidases, leads to a delay in the onset of differentiation (107). If the amounts of ROS are high or the exposure to ROS is long, cells will arrest in all phases and undergo apoptosis (106). ROS increase induces the expression of cyclin kinase inhibitor p21, the inhibition of CDK2, the expression of Chk1 and the decrease of Cdc25c, which lead to subsequent G1 phase, S phase and G2/M phase arrest respectively (106). Besides its role in cell cycle progression, ROS also performs as intracellular messengers and affect different transcription factors and intracellular signaling pathways (100). Low levels of ROS induce Nrf2, a transcription factor coding for the antioxidant enzymes (108). Intermediate amount of ROS triggers the activation of two transcription factors, nuclear factor-κB (NF-κB) and activator protein (AP)-1 (109). H_2O_2 can activate NF-κB, making it dissociate from IκB and translocate to the nucleus (110). H_2O_2 can also upregulates AP-1 activity through ERKs, JNKs and p38 (111). ROS can also participate in signal transduction pathways through activating mitogen-activated protein kinases (MAPK) pathway (112) and Janus kinase/signal transducers and activators of transcription (JAK/STAT) pathway (113). However, high amount of ROS induces opening of the mitochondrial permeability transition pore, leading to apoptosis (114).

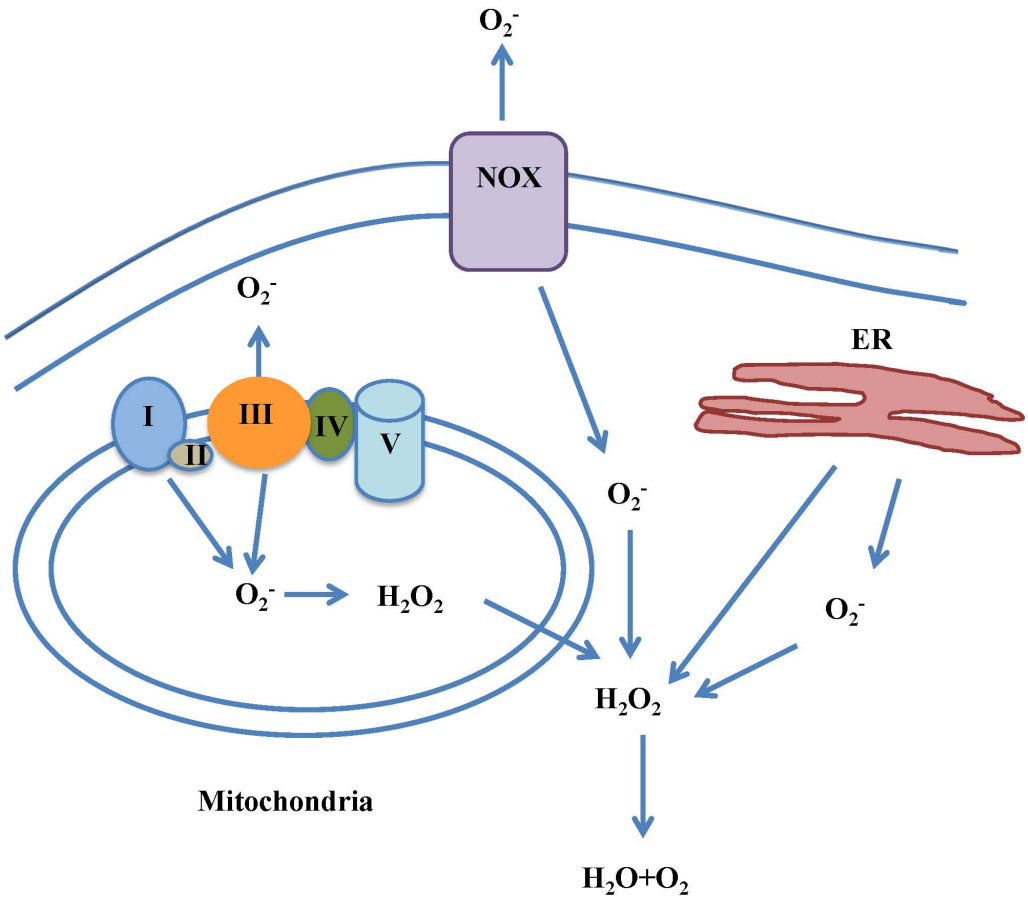

Figure 2. Major sources of cellular ROS. Mitochondrial electron transport chain, NADPH oxidase (NOX) complex, and the endoplasmic reticulum (ER) system are primary generators for ROS.

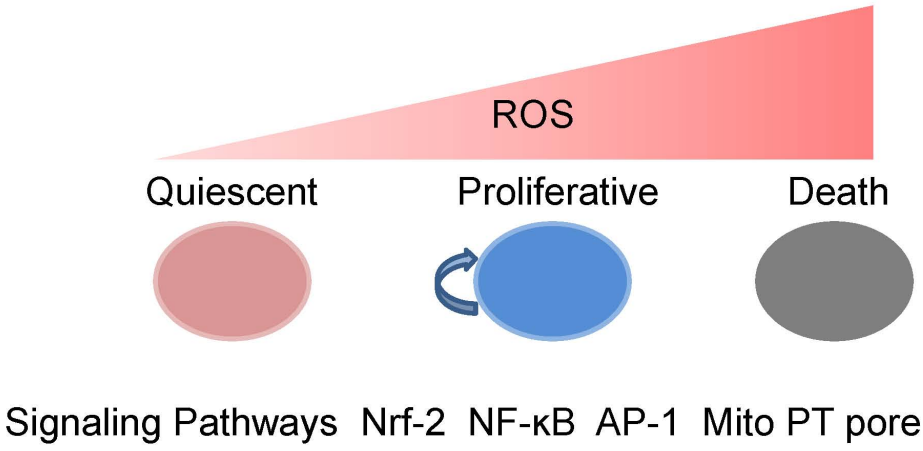

Figure 3. ROS levels and cell status. Quiescent cells maintain low levels of ROS. An intermediate increase of ROS induces Nrf-2, NF-κB and AP-1 signaling, and triggers cell proliferation. A high amount of ROS induces perturbation of mitochondrial permeability transition pore (Mito PT pore), leading to apoptosis or necrosis.

ROS IN CANCER

ROS may be a driving force for cancer initiation and progression. DNA damage and mutation caused by ROS are considered as a major cause of cancer (115). Most of ROS-induced mutations seem to involve modification of guanine, causing G→T transversions (116-118). If oncogenes or tumor suppressor genes are related, the mutation can result in cancer initiation or progression (115). As an evidence, extensive oxidative modifications in DNA has been observed in cancers (119), in which the hydroxylation of guanine in the 8-position (8-OHdG) is the most frequent and most mutagenic lesion. Cigarette smoke can cause the accumulation of 8-OHdG, which causes lack of base pairing specificity and misreading of the modified base and adjacent residues, thus leading to breast cancer and liver cancer (115). Sustained ROS may also trigger epithelial–mesenchymal transition (EMT), invasion and migration in cancer cells (120). Repeated treatment with a low dose of H_2O_2 in mammary epithelial cells results in EMT like morphology transformation and invasiveness (121). ROS can also induce urokinase plasminogen activator receptor expression and stimulate gastric cancer cell invasiveness and metastasis (122).

Compared with normal cells, cancer cells have shown increased levels of ROS (123-125). ROS generation is induced after the expression of several oncogenes including H-Ras and c-Met (126-128). The mitochondrial DNA with mutations from highly metastatic tumor cell line can confer high metastatic potential to poorly metastatic cell line, which is likely mediated by ROS overproduction and can be blocked by a ROS scavenger *N*-acetylcysteine (NAC) (129). Since cancer cells have shown increased ROS status, further increasing ROS may make them more vulnerable to the damage than normal cells (130). Compounds which promote ROS generation in cancer cells have shown promising anticancer activities.

Elesclomol, a compound that increases ROS production, has shown therapeutic activity in melanoma (130). Other compounds which interfere with the antioxidant, glutathione have also shown effectiveness in cancer therapy. Both phenethyl isothiocyanate (PEITC) and buthionine sulphoximine (BSO) can lead to a decrease of cellular GSH, causing cancer cell death (131, 132).

ANTIOXIDANT SYSTEM

Cells are capable of keeping themselves in an oxidation-reduction reactions (redox) homeostasis state because of several antioxidant defenses including ROS-scavenging enzymes and small scavenger molecules (133). There are three major intracellular ROS-scavenging enzymes: superoxide dismutases (SOD), catalases and peroxidases (Figure 4). The SODs that convert superoxide to hydrogen peroxide are the first and most important line of antioxidant enzymes against ROS (134). Three distinct isoforms of SOD have been identified in mammals: SOD1 (CuZn-SOD), SOD2 (Mn-SOD), and SOD3 (Ec-SOD) (135). The primary locations of SOD1, SOD2 and SOD3 are cytoplasm, mitochondria and outside of cytoplasm respectively. Catalases and peroxidases catalyze the reaction of hydrogen peroxide into water. Peroxidases include glutathione peroxidase (GPX), peroxiredoxin (PRX), thioredoxin (TRX), thioredoxin reductase (TR), glutaredoxin (GRX), sulfiredoxin and sestrin. GPx is the most prominent of them.

The intracellular non-enzymatic antioxidants are composed of vitamins like vitamin C, vitamin E, proteins like β-carotene, albumin and GSH (136). GSH is present in millimolar concentrations in cells and is the major component in maintaining redox homeostasis. GSH is synthesized by two enzymes, γ-glutamylcysteine synthetase (γ-GCS), which is the rate-limiting enzyme, and glutathione synthetase (137).

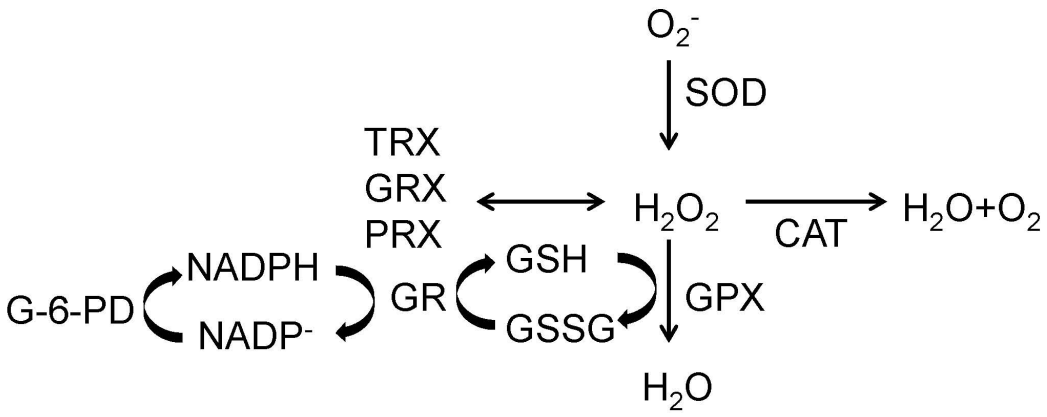

Figure 4. Three major ROS-scavenging enzymes in cells: superoxide dismutases (SOD), catalases and peroxidases. SOD, superoxide dismutases; CAT, catalase; TRX, thioredoxin; GRX, glutaredoxin; PRX, peroxiredoxin; GPx, glutathione peroxidase; GR, glutathione reductase; GSH, glutathione; GSSG, oxidized glutathione; G6PDH, glucose-6 phosphate dehydrogenase.

Nuclear factor E2-related factor 2 (Nrf2), a basic leucine zipper transcription factor that controls the genes coding for antioxidant enzymes, plays a crucial role in protecting cells against oxidative stress. Phosphorylation of Nrf2 at Serine-40 by protein kinase C was reported to trigger its nuclear translocation that is likely a critical signaling event leading to antioxidant response element (ARE)-mediated cellular antioxidant response (138). Nrf2 forms a heterodimer with musculoaponeurotic fibrosarcoma oncogene homolog, thereby binding to ARE to regulate the basal and inducible expression of more than 200 genes including antioxidant genes (139). Classic Nrf2-target genes includes SOD, glutathione S-transferase (GST), NAD(P)H: quinone oxidoreductase (NQO)1, NQO2, γ-GCS, glutamate cysteine ligase (GCL), GPx, TRX, TrxR, PRX, and heme oxygenase 1 (HO-1) (139). An important negative regulator of Nrf2 is a cytosolic protein Keap1. Under normal conditions, Keap1 binds with Nrf2 leading to its proteasomal degradation (140). ROS cause dissociation of Nrf2 from Keap1, leading to its translocation to the nucleus, which activates ARE, thus up-regulates a lot of ROS scavenging enzymes.

Forkhead box class O (FoxO) family are also critical regulators of oxidative stress and exert this function at least partially by modulating the expression of several antioxidant enzymes (141). Oxidative stress activates FoxOs via phosphorylation by the Jun N-terminal kinase (JNK), which increases the expression of SOD2 and catalase (142).

ROS IN STEM CELLS

ROS are known to play a role in affecting the fates of normal stem cells (143). Stem cells were thought to maintain low levels of ROS. Elevated ROS has been observed to induce differentiation of embryonic stem cells into cardiovascular and mesendodermal cells (144, 145). NSCs and hematopoietic stem cells (HSCs) contain lower levels of ROS than their mature progeny, while increased ROS levels are associated with lowered self-renewal capacity, increased cell cycling and reduced viability (146-148). Studies of genetically manipulated mice have deepened the understanding of ROS effects on stem cells. Ataxia telangiectasia mutated gene deficient ($Atm^{-/-}$) mice display increased levels of ROS, which lead to depletion of normal HSCs after serial transplantation (148). FoxOs are essential for the regulation of hematopoietic stem and progenitor cells. FoxO3a knockout mice showed elevated ROS that resulted in loss of HSC self-renewal capacity (149). PR domaincontaining16 (Prdm16) deficiency led to increased ROS levels and depletion of hematopoietic and neural stem cells (150). All these stem cell abnormalities can be restored or partially rescued by treatment with antioxidants (148-150).

However, recent evidence suggests that appropriate levels of ROS are required to promote proliferation and survival of stem and progenitor cells. AKT1/2 double-deficient ($AKT1^{-/-}/AKT2^{-/-}$) HSC have been found to persist in the G_0 phase of the cell cycle and demonstrate decreased ROS (151). Pharmacologically increasing ROS levels promotes the HSC proliferation and differentiation. Proliferative NSCs maintain a high ROS status and are highly responsive to ROS stimulation (152). ROS-mediated self-renewal and neurogenesis are dependent on PI3K/Akt pathway, and can be inhibited by NOX or PI3K

inhibitors. Taken together, ROS is tightly controlled in normal stem cell and keeping ROS at an appropriate level is crucial to maintaining stem cell functions.

Redox status of cancer stem cell has not been well-characterized so far. Little is known about whether ROS regulate any signaling pathways in CSCs. $CD24^{-/low}/CD44^{+}$ breast cancer stem cells are enriched after radiation, perhaps due to lower levels of ROS in these cells (153). It has also been found that human and murine breast cancer stem cells contain lower cellular levels of ROS compared to the corresponding non-tumorigenic cells, which is likely related to their high ROS-scavenging capacity (46). Human gastrointestinal cancer stem-like cells with a high level of CD44 expression display an enhanced capacity for glutathione synthesis and defense against ROS, probably by stabilizing a glutathione substrate transporter xCT (154). CD44 ablation by siRNA depletes cellular glutathione and increases ROS in cancer cells (155). It has been shown salinomycin is effective in inhibiting prostate cancer cell including CSCs, which is probably due to the induction of ROS (156).

3. CANCER CELL METABOLISM

Otto Warburg observed that, even in the presence of ample oxygen, cancer cells prefer to produce energy by a high rate of glycolysis followed by lactic acid fermentation, rather than by a comparatively low rate of glycolysis followed by oxidative phosphorylation like most normal cells, a phenomenon known as the "Warburg effect" (157). Although the Warburg effect has been generally accepted as a metabolic hallmark of cancer, its causal relationship with cancer progression remains unclear (158)

Why do cancer cells that have a great need for ATP use such a low efficient way of metabolism? Warburg proposed that cancer cells have a permanent impairment of oxidative phosphorylation resulting in a compensatory increase of glycolysis to cope with a lack of ATP generation (159). While later studies have found that mitochondrial defects are rare and most tumor cells retain the capacity for oxidative metabolism (160, 161). The high glycolytic rate provides several advantages for proliferative cancer cells as long as glucose supplies are not limited. First, it produces ATP at a higher rate than oxidative phosphorylation and allows cells to use the most abundant extracellular nutrient, glucose (162). Although the yield of ATP per mol glucose consumed is low, when cancer cells are in resource competition with normal cells that produce ATP at a lower rate but a higher yield, they consume the resource more rapidly and have a growth advantage over normal cells(163). Second, aerobic glycolysis allows cancer cells for ATP production in the absence of oxygen, which help the cancer cells proliferate in hypoxic conditions (164). Finally, aerobic glycolysis provides a biosynthetic advantage for cancer cells by producing intermediates for biosynthetic pathways including ribose sugars for nucleotides, glycerol and

citrate for lipids, nonessential amino acids and NADPH. So the Warburg effect benefits both bioenergetics and biosynthesis (162).

Not only the tumor microenvironment but also oncogene activation can drive metabolic changes and lead to increased glucose consumption, decreased oxidative phosphorylation, and accompanying lactate production (158). Due to the high proliferation of cancer cells, hypoxia tends to be widespread in solid tumors. When cancer cells outgrow the recruited endothelial cells, new disorganized blood supplies usually form and further contribute to hypoxia. Therefore, the anaerobic use of glucose through glycolysis is required for cancer cells survival (165). Cells transformed by the oncogenes V-Src or H-Ras display increased expression of HIF-1 or VEGF and exhibit increased rates of aerobic glycolysis (165). Additionally, loss of tumor suppressor p53 prevents the synthesis of cytochrome c oxidase protein, which interferes with mitochondrial oxidative phosphorylation (158).

The dependence of cancer cells on increased glucose uptake for aerobic glycolysis has been proven useful for tumor detection and monitoring. [^{18}F]fluorodeoxyglucose positron emission tomography (FDG–PET) imaging that uses a radioactive glucose analogue to detect regions of high glucose uptake has been widely applied in various tumor diagnosis and evaluation (162).

REGULATION OF CANCER CELL METABOLISM

The PI3K/Akt/mTOR pathway is a master regulator of aerobic glycolysis in cancers. This pathway is activated by mutation in PI3K complex, mutations in tumor suppressor genes or by aberrant signaling from receptor tyrosine kinases (162). Akt stimulates glycolysis and increases lactate production in either nontransformed cells or cancer cells by increasing the expression and membrane translocation of glucose transporters and by phosphorylating key glycolytic enzymes, such as hexokinase and phosphofructokinase 2 (166, 167). The activation of this pathway also stimulates protein and lipid synthesis and cell growth (160).

A key transcription factor hypoxia-inducible factor-1 (HIF-1) regulates glucose metabolism under low oxygen conditions. Under normal oxygen conditions, HIF1 can be stabilized by oncogenic pathways including PI3K and mutations in tumor suppressors such as von Hippel–Lindau tumour suppressor (VHL), succinate dehydrogenase (SDH) and fumarate hydratase (FH) (162). HIF-1 activation increases the transcription of genes encoding glucose transporter and glycolytic enzymes (168). HIF-1 can also induce expression of pyruvate dehydrogenase kinase 1 (PDK1), which inhibits the mitochondrial pyruvate dehydrogenase (PDH) complex and reduce the entry of pyruvate into the tricarboxylic acid (TCA) cycle and increases conversion of pyruvate to lactate (169, 170).

Another metabolic regulator of cancer cell is the oncogenic transcription factor c-Myc. Overexpression of c-Myc collaborates with HIF-1 to promote glycolysis by induction of glucose transporter and glycolytic enzymes such as hexokinase 2 and PDK1 (171, 172). Additionally, c-Myc transformed cells require glutamine for survival and depriving these

cells of glutamine leads to a depletion of TCA cycle intermediates. c-Myc increases glutaminolysis which may thus generate more antioxidant glutathione for cancer cells (162).

TARGETING CANCER CELL METABOLISM

Given that cancer cells depend on changes in metabolism to support their survival and growth, targeting cancer cells' metabolism has become an important area of research. Although there have been attempts to block the glycolytic pathway in tumor cells using compounds such as 2-deoxyglucose (2-DG) and 3-bromopyruvate (3-BrPA), effective strategies have not been devised (173-175). Several metabolic enzymes have been considered as candidate targets (Figure 5), and promising results have been obtained by using some compounds (176). Various compounds have been shown to block glucose uptake in cancer cells, but none of them are specific glucose transport inhibitors. Glucose transporter 1 (Glut1) and Glucose transporter 3 (Glut3) are expressed at much higher levels in cancer cells than in normal cells, suggesting that these transporters can be possible therapeutic targets. A competitive inhibitor of glucose, 2-deoxy-D-glucose (2-DG) is phosphorylated by hexokinase to produce 2-deoxyglucose-6-phosphate and competes with enzymes that metabolize glucose-6-phosphate (176). Cancer cells preferentially express hexokinase 2 (HK2) and repression of this enzyme is likely to be toxic to cancer cells. 3-BrPA is an alkylating agent that has been shown to inhibit HK2 and glyceraldehyde-3-phosphate dehydrogenase (GAPDH), two key enzymes in the glycolytic pathway (173, 177). The derivative of 3-BrPA, 3-bromo-2-oxopropionate-1-propyl ester (3-BrOP), was developed by our laboratory. It has similar mechanisms of action as 3-BrPA and is chemically more stable, and has been shown to be highly potent in causing ATP depletion in cancer cells (178). Another glycolytic enzyme preferentially expressed by cancer cells is pyruvate kinase M2 (PKM2). Targeting PKM2 by inhibitors or shRNA can decrease cancer cell proliferation and tumorigenicity (179, 180).

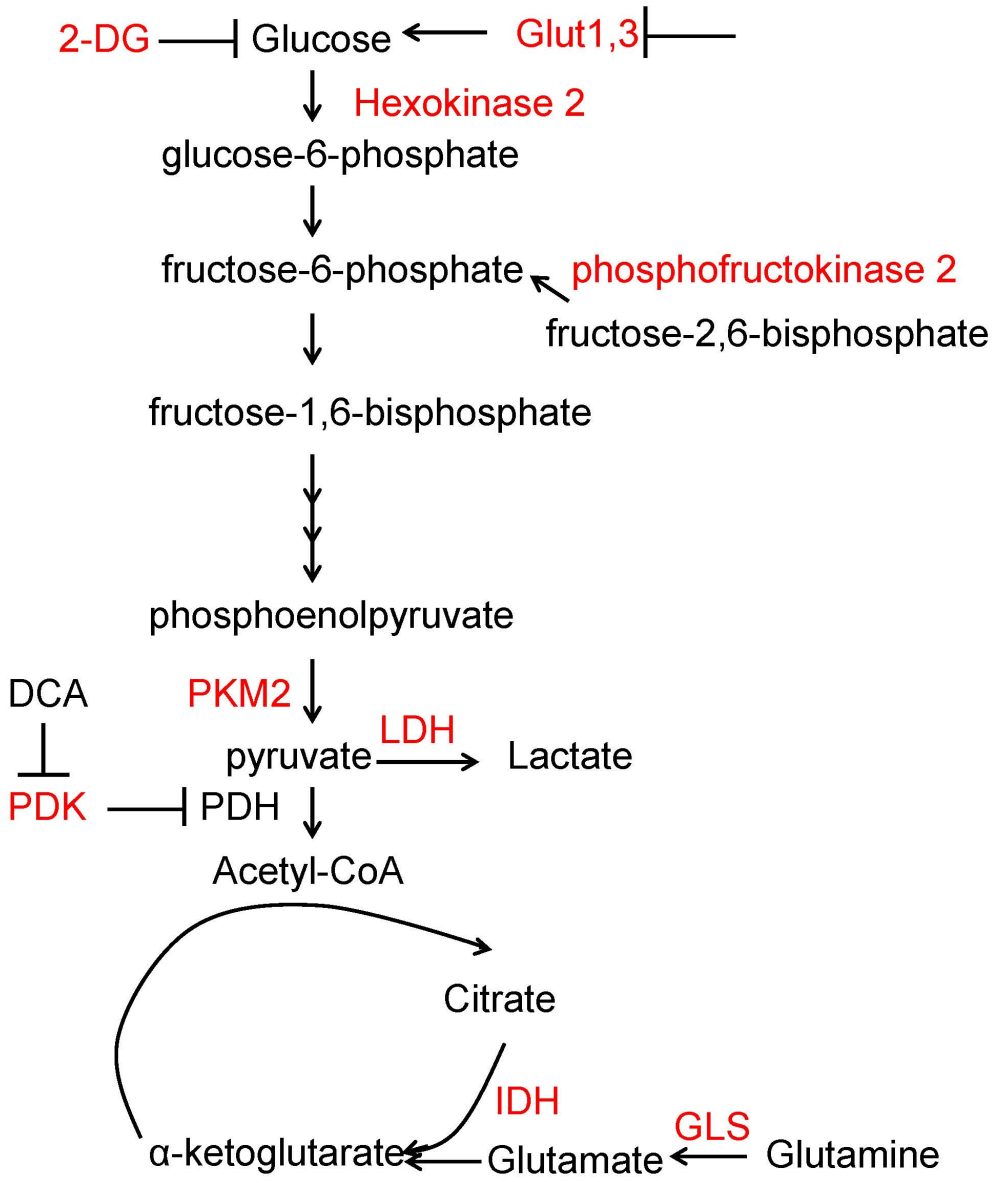

Figure 5. Targeting metabolic enzymes in cancer. The metabolic enzymes that are considered as therapeutic targets for cancer (shown as red in the figure). GLS, glutaminase; GLUT, glucose transporter; IDH, isocitrate dehydrogenase; LDH, lactate dehydrogenase; PDK, pyruvate dehydrogenase kinase; PKM2, pyruvate kinase M2 isoform.

HYPOTHEIS AND SPECIFIC AIMS

Although cancer stem cells (CSCs) have been isolated from various types of cancer and their microenvironment is considered to be crucial for maintaining their stemness, the metabolic characteristics and mitochondrial function of cancer stem cells have not been well investigated. When cultured under serum-free conditions, CSCs can maintain their self-renewal and multi-lineage differentiation abilities; while adding serum into the culture causes their differentiation. It remains unknown how serum induces differentiation in CSCs and whether the metabolism differs between CSCs and other cancer cells.

I **hypothesize** that GSCs have low mitochondrial activity and mainly depend on glycolysis for energy production compared with their differentiated progenies, and that such metabolic properties can be utilized for designing new therapeutic strategies to eliminate GSCs. Specifically, the **major goals** of this study are to compare the mitochondrial respiratory function, glycolytic metabolism, and generation of reactive oxygen species in GSCs and in the downstream progeny cells induced by differentiation factors like FBS, to evaluate the role of glycolysis and ROS in GSCs survival and drug sensitivity, and to test new therapeutic strategies to effectively kill the drug-resistant GSCs.

Considering the important role of CSCs in cancer development of disease recurrence, this proposed research project is of high **significance** in that it will provide new insights into cancer stem cell metabolism with potentially important therapeutic implications.

The specific aims of my thesis project are to:

Specific Aim 1. Evaluate the role of mitochondria and ROS in mediating GSC differentiation in response to serum induction.

Specific Aim 2. Investigate the underlying mechanisms of how serum induces GSC differentiation.

Specific Aim 3. Design new therapeutic strategies to effectively kill GSCs based on their metabolic properties.

CHAPTER 2

MATERIALS AND METHODS

Cell Lines and Cell Culture

GSC11, GSC23 and GBM3752 cell lines were isolated from three fresh surgical specimens of glioblastoma multiforme by Dr Howard Colman and Dr Xiao-nan Li's groups. GSC11 and GSC23 were grown in Dulbecco's Modified Eagle Medium: Nutrient Mixture F-12 (DMEM/F12) medium (Mediatech Inc; Manassas, VA) supplemented with B27 (Invitorgen; Carlsbad, CA), 20ng/ml epidermal growth factor (Miltenyi Biotec; Auburn, CA), 20ng/ml of basic fibroblast growth factor (Miltenyi Biotec; Auburn, CA) and 2 mM L-glutamine (Mediatech Inc; Manassas, VA). GBM3752 cells came from orthotopic tumors in murine brain, as previously described (181) and were cultured in the same supplemented DMEM/F12 medium of GSC11 and GSC23 for less than 5 passages. Differentiation was induced with 5% FBS (Sigma-Aldrich; St. Louis, MO). For NAC treatment, cells were cultured under the 5% FBS containing medium with different concentrations of NAC (Sigma-Aldrich). The glioma cell line U87 and non-malignant human astrocytes (NHAs) were maintained in DMEM (Mediatech) supplemented with 10% FBS. Cells were cultured in a humidified incubator maintained at 37°C with 5% CO_2 for 20 to 45 passages. Cells were treated with accutase (Sigma-Aldrich) before splitting or each treatment. The cells cultured under hypoxic conditions were maintained in a chamber with 2% O_2.

Chemicals and Reagents

NAC, rotenone, antimycin, 4(2′-aminoethyl) amino-1,8-dimethylimidazo(1,2-a) quinoxaline (BMS-345541), carmustine (BCNU), temozolomide (TMZ), and 3-BrPA were purchased from Sigma-Aldrich. 3-BrOP was synthesized by esterification of 3-bromo-2-

oxopropionate (Sigma-Aldrich) with 1-propanol (Sigma-Aldrich) under acidic conditions followed by neutralization with sodium carbonate and evaporation of the excess 1-propanol under a vacuum (178).

RNA Isolation and RNA Microarray Analysis

GSC11 cells were cultured in stem cell medium or differentiated medium for 1, 3, and 7 days in triplicate. Total RNA was extracted from 12 samples using the RNeasy Mini kit (QIAGEN Inc; Valencia, CA). Sample labeling was performed with an RNA amplification kit according to the manufacturer's instructions (Applied Biosystems; Foster City, CA). We used 700 ng of total RNA for labeling and hybridization on HumanHT-12 v3 expression beadchip (Illumina Inc; San Diego, CA) according to the manufacturer's protocols (Illumina). After the bead chips were scanned with a BeadArray Reader (Illumina), the microarray data were normalized using the quantile normalization method in the Linear Models for Microarray Data (LIMMA) package in the R language (http://www.r-project.org). The expression values of each gene were log2-transformed before further analysis. Primary microarray data are available in the National Center for Biotechnology Information Gene Expression Omnibus public database. BRB-ArrayTools were primarily used for statistical analysis of gene expression data (182). The t test was applied to identify the genes significantly different between two groups when compared. Cluster analysis was performed using the software programs Cluster and Heatmap was generated by Treeview (183).

Real-Time PCR Analysis

The total RNA was reverse transcribed using a complementary DNA (cDNA) synthesis kit (Fermentas Inc; Glen Burnie, MD). The quantitative polymerase chain reaction analyses were carried out in a 25 µl reaction mixture that contained 1µl cDNA, 0.1µg oligonucleotide primer pairs, 12.5 µl SYBR Green Mix (Invitrogen) and diethylpyrocarbonate-treated water with the following primer sets (Table 2).

Table 2. Human PCR primers for detecting levels of mRNA expression.

Gene	Forward	Reverse
SOX2	GCCTGGGCGCCGAGTGGA	GGGCGAGCCGTTCATGTAGGTCTG
Olig2	TGCGCAAGCTTTCCAAGA	CAGCGAGTTGGTGAGCATGA
CD133	CAGTCTGACCAGCGTGAAAA	GGCCATCCAAATCTGTCCTA
Notch1	GTGACTGCTCCCTCAACTTCAAT	CTGTCACAGTGGCCGTCACT
APH1B	TTTCCGCGGTGGCCATGACT	GAAGTGCTGGTTCCCTGAGG
DLL1	CCTACTGCACAGAGCCGATCT	ACAGCCTGGATAGCGGATACAC
DTX3	TCCCTAAATGCCAGACTTGG	GGACAGGACGAACGACATTT
HES5	GCACCAGCCCAACTCCAAAC	TGCAGGCACCACGAGTAGCC
LFNG	GATGACTGCACCATTGGCTACA	GGCACCTGCTGCAGGTTCT
MFNG	GCGGTACCACTTGAACCTGT	ATGTCTGTTCCCTGGTCCTG

Human Taqman probes were also used for detecting CD133, SOX2, Olig2 and 18S (Table 3).

Table 3. Human Taqman primers for detecting levels of mRNA expression. Taqman primers from Applied Biosystems for the indicated genes and their sequence ID are provided.

Primer	Assay I.D.
CD133	Hs01009250_m1
SOX2	Hs01053049_s1
Olig2	Hs00377820_m1
18S	Hs03928985_g1

Flow Cytometric Analysis of CD133

The cells were dissociated into single cells by using Accutase reagents (Sigma-Aldrich) and were stained by allophycocyanin (APC)-conjugated CD133/1 clone AC133 antibody (MACS Miltenyi Biotec, Cologne, Germany) or IgG2b-APC (MACS) according to the manufacturer's instructions. 10µl propidium iodide (PI) was added before flow cytometry was performed.

Immunocytochemistry

Human neural stem cell functional identification kit (R&D Systems; Minneapolis, MN) was used for immunocytochemistry assay. Cells were grown on chamber slides coated

with laminin or in flasks and fixed with 10% formalin and permeablized with 0.3% Triton X-100 or fixed with -20°C 100% methanol. After blocked with 3% Goat serum+10%BSA/PBS for 30-60 minutes, cells were incubated with the primary antibodies diluted in 1%BSA/PBS over night and washed with PBS for 3 times. FITC conjugated goat anti-mouse IgG or Rhodamine red conjugated goat anti-mouse IgG were diluted in 1%BSA/PBS and added onto the cells. The slides were washed with PBS for 3 times, stained with 4',6-Diamidino-2-Phenylindole, Dihydrochloride (DAPI) and observed under confocal microscope (Nikon).

Immunoblotting

Cultured cells were washed in PBS and homogenized in lysis buffer. Whole lysate was used and 20 μg protein was applied for each sample. Cell lysates were separated by electrophoresis on 10% or 12% sodium dodecyl sulfate polyacrylamide gel electrophoresis and transferred to nitrocellulose membranes. After blocking with 5% non-fat milk/PBST for 1 hour, the membranes were incubated overnight with primary antibodies at 4°C. Rabbit anti-human SOX2 (Cell Signaling Technology Inc; Danvers, MA), rabbit anti-human Olig2 (Abcam; Cambridge, MA), mouse anti-human CD133 (MACS Miltenyi Biotec), rabbit anti-human Catalase (EMD Chemicals; Gibbstown, NJ), sheep anti-human SOD1 (EMD Chemicals), rabbit anti-human SOD2 (Santa Cruz Biotechnology Inc; Santa Cruz, CA), rabbit anti-human γ-GCSc (Santa Cruz), mouse anti-human phospho-IκBα (Cell Signaling; Danvers, MA), mouse anti-human IκBα (Cell Signaling), rabbit anti-human phosphor-p65 (Cell Signaling), rabbit anti-human p65 (Cell Signaling), rabbit anti-human phosphor-H_2AX

(EMD Millipore; Billerica, MA) rabbit anti-human H2AX (EMD Millipore) and mouse anti-human β-actin (Sigma-Aldrich) were used as primary antibodies. The primary antibody was incubated at 4°C overnight and the secondary antibody was incubated for 1 hour at room temperature.The primary antibodies were detected with horseradish peroxidase-conjugated secondary antibodies. The membranes were developed using a Pierce Supersignal West Pico Chemiluminescent Substrate (Fisher Scientific Inc; Pittsburgh, PA).

Measurement of Intracellular ROS

Cells were plated in 6 well plates in stem cell medium or FBS-containing medium for 1, 3, or 7 days. Before performing the experiments, all samples were collected and dissociated into single cells by accutase. We washed cells with PBS once and resuspended them in prewarmed PBS containing freshly made solutions of 1μM CM-H2DCFDA or 5μM MitoSOX-Red (Molecular Probes; Eugene, OR) and incubate them at 37°C for 30 and 15 minutes, respectively. After loading, we spun the cells in PBS, washed them in PBS twice and performed the flow cytometric analysis.

Glutathione Assay

Measurement of total intracellular glutathione was performed by using a glutathione assay kit according to the manufacturer's instructions (Cayman Chemical, Ann Arbor, MI, USA). The GSC cells were cultured in serum-free for 7 days or cultured in 5% FBS-containing medium for 1, 3 or 7 days. Subsequently, the cells were washed with PBS, harvested by centrifuging or by using a rubber policeman and were sonicated in cold MES

buffer. A small portion of the supernatant was kept for the BCA protein assay (Pierce, Rockfold, IL). 1% 2-vinylpyridine solution was added to the residual supernatant for deproteinization and kept at -80°C till measurement.

Oxygen Consumption Assay

Samples were harvested and dissociated into singles cells by accutase, washed with PBS once and suspended in fresh 37°C medium pre-equilibrated with 21% oxygen at 4~10 million cells/ml in stem cell medium. Oxygen consumption was measured in 1-ml medium in a sealed respiration chamber equipped with a thermostat control and microstirring device using an Oxytherm electrode unit (Hansatech Instruments Ltd; Norfolk, UK) at 37°C for 10 to 20 minutes. Oxygen consumption by these cells in the chamber was measured and constantly monitored at 37°C using a Clark-type oxygen electrode (Hansatech Instruments). The oxygen consumption was expressed in nanomoles of O_2 consumed as a function of time (nmol/ml/minute).

Cell Viability Assay

Cell-growth inhibition was assayed using a colorimetric assay with MTS (Promega). Briefly, GSCs were seeded in 96-well plates and then treated with indicated compounds at various concentrations. After 72 hours of incubation, 40 μl of the MTS solution was added to each well and then incubated for another 4 hours. The absorbance in each well at 490 nm was measured using a Multiskan plate reader (Thermo Scientific). Cell apoptosis and necrosis were measured using flow cytometric analysis of cells double-stained with FITC-

annexin-V and propidium iodide. Briefly, samples were collected, dissociated, washed with cold PBS, and suspended in the annexin-V binding buffer, and then stained with annexin-V for 15 minutes at room temperature, washed, and stained with PI. The samples were analyzed using a FACSCalibur flow cytometer equipped with the CellQuest Pro software program (Becton-Dickinson).

Tumor Sphere Forming Assay

GSCs were treated with indicated compounds for 3 hours and then seeded in fresh medium in 96-well plates at cell numbers from 10 to 1000 cells per well and incubated at 37°C under normoxia condition; neurospheres were counted under a microscope (Nikon) after 3 weeks of incubations.

Glucose Uptake Assay

GSCs were induced by 10% FBS for 20 days and then compared with the control GSCs. Briefly, the medium in the cell culture were replaced with the glucose-free medium and incubated for 2 hours at 37°C, and then incubated with [^{3}H]-2-deoxyglucose (0.4 μCi/ml) for another hour. After washing with cold PBS, each sample was suspended in 0.5 ml of water and transferred to a vial with 3 ml of scintillation fluid. The radioactivity of the samples was detected using a liquid scintillation machine (Beckman Coulter).

Lactate Production Assay

To measure the lactate production by GSCs in long-term culture, GSCs were plated in six-well plates with the fresh medium for indicated times. Aliquots of the culture medium were analysed by an Accutrend lactate analyzer (Roche). To measure the lactate production in short-term culture, cells were plated in 96-well plates and treated with indicated compounds for 3 hours. A colorimetric lactate assay kit was used according to the manufacturer's protocol (Eton Bioscience). Absorbance in each well at 490 nm was measured using a Multiskan plate reader.

ATP Depletion Assay

GSCs were plated in 96-well plates and then treated with indicated compounds for 3 or 6 hours, 100 μl of mixed CellTiter-Glo luminescent reagent (Promega) was added to each well and incubated for 10 minutes on an orbital shaker. Luminescence in each well was measured using a Fluoroskan luminescence scanner (Thermo Scientific).

Single-Cell Gel Electrophoresis Assay (Comet Assay)

After GSCs were treated with indicated compounds for 3 hours, cell suspensions mixed with 0.5% low-melting-point agar was placed onto a 24 × 50-mm slide precoated with 1% normal-melting-point agar. After agar distribution and solidification, slides were soaked in a prechilled fresh lysing solution (2.5 μM NaCl, 100 mM ethylenediaminetetraacetic acid, 10 mM Tris-HCl, 1% Triton X-100, pH 10) for 1 hour at

4°C. After rinsing with 0.4 M Tris buffer (pH 7.5), slides were placed in a reservoir filled with fresh electrophoresis buffer (300 mM NaOH, 1 mM ethylenediaminetetraacetic acid, pH >13) for 15 minutes and electrophoresed for another 15 minutes (25 V, 300 mA). Slides were then stained with CYBR Green I (Trevigen) and photographed under a fluorescent microscope (Nikon). The tail DNA percentage, which indicates damaged DNA, was analyzed using the Casp software program (version 1.2.2) provided by the CASPLab Comet Assay Project.

GAPDH Enzymatic Activity Assay

Purified GAPDH enzyme from rabbit muscle (Sigma-Aldrich) or protein extracts prepared from GSC11 cells were used in the GAPDH assays in vitro, using GAPDH Assay Kit (ScienCell) according to the manufacturer's protocol. Purified GAPDH was incubated in vitro with the indicated compounds (BCNU and 3-BrOP) for 30 minutes, then added to a mixture of 6.67 mM 3-phosphoglyceric acid, 3.33 mM L-cysteine, 117 μM β-NADH, 1.13 mM ATP, 3.33 U/ml 3-phosphoglycerate kinase, and 100 mM triethanolamine buffer (pH 7.6), and change in NADH fluorescence was then monitored using a Fluoroskan spectrometer every minute for up to 20 minutes. For analysis of GAPDH activity in cell extracts, GSC11 cells were first incubated with or without 3-BrOP, BCNU, or their combination for 30 min, and protein lysates were prepared and immediately used for GAPDH activity assay without addition of 3-BrOP or BCNU in vitro.

Tumorigenicity in Subcutaneous Mouse Xenografts

GSC11 cells cultured under neural sphere culture conditions (GSC medium) as mentioned above were divided into 4 groups. One group continued to be cultured in the GSC medium, another group was cultured in GSC medium supplemented with 5%FBS, the third group was cultured in GSC medium in the presence of 20mM NAC and the last group was cultured in GSC medium with 5% FBS and 20mM NAC. After 7 days, cells were collected, treated with accutase into single cells and inoculated into the right flank of nude mice at 2×10^6 cells/mouse. The mice were euthanized when the tumor diameter was greater than 20 mm.

3-BrOP and BCNU Treatment

GSC11 cells were cultured in GSC medium and made into single cells by accutase. The same amount of GSC11 cells were exposed to PBS, 20μM BCNU, 20μM 3-BrOP or 20μM BCNU and 20μM 3-BrOP in GSC medium and cultured at 37°C. After 6 hours, cells were collected, washed and inoculated into SCID mice brain at 2×10^5 cells/mouse. The mice were euthanized when they developed signs of neurological deficit or became moribund.

Statistical Analysis

Data were analyzed using GraphPad Prism 5 (GraphPad Software). Data graphed with error bars represent mean and SEM from experiments done in triplicate unless

otherwise noted. A two-sided Student's t test was used to determine the significance of any differences. Survival curves were compared between different groups by Logrank Test.

CHAPTER 3

Mitochondrial function and ROS increase in serum-induced GSC differentiation

Establishment of GSC culture and induction of aberrant differentiation by serum

We used three human glioblastoma stem cell lines (GSC11, GSC23, and GBM3752) in this study. GSC11 and GSC23 were originally derived from fresh surgical specimens of adult glioblastoma multiforme and maintained in serum-free neural sphere culture medium (184, 185). GBM3752 cells were derived from fresh surgical specimen of glioblastoma multiforme, inoculated into SCID mice's brain and passed in SCID mice as orthotopic brain tumors (181). GBM3752 cells were prepared freshly for *in vitro* study in serum-free medium during the first several passages. These cells all grew in serum free stem cell medium (DMEM/F-12 medium) containing EGF and bFGF, and exhibited the morphology of stem-like neurospheres (Figure 6). The presence of serum (5% FBS) in culture medium caused a significant change in cell morphology, manifested by a loss of neurosphere formation and the appearance of differentiated cells attaching to the culture dishes (Figure 6).

About 50%-60% of GSC11 and GSC23 cultured under serum free medium were CD133-positive cells (Figure 7A). Adding FBS into the culture medium caused a substantial decrease of CD133 expression in a time-dependent manner (Figure 7A-B). After 3 days cultured in serum-containing medium, the percentage of $CD133^+$ cells dropped to 30-45% in GSC11 cells, which was significantly decreased compared to the cells cultured in serum-free medium. After 7 days cultured in serum-containing medium, the percentage of $CD133^+$ GSC11 cells further dropped to around 20%. The decrease of CD133 expression was confirmed by western blot (Figure 7C). The similar time-dependent decrease of $CD133^+$ was also observed in GSC23 cells (Figure 7D-E).

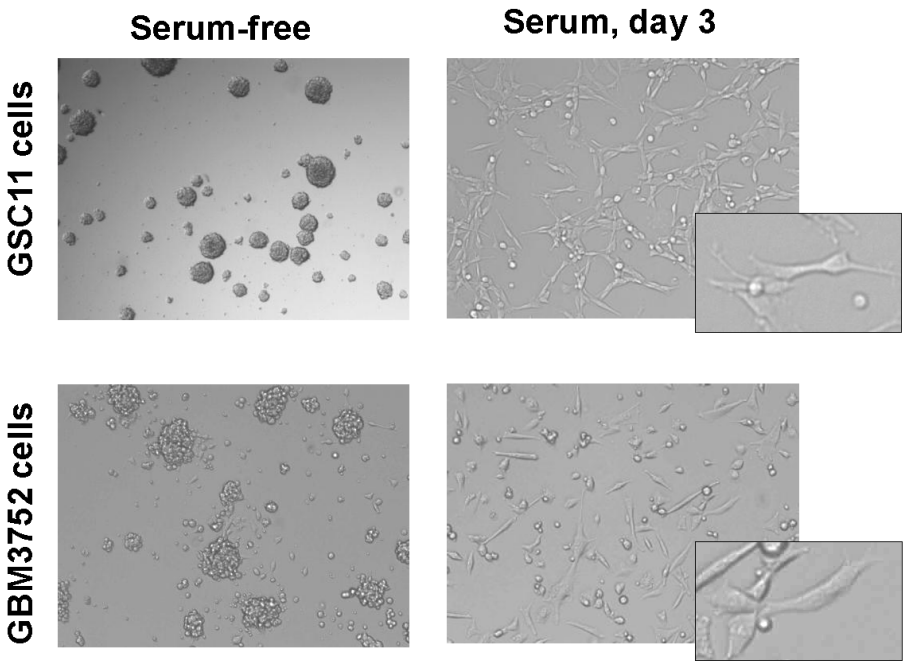

Figure 6. Serum induces GSCs aberrant differentiation. Glioblastoma stem cells (GSC11 and GBM3752) formed neurospheres in the serum-free medium supplemented with EGF and bFGF. Exposure of the cells to serum (5% FBS) for 3 days led to a loss of neurosphere formation in both cell lines.

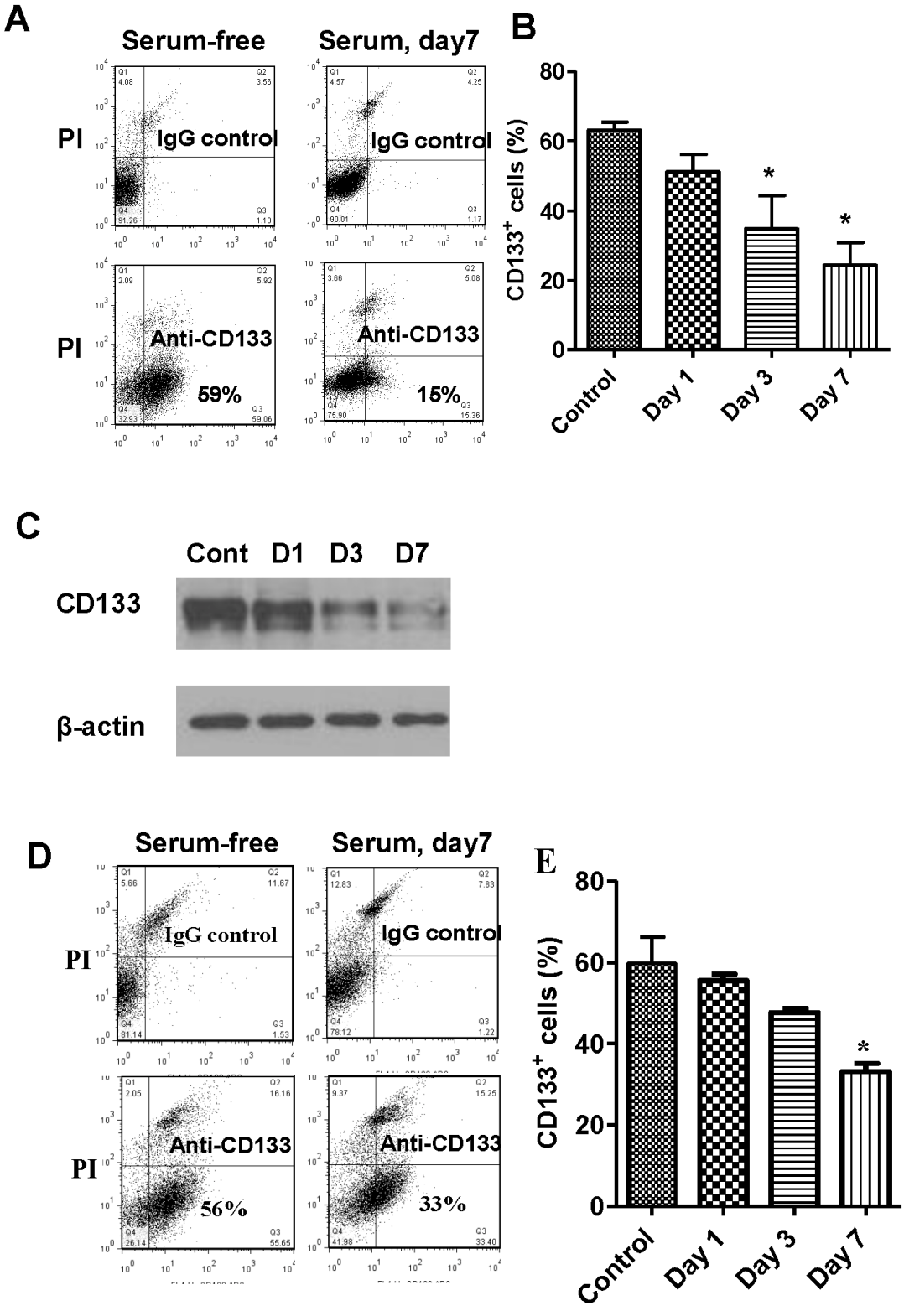
A
Serum-free
Serum, day7
PI
IgG control
IgG control
PI
Anti-CD133
59%
Anti-CD133
15%
B
CD133+ cells (%)
80
60
40
20
0
*
*
Control
Day 1
Day 3
Day 7
C
Cont
D1
D3
D7
CD133
β-actin
D
Serum-free
Serum, day7
PI
IgG control
IgG control
PI
Anti-CD133
56%
Anti-CD133
33%
E
CD133+ cells (%)
80
60
40
20
0
*
Control
Day 1
Day 3
Day 7

Figure 7. Serum causes CD133 decrease. (A) Flow cytometric analysis of CD133 expression in GSC11 cells before and after exposure to serum for 7 days. (B) Quantitation of the percentage of CD133+ cells before and after GSC11 cells exposed to serum for 1, 3, and 7 days. *, $P<0.05$. (C) Western blot analysis of CD133 expression in GSC11 cells before and after exposure to serum for 1, 3, and 7 days as indicated. (D) Flow cytometric analysis of CD133 expression in GSC23 cells before and after exposure to serum for 7 days. (E) Quantitation of the percentage of CD133+ cells before and after GSC23 cells were exposed to serum for 1, 3, and 7 days. *, $P<0.05$.

Quantitative RT-PCR and western blot analyses of GSC11 cells revealed a significant decrease in mRNA expression of SOX2 and Olig2, two transcription factors that are important for neural stem cells and neural progenitor cells, in serum-induced cells (Figure 8A). The mRNA expression of Notch1, a molecule important for promoting neural stem cell function(186), was also significantly down regulated in serum-induced cells (Figure 8A). The downregulation of SOX2 and Olig2 was also detected on protein levels by western blot (Figure 8B). In contrast, the expression of a differentiation marker ANXA1 was significantly increased after exposure of GSC11 cells to serum (Figure 8B). Similar results were obtained from GSC23 cells (Figure 8C-D).

High expression levels of a neural stem cell marker Nestin was detected in GSC spheres by immunocytochemistry (Figure 9). The exposure to FBS did not cause obvious change in Nestin expression. Glial fibrillary acidic protein (GFAP), a marker which is often detected in astrocytes, was also detected in GSC spheres by immunocytochemistry (Figure 10). Serum exposure did not cause substantial change of GFAP expression. Low level expression of a neuron marker β-III tubulin and an oligodendrocyte marker O4 was detected in GSC cells and serum induction caused an upregulation of both proteins (Figure 11).

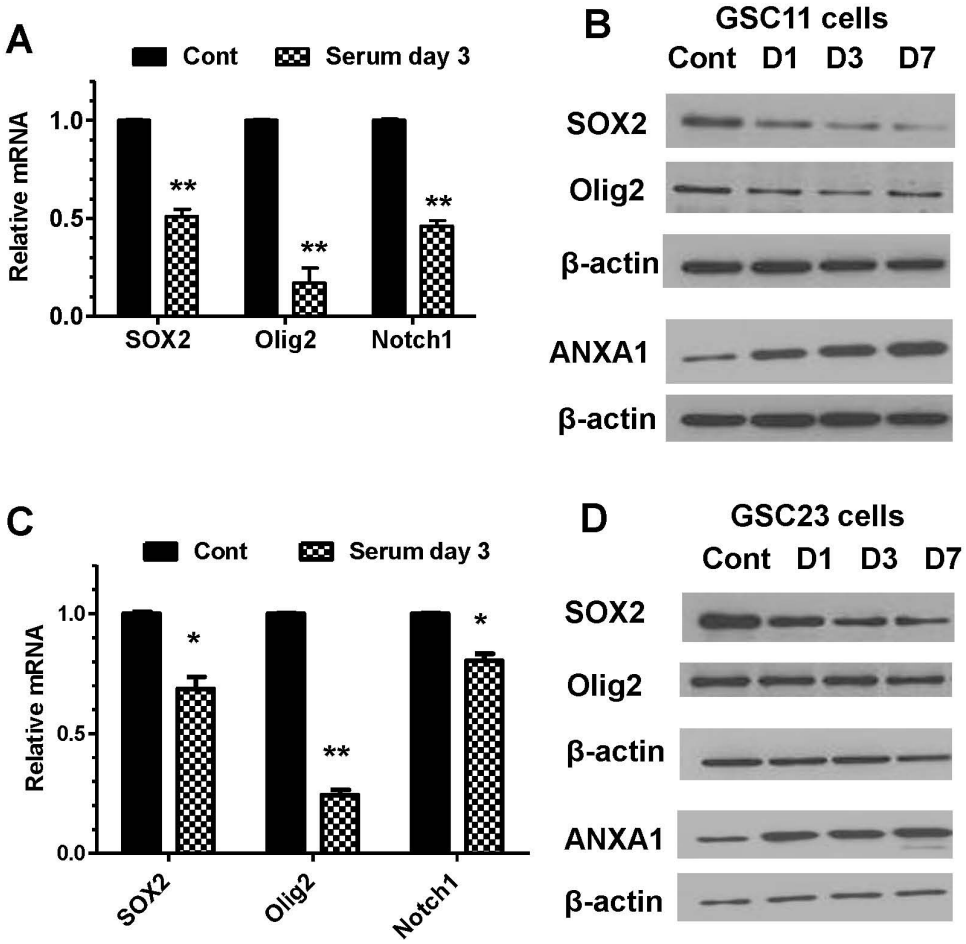

Figure 8. Serum causes decreases of SOX2, Olig2 and Notch1 and an increase of ANXA1. (A) Expression of SOX2, Olig2, and Notch1 mRNA in GSC11 cells before and after exposure to serum for 3 days. Expression of mRNA was measured by quantitative real-time PCR. **, P<0.001 *, P<0.05. (B) Effect of serum exposure on protein expression of stem cell markers SOX2 and Olig2 and differentiation marker ANXA1. GSC11 cells were exposed to 5% FBS for 1, 3, and 7 days (D1, D3, D7). SOX2, Olig2, ANXA1 were detected by western blot analysis. (C) Expression of SOX2, Olig2, and Notch1 mRNA in GSC23 cells before and after exposure to serum for 3 days. Expression of mRNA was measured by quantitative real-time PCR. **, P<0.001 *, P<0.05. (D) Effect of serum exposure on protein expression of stem cell markers SOX2 and Olig2 and differentiation marker ANXA1. GSC23 cells were exposed to 5% FBS for 1, 3, and 7 days (D1, D3, D7) as indicated, and cellular proteins were analyzed for expression of SOX2, Olig2 and ANXA1 by western blotting.

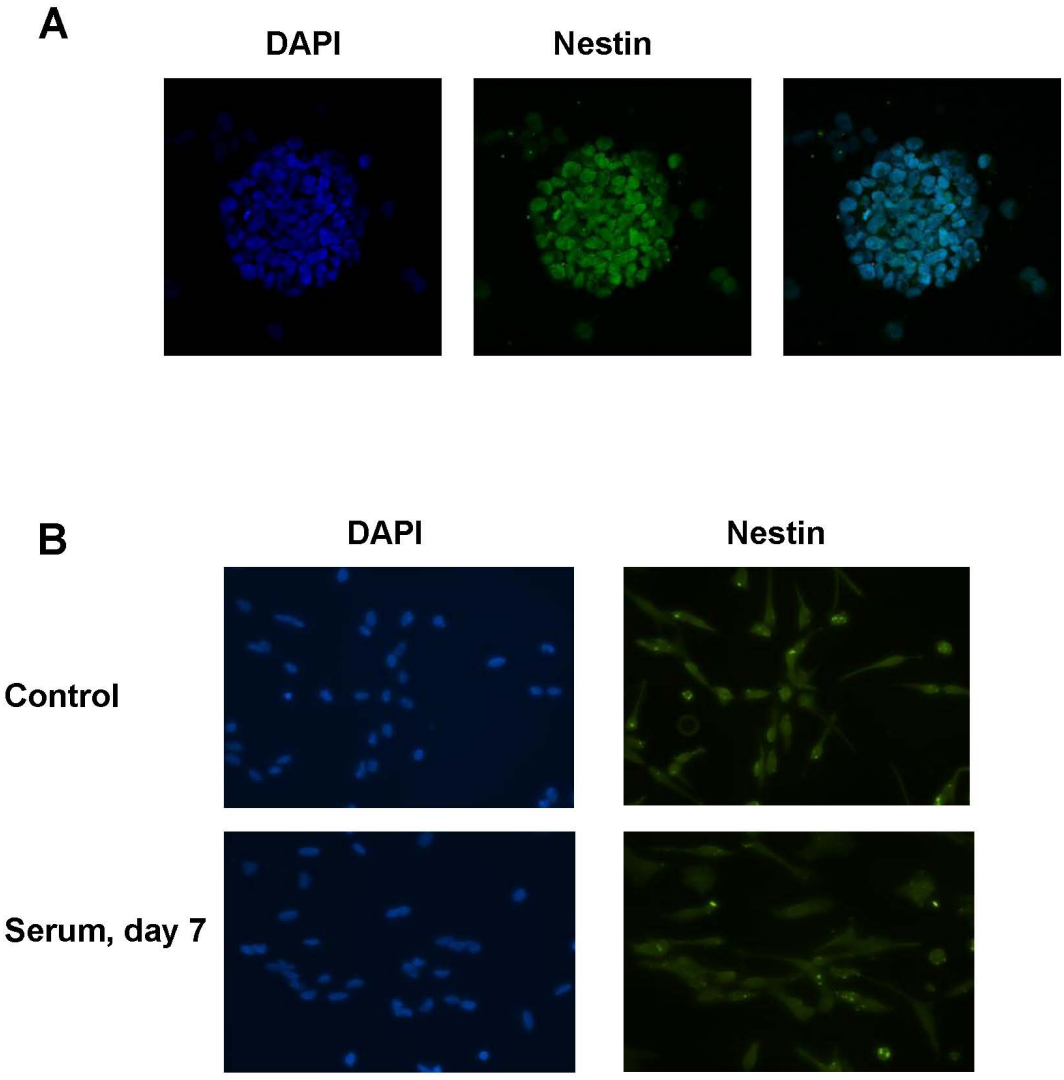

Figure 9. GSCs express Nestin. (A) Expression of Nestin (green) in GSC11 neurospheres was detected by immunocytochemistry staining. Counterstaining of the nuclei with DAPI is depicted (blue). (B) Immunocytochemistry staining of Nestin (green) and DAPI (blue) in GSC11 cells cultured in GSC medium or exposed to 5% FBS for 7 days.

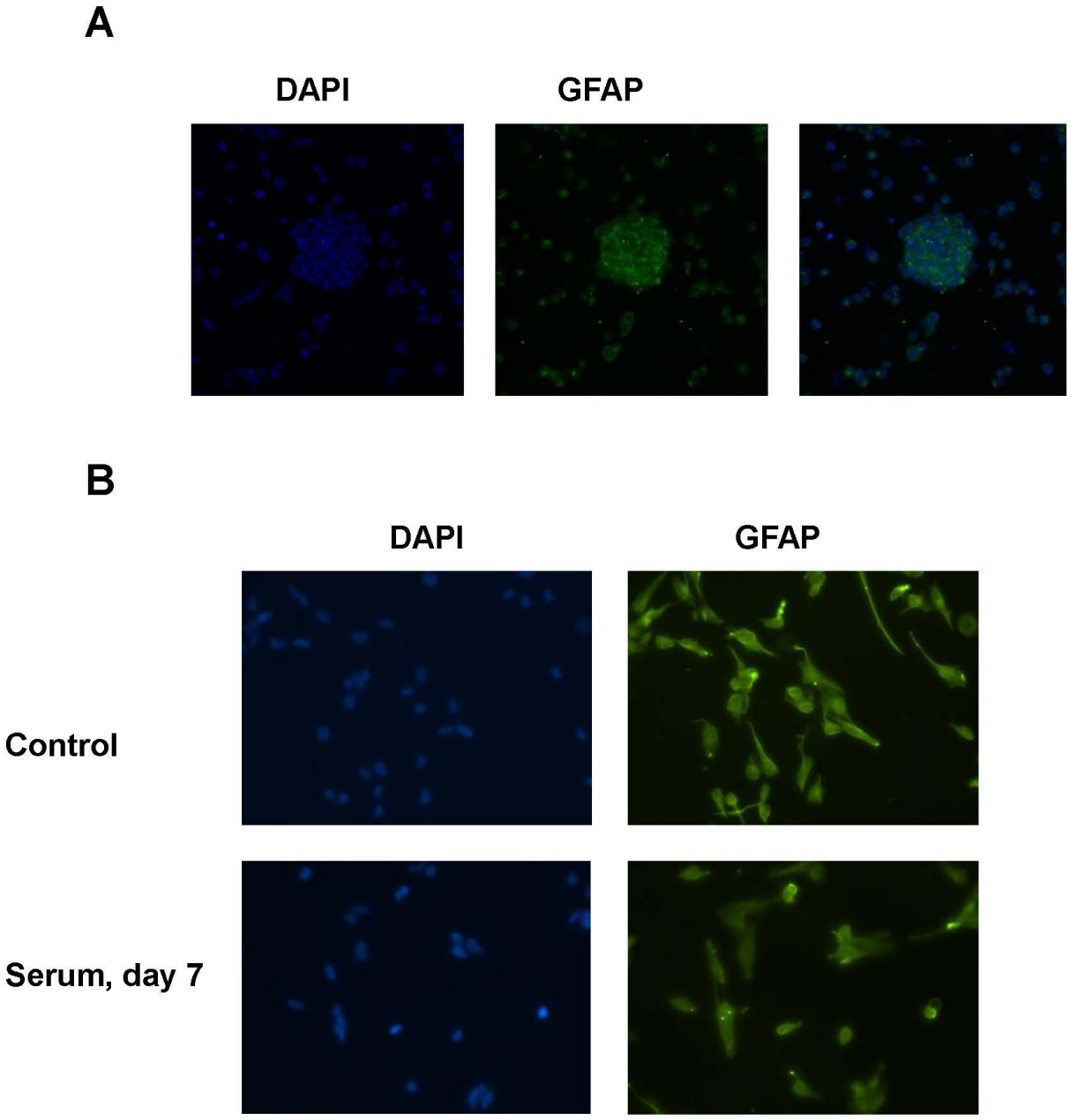

Figure 10. GSCs express GFAP. (A) Expression of GFAP (green) in GSC11 neurospheres by Immunocytochemistry staining. Counterstaining of the nuclei with DAPI is depicted (blue). (B) Immunocytochemistry staining of GFAP (green) and DAPI (blue) in GSC11 cells cultured in GSC medium or exposed to 5% FBS for 7 days.

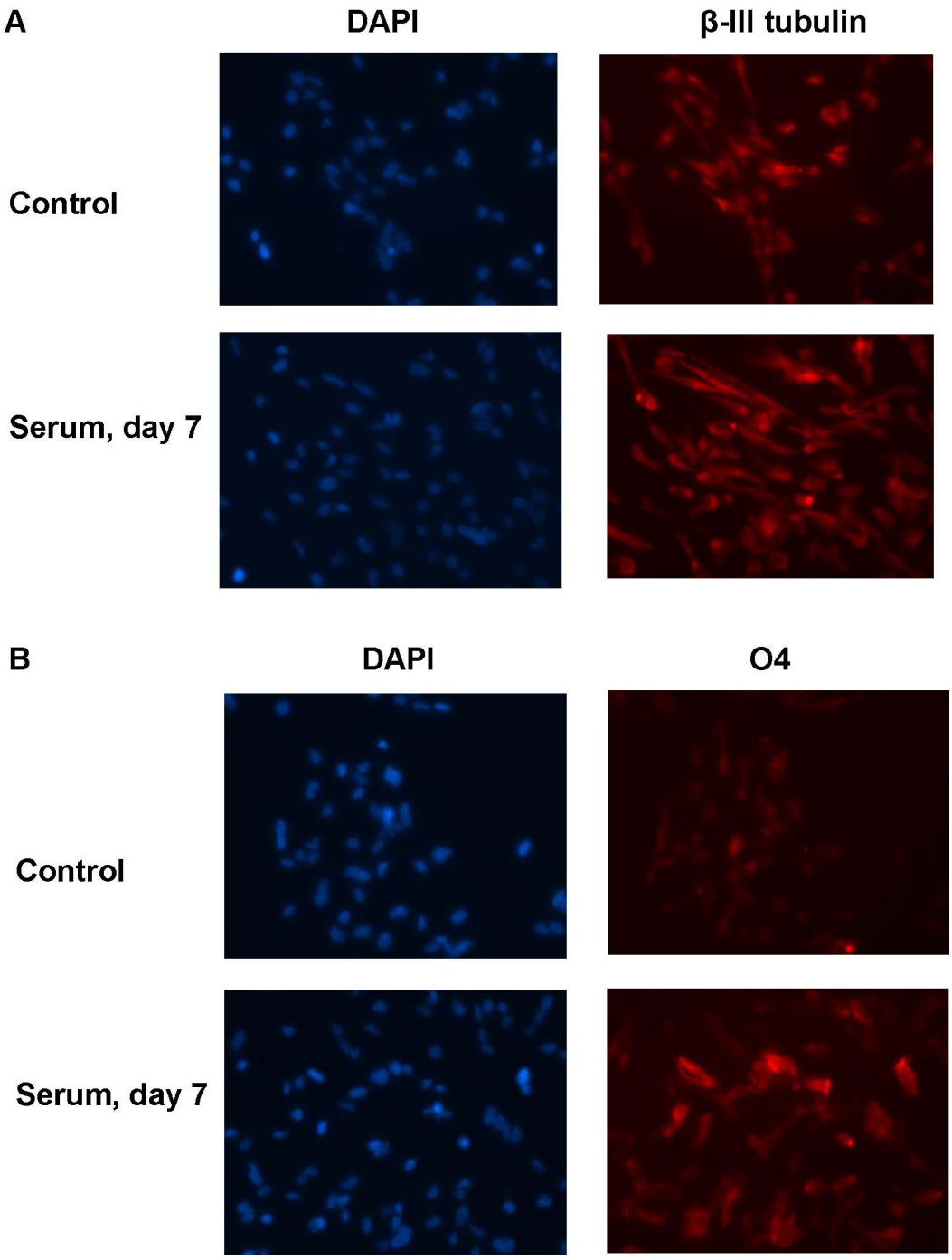

Figure 11. Expression of β-III tubulin and O4 increases in serum-induced GSC11 cells. (A) Immunocytochemistry staining of β-III tubulin (red) and DAPI (blue) in GSC11 cells cultured in GSC medium or exposed to 5% FBS for 7 days. (B) Immunocytochemistry staining of O4 (red) and DAPI (blue) in GSC11 cells cultured in GSC medium or exposed to 5% FBS for 7 days.

FBS causes gene expression change in aberrant differentiated cells

To investigate the molecular events and potential alterations of signaling pathways in response to serum-induced differentiation in the glioblastoma stem cells, we treated GSC11 cells with 5% FBS for 1, 3, and 7 days in triplicate cultures, and isolated RNA from each sample for determination of gene expression profiles. As shown in Figure 12A, clustering analysis of the gene expression data from microarray analysis revealed that the serum-treated GSC11 cells exhibited gene expression profiles distinct from that of the GSC11 cells cultured in serum-free medium. There was a further shift of gene expression profiles as the time of serum exposure prolonged. The fact that three separate samples of the same time point (biological triplicates) displayed similar gene expression patterns and clustered in the same group reflects the high reproducibility of this experimental system. Using the Ingenuity Pathway Analysis software, we compared the gene expression between GSCs and aberrant differentiated cells and we found that the Nrf2 mediated oxidative stress response pathway was the most significant alteration (p = 0.00045) in cells cultured under serum condition for 1 day. On the first day of initiating differentiation, the molecules related to Nrf2 mediated oxidative stress response pathway were significantly altered (Figure 12B). Table 4 shows the genes involved in oxidative stress response identified by this analysis in GSC11 cells. Among the genes identified, SOD2, catalase, NQO1, peroxiredoxin 1, thioredoxin reductase 1, and glutamate-cysteine ligase are involved in ROS scavenging. These results suggest that serum-induced differentiation of GSCs was likely associated with oxidative stress.

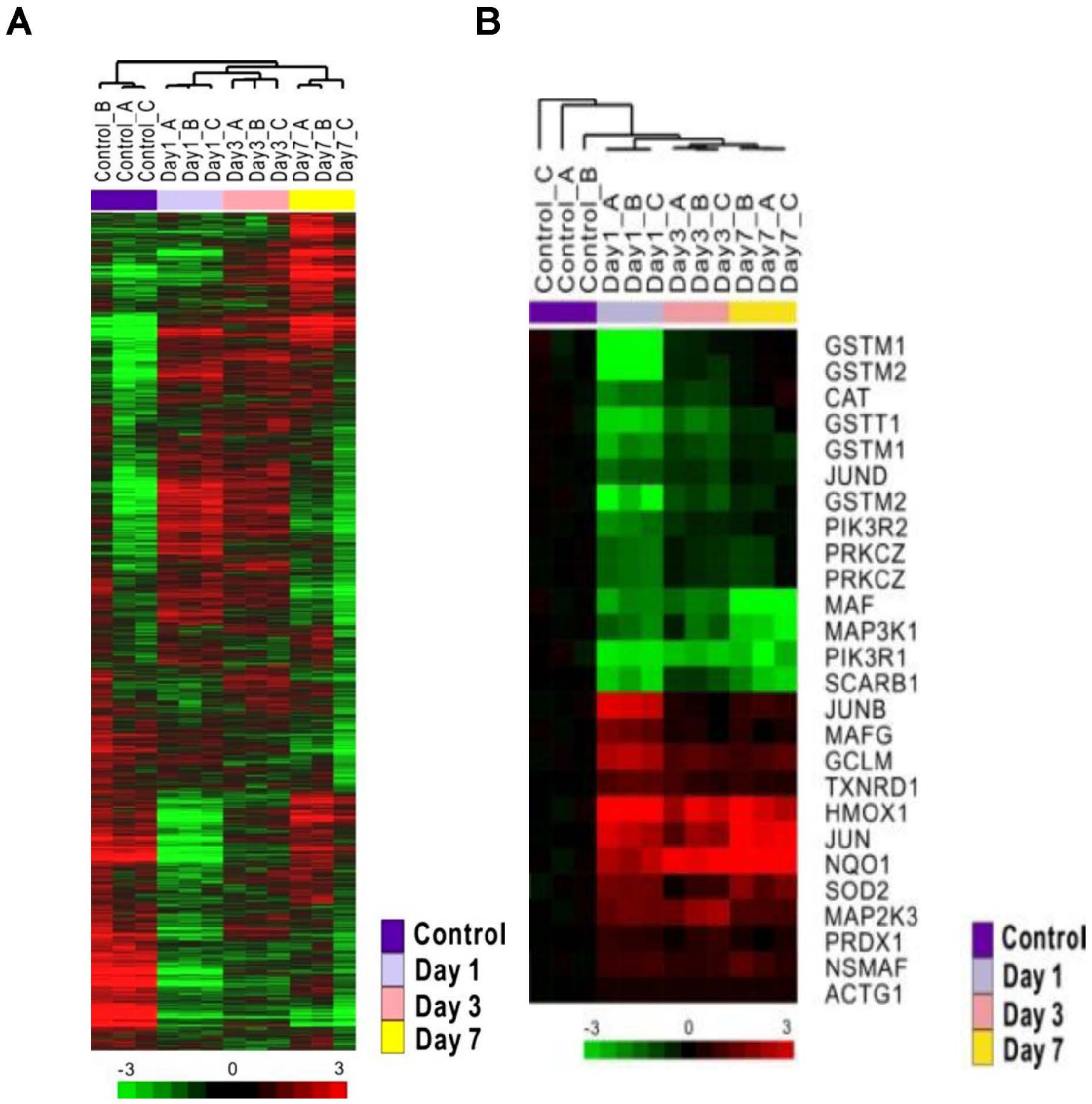
A
Control_B
Control_A
Control_C
Day1_A
Day1_B
Day1_C
Day3_A
Day3_B
Day3_C
Day7_A
Day7_B
Day7_C
-3
0
3
Control
Day 1
Day 3
Day 7
B
Control_C
Control_A
Control_B
Day1_A
Day1_B
Day1_C
Day3_A
Day3_B
Day3_C
Day7_B
Day7_A
Day7_C
GSTM1
GSTM2
CAT
GSTT1
GSTM1
JUND
GSTM2
PIK3R2
PRKCZ
PRKCZ
MAF
MAP3K1
PIK3R1
SCARB1
JUNB
MAFG
GCLM
TXNRD1
HMOX1
JUN
NQO1
SOD2
MAP2K3
PRDX1
NSMAF
ACTG1
-3
0
3
Control
Day 1
Day 3
Day 7

Figure 12. The gene expression changes in aberrant differentiated cells. (A) Overall gene expression pattern of GSC11 cells. GSC11 cells maintained in serum-free stem cell medium were exposed to 5% FBS for 1, 3, and 7 days (each time point had triplicate culture flasks A-C). After variance filtering, a total of 7613 probes were used for unsupervised hierarchical clustering with the similarity metric of uncentered correlation. The red and green colors represent high and low expression, respectively, as indicated in the log2-transformed scale bar. (B) Expression pattern of genes associated with the Nrf2-mediated oxidative stress response pathway. Genes with expression showing significant difference between control and 1 day in serum-free condition in GSC11 cells were selected by two-sample t-test ($P < 0.001$). Expression values of each gene in 1, 3 and 7 days were normalized by its mean value of controls, and visualized.

Table 4. The significantly changed genes in the Nrf2-mediated oxidative stress response pathway.

Gene	p value(Day1 vs Control)	Fold change (Day1 vs Control)
GSTM1	0.0008	-3.18
GSTM2	4.3E-05	-3.44
CAT	0.00078	-1.83
GSTT1	0.00028	-2.49
GSTM1	0.00043	-2.06
JUND	0.00068	-1.65
GSTM2	0.00057	-2.82
PIK3R2	0.0002	-1.89
PRKCZ	0.00011	-1.76
MAF	0.0008	-2.02
MAP3K1	0.00091	-1.78
PIK3R1	0.00029	-2.63
SCARB1	6.1E-05	-2.39
JUNB	6.7E-05	2.53
MAFG	0.00044	1.76
GCLM	6.8E-05	2.26
TXNRD1	2.7E-05	1.60
HMOX1	0.00017	3.06
JUN	7.5E-05	2.37
NQO1	0.00042	2.22
SOD2	0.00051	1.78

MAP2K3	0.00061	1.71
PRDX1	0.00029	1.30
NSMAF	0.00063	1.41
ACTG1	0.00057	1.17

Serum induces increase of mitochondrial superoxide

The observations that exposure of GSCs to serum caused a consistent oxidative stress response prompted us to test possible changes in cellular redox status. Since mitochondria are the major sites of ROS production, we used MitoSox Red to detect mitochondrial superoxide (O_2^-) and 5-(and-6)-chloromethyl-2,7-dichlorodihydrofluorescein diacetate acetyl ester (DCF-DA) to measure total cellular H_2O_2 and other ROS. We found that serum induced a substantial increase of mitochondrial O_2^- in a time-dependent manner, with an increase of median value from 46 units in control cells (without serum) to 67, 188, and 268 units on day 1, day 3, and day 7 after serum exposure, respectively (Figure 13A). Total cellular H_2O_2 and other ROS as measured by DCF-DA also showed an increase, from 84 units in the control to 112, 126, and 159 units on day 1, day 3, and day 7, respectively (Figure 13B). Similar results were also observed in GSC23 (Figure 13C-D) and GBM3752 (Figure 13E-F), suggesting that the induction of mitochondrial O_2^- generation might be an important early event in serum-induced differentiation of GSCs.

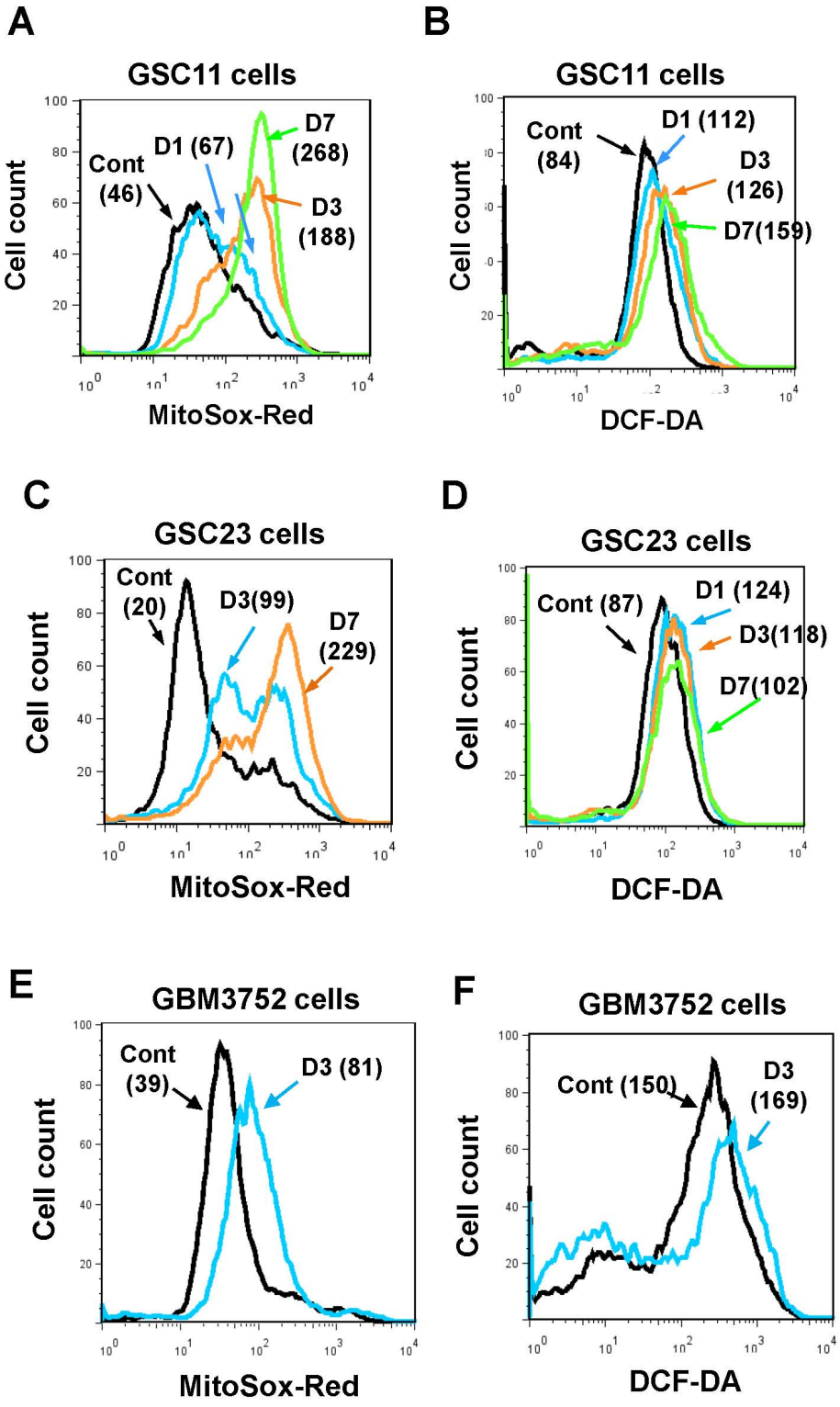
A
GSC11 cells
Cell count
MitoSox-Red
Cont (46)
D1 (67)
D7 (268)
D3 (188)
B
GSC11 cells
Cell count
DCF-DA
Cont (84)
D1 (112)
D3 (126)
D7(159)
C
GSC23 cells
Cell count
MitoSox-Red
Cont (20)
D3(99)
D7 (229)
D
GSC23 cells
Cell count
DCF-DA
Cont (87)
D1 (124)
D3(118)
D7(102)
E
GBM3752 cells
Cell count
MitoSox-Red
Cont (39)
D3 (81)
F
GBM3752 cells
Cell count
DCF-DA
Cont (150)
D3 (169)

Figure 13. Effect of serum on mitochondrial superoxide and cellular ROS. Mitochondrial superoxide was measured by flow cytometric analysis after cells were stained with MitoSOX-Red. Cellular ROS were detected using CM-H2-DCFDA staining followed by flow cytometric analysis. The numbers in parentheses indicate the median fluorescent intensity. (A) Increase of mitochondrial superoxide in GSC11 cells after exposure to 5% FBS for 1, 3, and 7 days (D1, D3, D7). (B) Analysis of total cellular H_2O_2 and other ROS in GSC11 cells before and after exposure to serum. (C) Increase of mitochondrial superoxide in GSC23 cells after exposure to 5% FBS for 1, 3, and 7 days. (D) Analysis of total cellular H_2O_2 and other ROS in GSC23 cells before and after exposure to serum for 3 and 7 days. (E) Increase of mitochondrial superoxide in GBM3752 cells after exposure to 5% FBS for 3 days (D3). (F) Analysis of total cellular H_2O_2 and other ROS in GBM3752 cells before and after exposure to serum for 3 days.

We then tested if the alterations in mitochondrial O_2^- and cellular ROS might cause stress response and upregulation of antioxidant enzymes. As shown in Figure 14, there was a time-dependent increase in expression of SOD2, a mitochondrial superoxide dismutase that converts O_2^- to H_2O_2. Interestingly, the cytosolic superoxide dismutase (SOD1) did not exhibit any significant change after serum exposure (Figure 14A). The expression of catalase, an enzyme that converts cellular H_2O_2 to water and oxygen, increased after serum incubation (Figure 14A). Similar results were obtained from GSC23 (Figure 14B). These data together suggest that the increased expression of SOD2 might be a specific stress response to elevated mitochondrial O_2^- generation induced by serum. SOD2 converted O_2^- to H_2O_2, which was then able to pass the mitochondrial membranes and further converted to O_2 and H_2O by catalase, resulting in a moderate overall increase of total cellular ROS detected by DCF-DA.

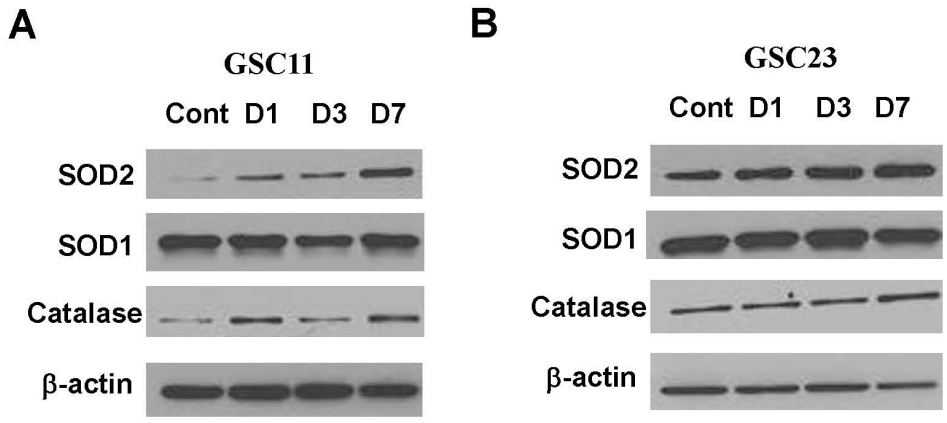

Figure 14. Effect of serum on expression of SOD1, SOD2 and catalase. (A) Western blot analysis of SOD1, SOD2, and catalase in GSC11 cells before and after exposure to serum for 1, 3 and 7 days (D1, D3, D7). (B) Western blot analysis of SOD1, SOD2, and catalase in GSC23 cells before and after exposure to serum for 1, 3 and 7 days (D1, D3, D7).

Total glutathione (GSH), the major endogenous antioxidant, became deficient in a time-dependent manner in the GSC11 aberrant differentiated cells (Figure 15A). For GSC23 cells induced by serum, total GSH increased on day 1 and decreased subsequently on day 3 and day 7 (Figure 15B). A rate limiting enzyme in GSH biosynthesis, γ-glutamylcysteine synthetase heavy subunit (γ-GCSc), increased in aberrant differentiated GSC11 on day 7 (Figure 15C). These results suggested that serum induction caused oxidative stress that led to an upregulation of GSH synthesis enzyme. But this stress response failed to provide sufficient GSH for the cells to scavenge the oxidative stress.

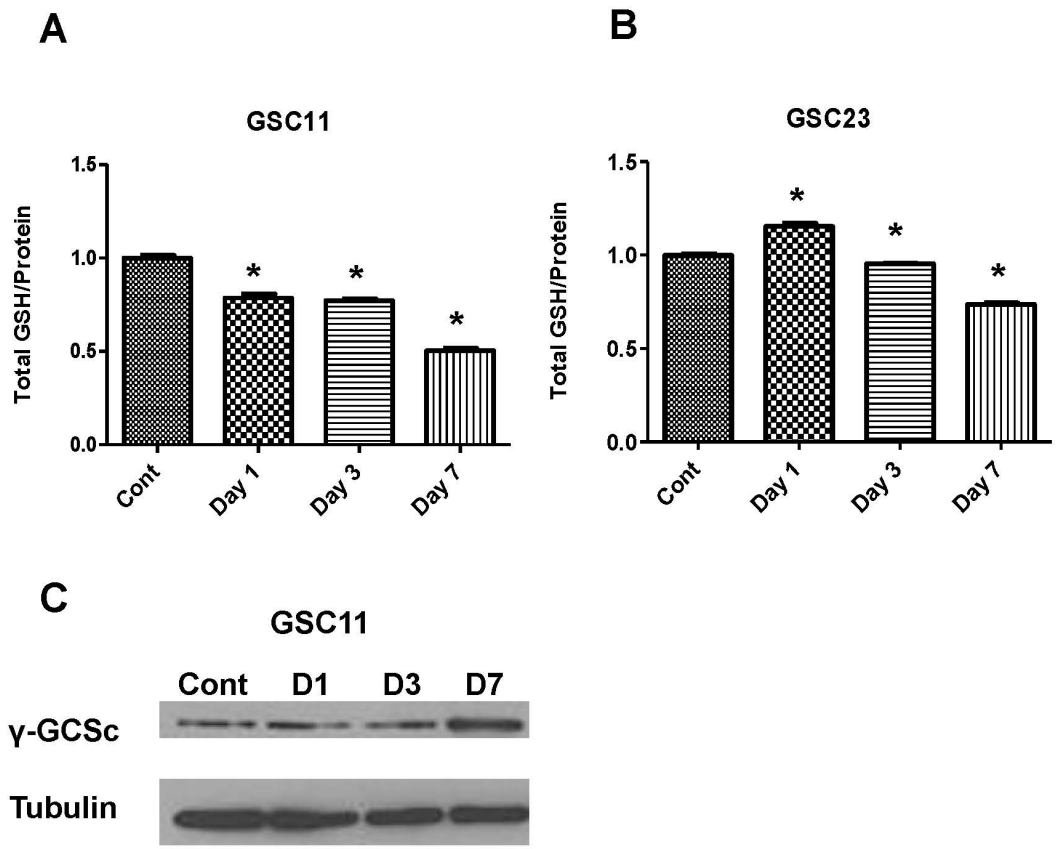

Figure 15. Serum induction causes glutathione depletion. (A)Total GSH/protein ratio in GSC11 cells before and after exposure to serum for 1, 3 and 7 days. (B) Total GSH/protein ratio in GSC23 cells before and after exposure to serum for 1, 3 and 7 days. (C) WB blot detection of γ-GCSc expression in GSC11 cells before and after exposure to serum for 1, 3 and 7 days.

Activation of mitochondrial respiration by serum in glioblastoma stem cells

Since mitochondrial superoxide is mainly generated during respiration due to a release of electrons from complexes I and III of the electron transport chain, we speculated that the increased mitochondrial O_2^- might be a result of active mitochondrial respiration induced by serum, and not a consequence of a slower superoxide elimination since SOD2 expression was increased. To test this possibility, we measured oxygen consumption by GSCs as an indicator of mitochondrial respiration. As shown in Figure 16A-B, exposure of GSC11 cells to serum led to a time-dependent significant increase of oxygen consumption, with approximately 100% increase by day 3. The increase in mitochondrial respiration was also consistently observed in GSC23 (Figure 16C) and GBM3752 cells (Figure 16D).

Since the oxygen consumption increase in aberrant differentiated cells might be due to mitochondria quantity increase or mitochondrial function increase, we further measured the mitochondria quantity by using a fluorescent dye, MitoTracker Green. Flow cytometric analysis showed that serum did not cause any significant change in mitochondrial mass (Figure 17A), suggesting that the increased respiration was mainly a functional activation of mitochondria instead of an increase of mitochondria biogenesis. Similarly, no significant changes in mitochondrial mass were observed in GSC23 (Figure 17B) and GBM3752 cells (Figure 17C).

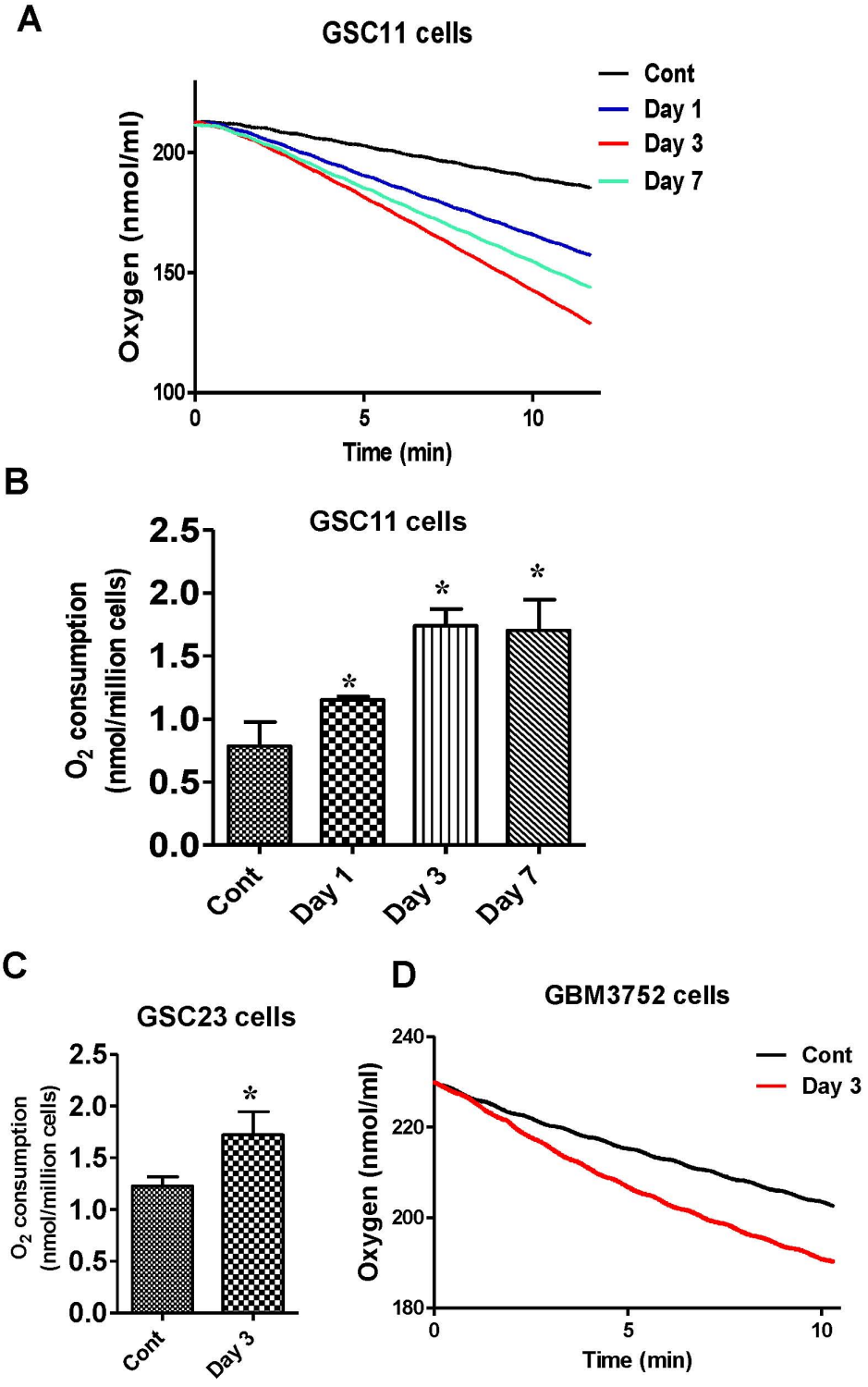
A
GSC11 cells
Cont
Day 1
Day 3
Day 7
Oxygen (nmol/ml)
200
150
100
0
5
10
Time (min)
B
GSC11 cells
O2 consumption (nmol/million cells)
2.5
2.0
1.5
1.0
0.5
0.0
*
*
*
Cont
Day 1
Day 3
Day 7
C
GSC23 cells
O2 consumption (nmol/million cells)
2.5
2.0
1.5
1.0
0.5
0.0
*
Cont
Day 3
D
GBM3752 cells
Cont
Day 3
Oxygen (nmol/ml)
240
220
200
180
0
5
10
Time (min)

Figure 16. Increase of mitochondrial respiration in aberrant differentiated cells. (A) Comparison of oxygen consumption in GSC11 cells before and after exposure to serum for 1, 3 and 7 days. Oxygen consumption was measured using an Oxytherm system as described in Methods. (B) Quantitative analysis of oxygen consumption in GSC11 cells exposed to serum for 1, 3, and 7 days. *, $P<0.01$. (C) Quantitative analysis of oxygen consumption in GSC23 cells exposed to serum for 3 days. *, $P<0.01$. (D) Comparison of oxygen consumption in GBM3752 cells before and after exposure to serum for 3 days.

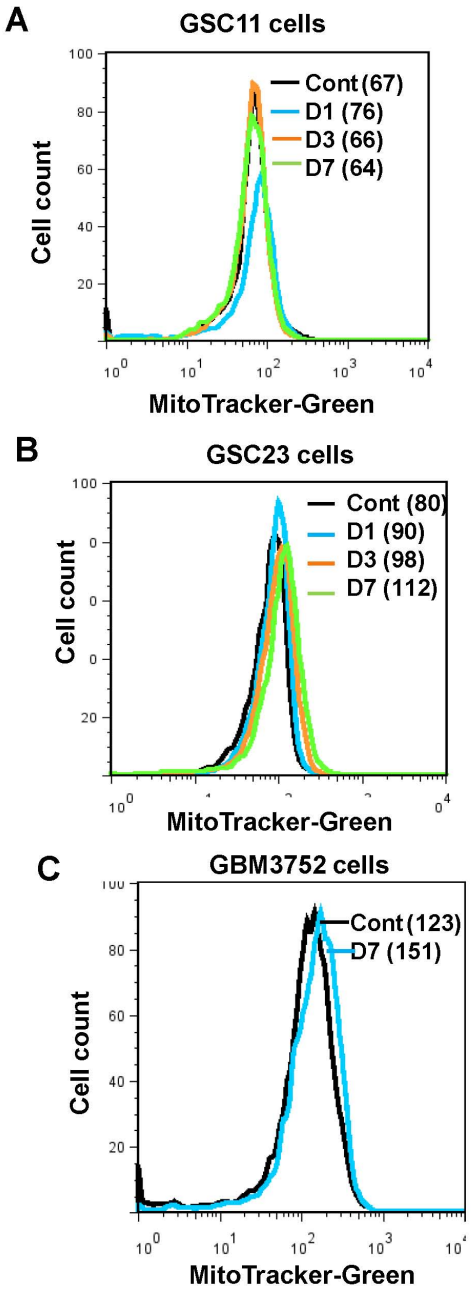

Figure 17. Serum does not induce mitochondria biogenesis. Mitochondrial mass was measured by MitoTracker-Green. No change in mitochondrial mass was found in GSC11 (A), GSC23 (B) and GBM3752 (C) cells after exposed to serum for 1 day (D1), 3 days (D3), or 7days (D7). The numbers in parentheses indicate the median fluorescent values.

CHAPTER 4

ROS mediate GSC differentiation in response to serum induction

Oxidative respiration inhibitor CCCP does not inhibit serum-induced aberrant differentiation.

The effect of carbonyl cyanide m-chloro phenyl hydrazone (CCCP), a mitochondrial uncoupling agent that causes an uncoupling of the proton gradient and reduces ATP synthesis, on aberrant differentiation was tested. Different dosages of CCCP were used to treat the GSC11 cells, which showed that 5μM of CCCP didn't cause much cell death (data not shown). Therefore, 2μM and 5μM of CCCP were used to test its effects on inhibiting the stem cell related gene expression change. 5 μM of CCCP prevented the decrease of CD133 induced by serum in GSC11 cells (Figure 18A), but no inhibition of SOX2 and Olig2 mRNA decreases was found by real-time PCR (Figure 18A). CCCP either didn't inhibit the decrease of SOX2 and increase of ANXA1 caused by serum on protein levels (Figure 18B). We measured the mitochondrial superoxide change in the GSC11 cells treated by CCCP. The results showed that CCCP did not inhibit the mitochondrial superoxide increase in aberrant differentiated cells (Figure 19).

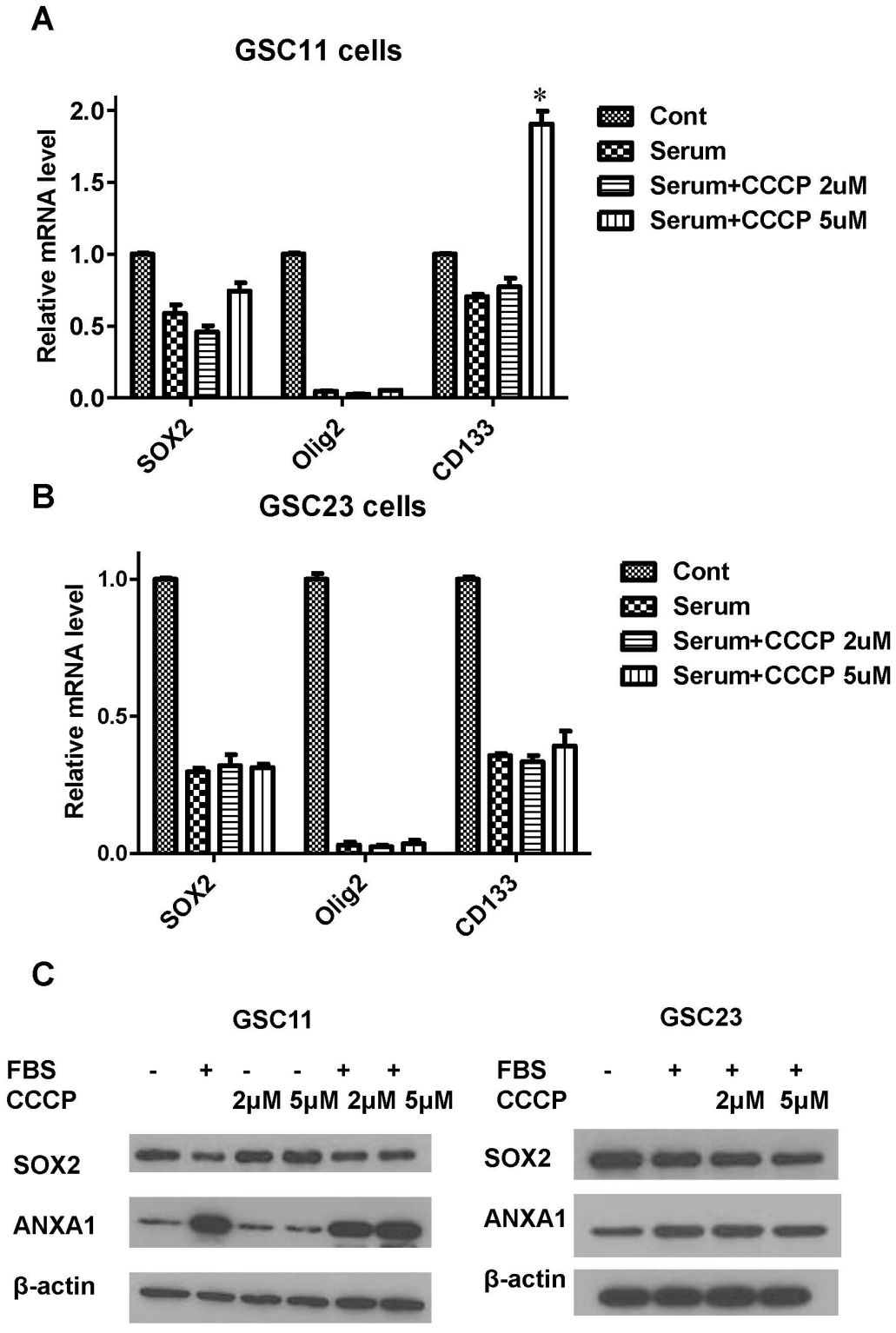
A
GSC11 cells
Relative mRNA level
2.0
1.5
1.0
0.5
0.0
*
SOX2
Olig2
CD133
Cont
Serum
Serum+CCCP 2uM
Serum+CCCP 5uM
B
GSC23 cells
Relative mRNA level
1.0
0.5
0.0
SOX2
Olig2
CD133
Cont
Serum
Serum+CCCP 2uM
Serum+CCCP 5uM
C
GSC11
FBS - + - - + +
CCCP 2μM 5μM 2μM 5μM
SOX2
ANXA1
β-actin
GSC23
FBS - + + +
CCCP 2μM 5μM
SOX2
ANXA1
β-actin

Figure 18. Effects of mitochondrial uncoupler CCCP on the expression of SOX2, Olig2, CD133 and ANXA1. (A) mRNA expression of SOX2, Olig2 and CD133 in GSC11 cells, as measured by quantitative RT-PCR. GSC11 were exposed to serum (5% FBS) for 3 days in the presence and absence of 2μM or 5μM CCCP. *, $p<0.05$. (B) mRNA expression of SOX2, Olig2 and CD133 in GSC23 cells, as measured by quantitative RT-PCR. GSC23 were exposed to serum (5% FBS) for 3 days in the presence and absence of 2μM or 5μM CCCP. *, $p<0.05$. (C) Protein levels of SOX2, Olig2 and CD133 in GSC11 and GSC23 cells, as measured by western blot. GSC11 and GSC23 cells were cultured with or without presence of serum (5% FBS) for 3 days in the presence and absence of 2μM or 5μM CCCP.

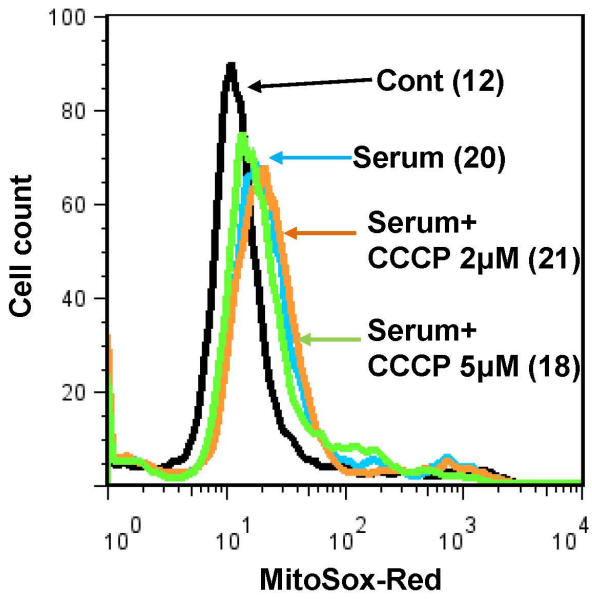

Figure 19. CCCP can't inhibit mitochondrial superoxide increase. Mitochondrial superoxide was measured by flow cytometric analysis after cells were stained with MitoSOX-Red. GSC11 cells were cultured in GSC medium or FBS-containing medium with or without the presence of 2μM or 5μM of CCCP for 1 day.

Compounds increasing mitochondrial superoxide cause CD133 decrease

In order to test whether the activation of mitochondrial function would affect serum induced aberrant differentiation, several mitochondrial electron transport chain inhibitors were used to disrupt mitochondrial function. Mitochondria ETC complex I inhibitor rotenone and complex III inhibitor antimycin were added with serum to the GSCs. Both ETC inhibitors caused an increase of mitochondrial superoxide (Figure 20). Neither of them prevented the GSCs from attaching to the flasks and showing differentiated morphology (Figure 21A). Adding rotenone or antimycin even caused further decreases of CD133 on both mRNA and protein levels (Figure 21B-C).

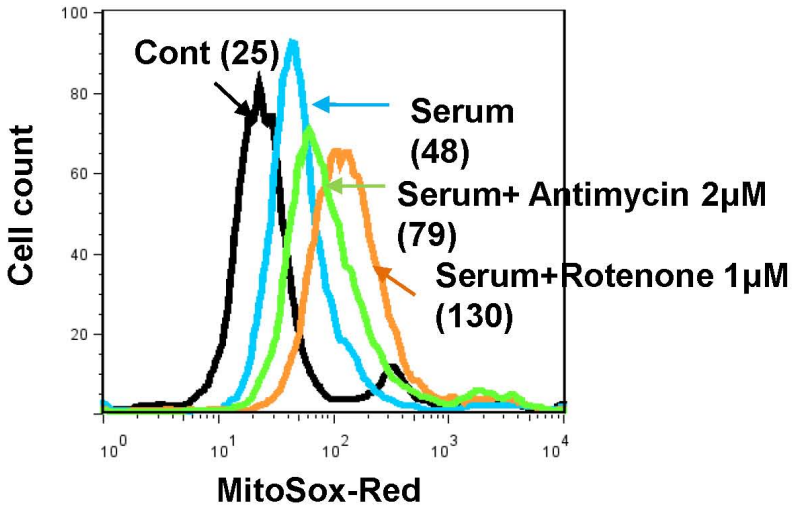

Figure 20. Mitochondrial electron transport chain inhibitors antimycin and rotenone cause increase of mitochondrial superoxide. Mitochondrial superoxide was measured by flow cytometric analysis after cells were stained with MitoSOX-Red. GSC23 cells were cultured in GSC medium or FBS-containing medium with 2μM antimycin or 1μM rotenone.

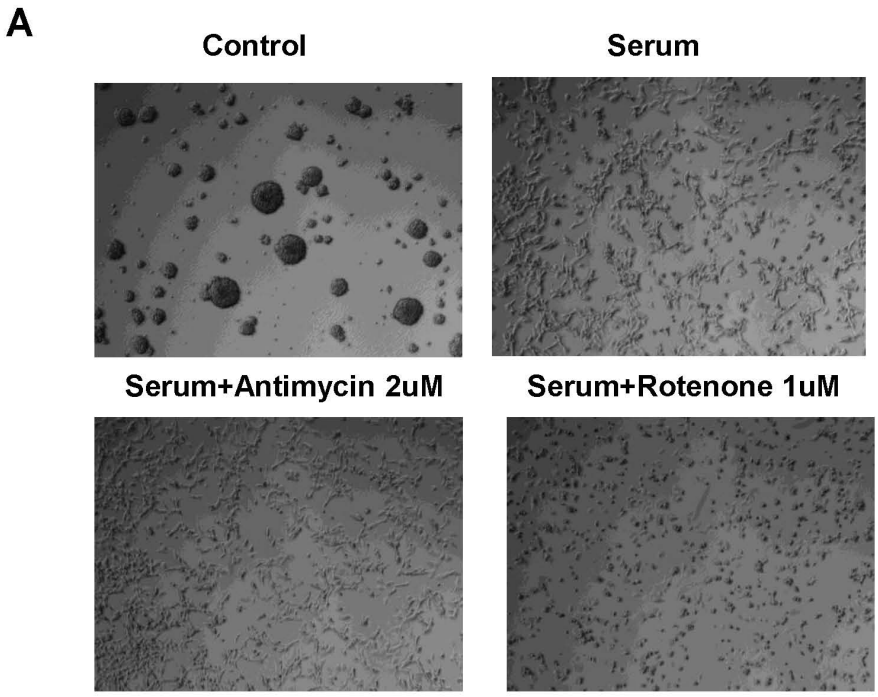
A
Control
Serum
Serum+Antimycin 2uM
Serum+Rotenone 1uM

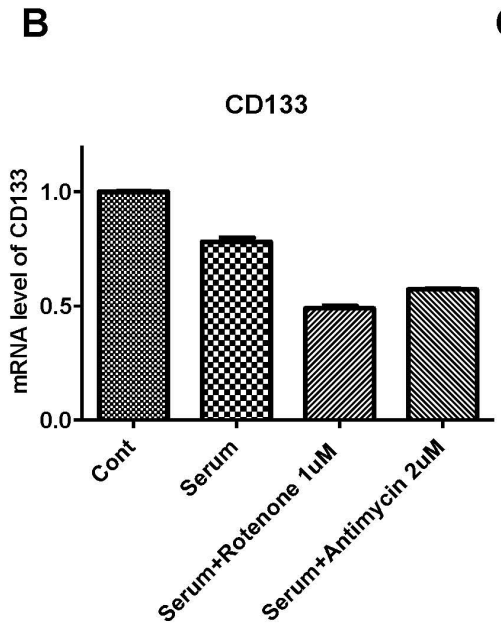
B
CD133
mRNA level of CD133
1.0
0.5
0.0
Cont
Serum
Serum+Rotenone 1uM
Serum+Antimycin 2uM

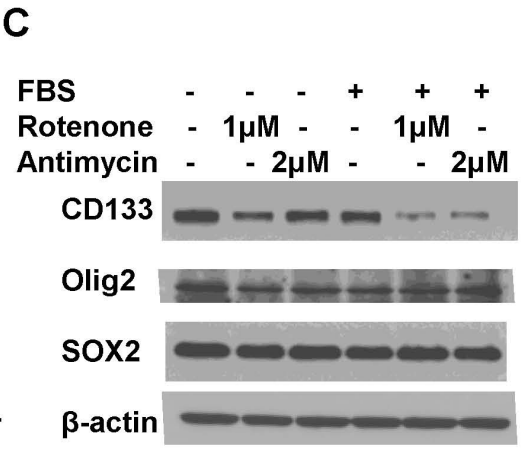
C
FBS - - - + + +
Rotenone - 1μM - - 1μM -
Antimycin - - 2μM - - 2μM
CD133
Olig2
SOX2
β-actin

Figure 21. Antimycin and rotenone cause further decrease of CD133 in serum-induced cells. (A) GSC11 cells were cultured in GSC medium or FBS-containing medium with 2μM antimycin or 1μM rotenone. (B) mRNA levels of CD133 were measured by real-time PCR after GSC23 cells were cultured in GSC medium or FBS-containing medium with 2μM antimycin or 1μM rotenone. (C) GSC23 cells were cultured in GSC medium or FBS-containing medium with or without the presence of 2μM antimycin or 1μM rotenone. Protein levels of CD133 were measured by western blot.

H_2O_2 causes the stem cell markers gene expression decrease

Exposure of GSCs to serum caused an increase in mitochondrial respiration and O_2^- generation. However, neither the mitochondria ETC inhibitors (rotenone and antimycin) nor the oxidative phosphorylation inhibitor (CCCP) prevented the stem cell markers decrease or differentiation marker increase. Rotenone and antimycin caused further increase of mitochondrial superoxide and induced further CD133 decreases. Therefore, it seems mitochondrial ROS instead of the activation of mitochondria itself plays an important role in aberrant differentiation. I further tested the potential role of ROS increase in serum-induced differentiation by using hydrogen peroxide. H_2O_2 caused a similar increase of mitochondrial ROS as serum did in GSC11 and GSC23 cells (Figure 22A-B). The short-term treatment of H_2O_2 led to significant decreases of SOX2, Olig2 and CD133 mRNA expression in GSC11 cells (Figure 22C). Similarly, the short-term treatment of H_2O_2 caused significant decreases of SOX2 and CD133 mRNA expression in GSC23 cells (Figure 22D).

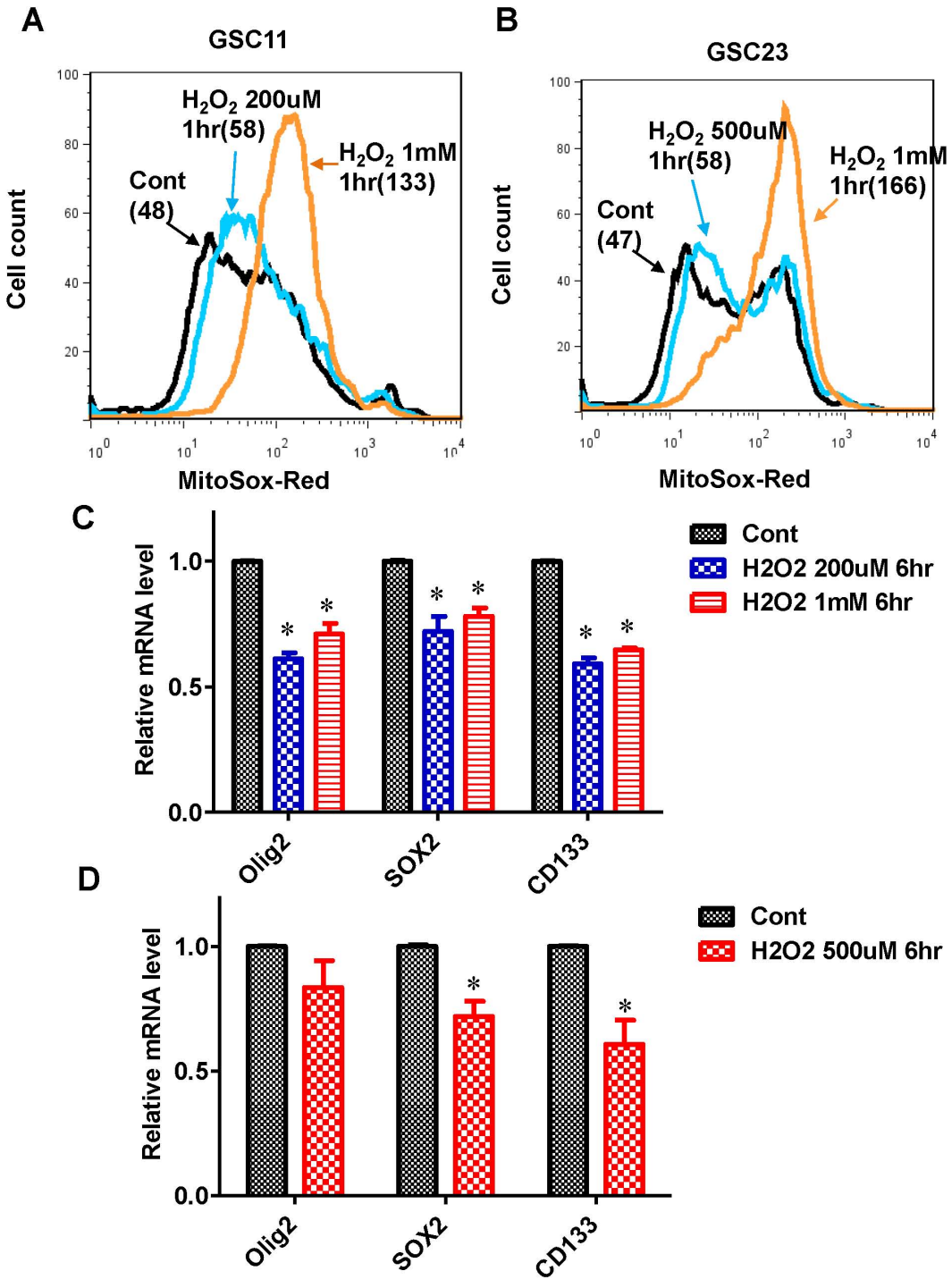
A
GSC11
Cell count
MitoSox-Red
Cont
(48)
H2O2 200uM
1hr(58)
H2O2 1mM
1hr(133)
B
GSC23
Cell count
MitoSox-Red
Cont
(47)
H2O2 500uM
1hr(58)
H2O2 1mM
1hr(166)
C
Relative mRNA level
Olig2
SOX2
CD133
Cont
H2O2 200uM 6hr
H2O2 1mM 6hr
D
Relative mRNA level
Olig2
SOX2
CD133
Cont
H2O2 500uM 6hr

Figure 22. Hydrogen peroxide causes mitochondrial superoxide increase and decreases of Olig2, SOX2 and CD133. (A) Mitochondrial superoxide was measured by flow cytometric analysis before or after GSC11 cells were treated with 200μM or 1mM of H_2O_2 for 1 hour. (B) Mitochondrial superoxide was measured by flow cytometric analysis before or after GSC23 cells were treated with 500μM or 1mM of H_2O_2 for 1 hour. (C) mRNA expression of SOX2, Olig2 and CD133 in GSC11 cells, as measured by quantitative RT-PCR. GSC11 were treated with 200μM or 1mM H_2O_2 for 6 times with 1 hour intervals. *, $p<0.05$. (D) mRNA expression of SOX2, Olig2 and CD133 in GSC23 cells, as measured by quantitative RT-PCR. GSC23 were treated with 500μM or for 6 times with 1 hour intervals. *, $p<0.05$.

Antioxidant NAC prevents the serum-induced differentiation

N-Acetyl-Cysteine (NAC), a precursor for glutathione synthesis with potent antioxidant property capable of reducing various types of ROS stress, was used to prevent the increase of mitochondrial O_2^- in serum-treated GSCs. As shown in Figure 23A, incubation of GSC11 cells with serum for 7 days caused a significant increase of mitochondrial O_2^-, and 20μM of NAC effectively suppressed such ROS increase. Similar results were obtained from GSC23 cells (Figure 23B).

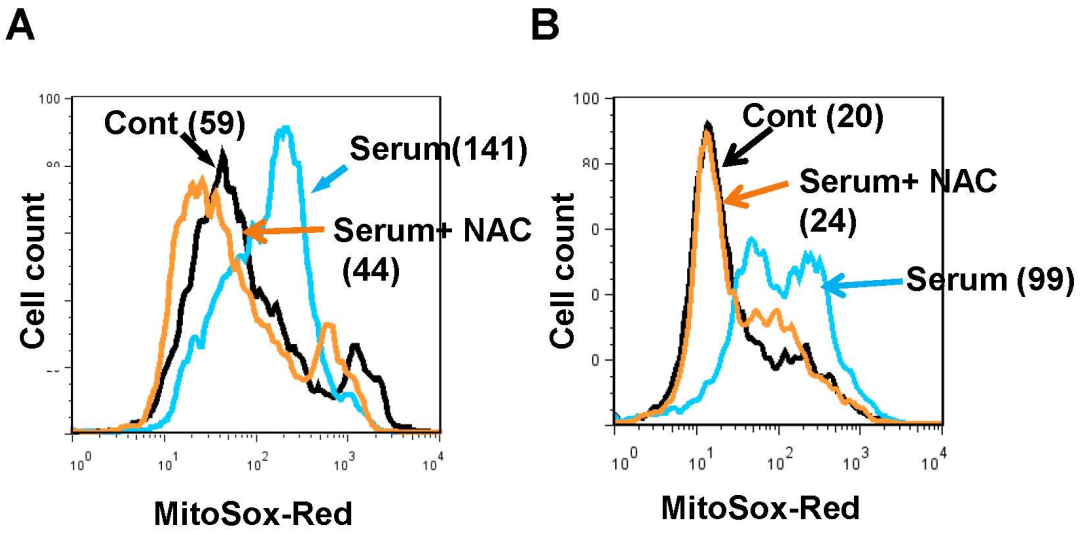

Figure 23. NAC suppresses serum-induced mitochondrial superoxide increase. Mitochondrial superoxide was detected by flow cytometry after cells were stained with MitoSox-Red. (A) GSC11 cells were cultured in serum-containing medium with or without the presence of 20mM NAC for 7 days. (B) GSC23 cells were cultured in serum-containing medium with or without the presence of 20mM NAC for 7 days.

Importantly, NAC was able to prevent serum-induced differentiation and keep the GSC11 cells in stem-like neurospheres (Figure 24A), and to preserve the expression of CD133 in GSC11 cells (Figure 24B), suggesting that the increase in mitochondrial superoxide might play an important role in mediating serum-induced GSC differentiation.

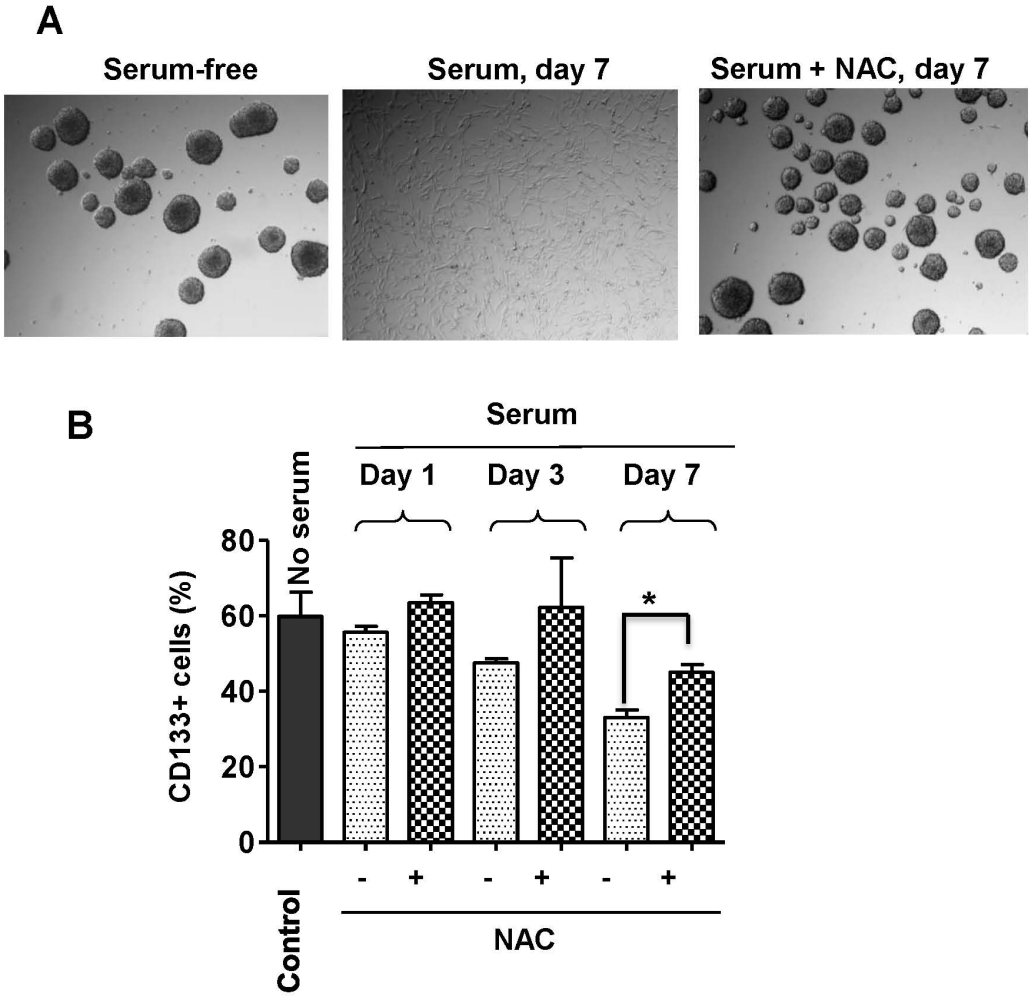

Figure 24. NAC prevents serum-induced aberrant differentiation. (A) Comparison of neurosphere formation in GSC11 cells cultured in serum-containing medium in the presence and absence of 20 mM NAC for 7 days. (B) NAC suppressed serum-induced loss of CD133 expression. GSC23 cells were exposed to serum for 1, 3, or 7 days in the presence or absence of 20 mM NAC as indicated, and CD133-possitive cells were measured by flow cytometric analysis.*, $P<0.05$.

Since there was a significant decrease in expression of SOX2, Olig2, and Notch1 during serum-induced differentiation, we tested if NAC could suppress serum-induced differentiation by preventing the down-regulation of these molecules important for stem cell maintenance. As shown in Figure 25A, quantitative RT-PCR revealed that addition of NAC to the serum-treated GSC11 cells largely prevented the decrease of SOX2 and Olig2 expression, suggesting that the expression of these two molecules might be redox-sensitive. Similar results were also observed in another glioblastoma stem line GSC23 (Figure 25B). Furthermore, gene expression analysis of molecules involved in the Notch pathway revealed that serum caused a significant decrease in the expression of Notch1, MFNG, LFNG, HES5, DTX3, and DLL1 in GSC11 cells (Figure 25C). The presence of antioxidant NAC largely prevented the down regulation of the Notch-related genes (Figure 25C), suggesting that cellular redox status might play a major role in Notch signaling.

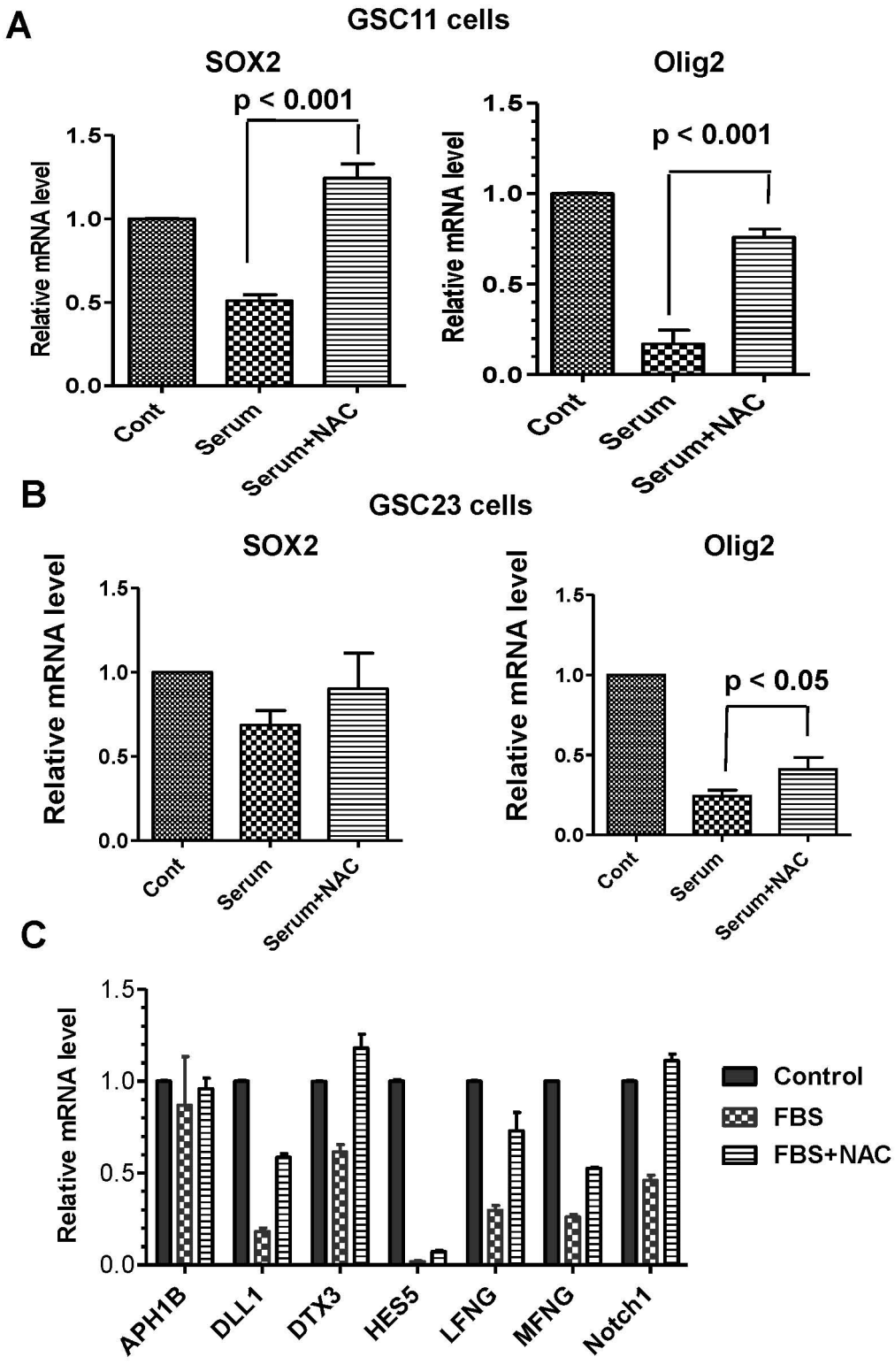
A
GSC11 cells
SOX2
p < 0.001
Relative mRNA level
1.5
1.0
0.5
0.0
Cont
Serum
Serum+NAC
Olig2
p < 0.001
Relative mRNA level
1.5
1.0
0.5
0.0
Cont
Serum
Serum+NAC
B
GSC23 cells
SOX2
Relative mRNA level
1.5
1.0
0.5
0.0
Cont
Serum
Serum+NAC
Olig2
p < 0.05
Relative mRNA level
1.5
1.0
0.5
0.0
Cont
Serum
Serum+NAC
C
Relative mRNA level
1.5
1.0
0.5
0.0
APH1B
DLL1
DTX3
HES5
LFNG
MFNG
Notch1
Control
FBS
FBS+NAC

Figure 25. Effect of antioxidant NAC on the expression of SOX2, Olig2 and Notch pathway. Antioxidant NAC suppressed serum-induced down regulation of SOX2 and Olig2 mRNA expression in GSCs, as measured by quantitative real-time PCR. GSC11 (A) and GSC23 (B) were exposed to serum (5% FBS) for 3 days in the presence and absence of 20 mM NAC. The expression of SOX2 and Olig2 messenger RNA in each sample was measured by quantitative RT-PCR. (C) Antioxidant NAC suppressed serum-induced down regulation of the notch pathway. GSC11 cells were incubated with serum (5%FBS) for 3 days in the presence or absence of 20 mM NAC. RNA was isolated from each sample and the expression of molecules involved in notch signaling was measured by quantitative real-time PCR.

Serum induction activates NFκB pathway

ROS seems to play an important role in mediating serum-induced differentiation. In order to clarify the possible mechanism of how mitochondrial ROS change causes the GSC differentiation, we analyzed the data of microarray and searched for significantly altered gene expressions in aberrant differentiated cells. A ROS regulating signaling, NFκB pathway seems to be a possible candidate. Its downstream targets CD44, IL8, IL11, Cyclin D1, TFP12 and PLAUR were significantly up-regulated in the aberrant differentiated cells (Table 5). We assayed the NFκB pathway by western blot and found phosphorylated IκBα and phosphorylated p65 were increased in serum-induced aberrant differentiated cells on day three in both GSC11 and GSC23, indicating the activation of NFκB pathway after serum induction (Figure 26).

Table 5. NFκB pathway downstream targets expression in the microarray analysis. The mRNA expression signal of GSC11 cells cultured in serum-free medium and 5%FBS-containing medium for 1, 3 and 7 days. P value was calculated by t-test based on the mRNA expression values. CD44-4, CD44 transcript variant 4; CD44-5, CD44 transcript variant 5; IL-8, interleukin 8; IL-11, interleukin 11; PLAUR, plasminogen activator urokinase receptor; TFP12, tissue factor pathway inhibitor 2.

	Average Value of Triplicate				p Value		
	Cont	**D1**	**D3**	**D7**	**Cont vs D1**	**Cont vs D3**	**Cont vs D7**
CD44 -4	6.39	11.97	10.72	12.79	9.55E-08	6.16E-07	7.61E-08
CD44-5	5.66	7.90	7.72	10.02	0.000149	6.61E-05	8.96E-08
IL-11	5.75	7.77	7.10	8.16	8.80E-05	0.000715	3.62E-05
Cyclin D1	11.52	12.79	12.34	12.21	1.07E-06	1.51E-06	0.000248
TFPI2	6.58	8.7	8.53	8.67	7.74E-05	1.11E-06	0.000336
IL-8	5.61	6.29	5.68	7.23	8.66E-05	0.090	9.85E-05
PLAUR	6.04	6.04	6.66	7.29	0.99	0.00037	0.000118

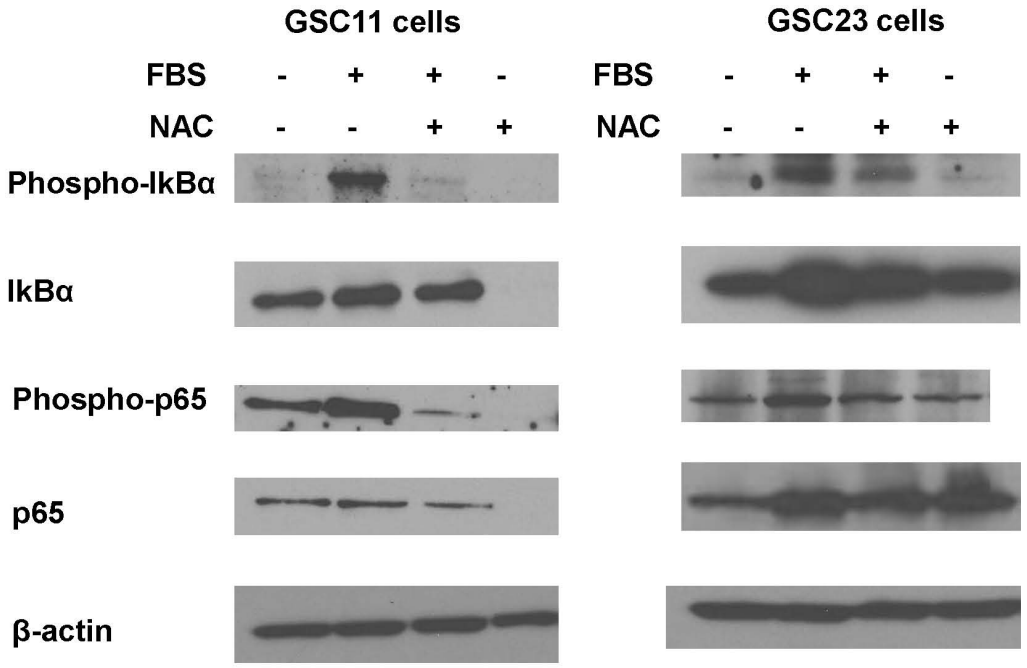

Figure 26. NFκB pathway activation by serum-induction. Protein samples were obtained from GSC11 and GSC23 cells cultured in serum-free or serum-containing medium in the presence or absence of 20mM NAC for 3 days. The protein expression of phospho-IKBα, IKBα, phosphor-p65, p65 and β-actin was assayed by western blot.

Inhibition of NFκB pathway prevents CD133 decrease and ANXA1 increase.

An IKK inhibitor, BMS-345541 was used to inhibit the activation of NFκB signaling in GSC11 cells. The western blot results showed the inhibition of NFκB pathway in serum-induced cells in a dose-dependent manner (Figure 27). 10 μM and 20 μM of BMS-345541 prevented the decrease of CD133 and inhibited the ANXA1 increase (Figure 27).

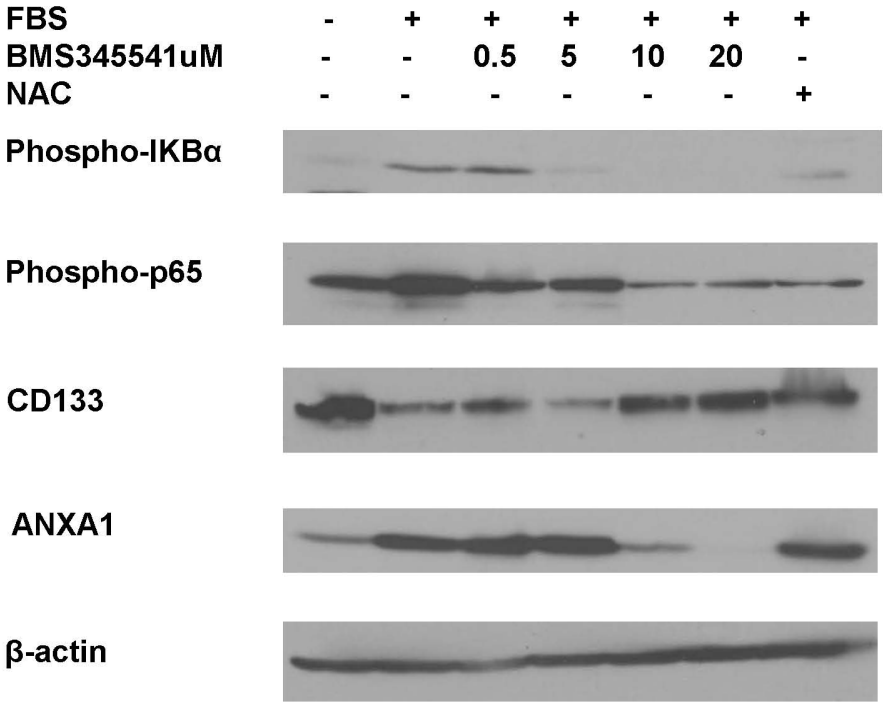

Figure 27. IKK inhibitor BMS-345541 prevents CD133 decrease and ANXA1 increase. GSC11 cells were cultured in serum-free or serum-containing medium with different dose of BMS345541 or 20mM of NAC. Cells were collected after 3 days and the expression of phospho-IKBα, phosphor-p65, CD133, ANXA1 and β-actin was assayed by western blot.

Serum induction promotes tumorigenesis and malignancy in vivo

In order to test the effect of serum induction on tumor formation, we cultured the GSC11 cells under different conditions for 7 days and inoculated the same number of cells subcutaneously into the right flank of nude mice. Interestingly, the mice inoculated with serum-induced cells all formed tumors (Figure 28A). However, only 2 out of 7 mice treated with cells cultured in serum-free medium (the control group) formed tumors. There were 4 mice in the NAC group and 5 mice in the serum plus NAC group formed tumors. The overall survival of the control group was significantly higher than the serum induction group, with a p value 0.0019 (Figure 28B). No significant difference of overall survival was found between the control group and NAC or serum plus NAC group.

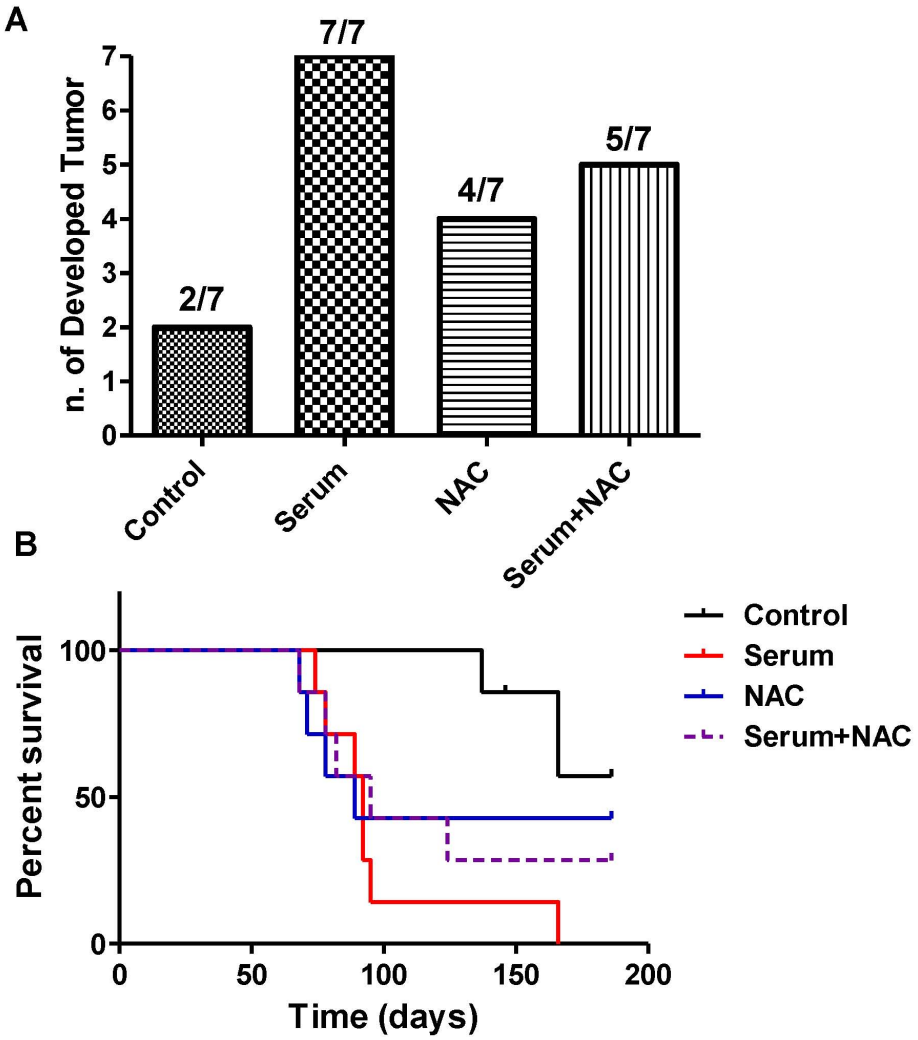

Figure 28. Serum induction increases tumorigenicity and malignancy in GSCs. GSC11 cells were cultured under serum-free medium or serum-containing medium in the presence of absence of 20mM NAC for 7 days. $2X10^6$ cells were inoculated subcutaneously into the right flank of each nude mouse. (A) Number of mice with visible tumors in each group. (B) Survival curves for the mice in each group. The mice were euthanized when the tumor diameter was greater than 20 mm.

CHAPTER 5

Targeting metabolism with 3-BrOP and BCNU in GSCs

GSCs exhibit high glycolytic activity and resistance to TMZ and BCNU but sensitivity to glycolytic inhibition.

GSC11 and GSC23 were cultured in the serum-free stem cell culture medium supplemented with EGF and bFGF. Under these culture conditions, the GSCs exhibited relatively low mitochondrial respiration as evidenced by a low oxygen consumption rate (Figure 29A). When the cells were induced to undergo differentiation by exposure to serum, mitochondrial respiration was substantially activated leading to approximately 90% increase in oxygen consumption after 20 days (Figure 29A), accompanied by a decrease in lactate production (Figure 29C) and a significant decrease in glycolytic index (Figure 29D). This data suggests the GSCs maintained in their stem stage had a low mitochondrial respiration and high glycolytic activity, and serum induction activated mitochondrial oxidative phsophorylation and reduced the need of glycolysis for energy production.

When GSC11 and GSC23 cells were treated with TMZ and BCNU for 72 hours, two drugs commonly used in the treatment of glioblastoma, the cells showed resistance to these conventional chemotherapeutic drugs. The MTS assay demonstrated that GSCs were more resistant to TMZ and BCNU under hypoxic conditions than under normoxic conditions (Figure 30). In contrast, GSCs were also sensitive to 3-BrOP under hypoxic conditions, with the similar or lower 50% inhibitory concentrations than those under normoxic conditions. These data are consistent with the observation that GSCs had low mitochondrial function and thus were more dependent on glycolysis, which was inhibited by 3-BrOP, a derivative of the alkylating agent 3-bromopyruvate known to inhibit two major glycolytic enzymes hexokinase II and GAPDH (74, 86, 187, 188).

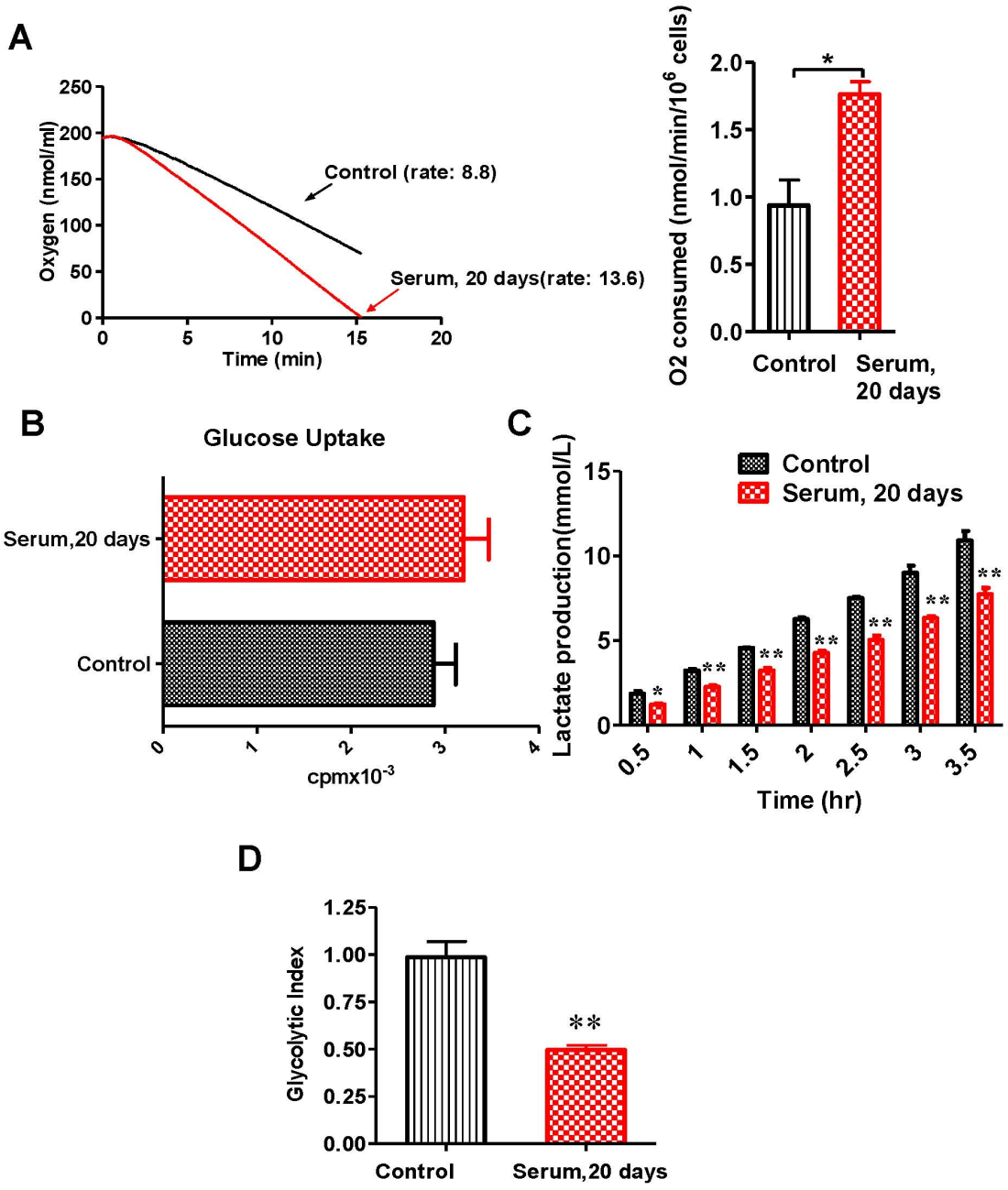
A
Oxygen (nmol/ml)
250
200
150
100
50
0
0
5
10
15
20
Time (min)
Control (rate: 8.8)
Serum, 20 days(rate: 13.6)
O2 consumed (nmol/min/10^6 cells)
2.0
1.5
1.0
0.5
0.0
*
Control
Serum, 20 days
B
Glucose Uptake
Serum,20 days
Control
0
1
2
3
4
cpmx10^-3
C
Lactate production(mmol/L)
15
10
5
0
Control
Serum, 20 days
0.5
1
1.5
2
2.5
3
3.5
Time (hr)
D
Glycolytic Index
1.25
1.00
0.75
0.50
0.25
0.00
Control
Serum,20 days

Figure 29. Serum induction causes decrease of glycolysis. (A) Comparison of oxygen consumption in GSC11 cells before and after exposure to serum for 20 days. Oxygen consumption was measured using an Oxytherm system as described in Methods. *, $P<0.05$. (B) Comparison of glucose uptake in GSC11 cells before and after exposure to serum for 20 days. (C) Lactate generation rates in GSC11 cultured in GSC medium and in serum-containing medium for 20 days. *, $P<0.05$; **, $P<0.01$. (D) Comparison of glycolytic index in GSC11 cells and serum-induced differentiated cells. **, $P<0.01$. Glycolytic index was calculated according to the formula $(L \times G)/O$, in which L is the cellular lactate production, G is the glucose uptake, and O is the oxygen consumption rate.

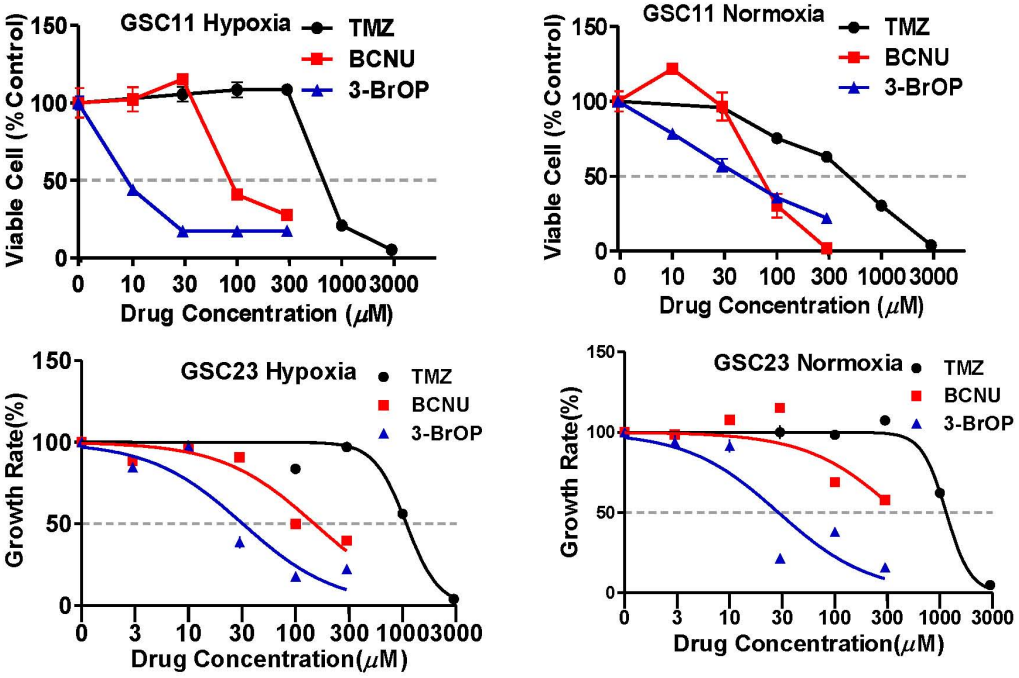

Figure 30. GSCs are resistant to chemotherapeutic agents but sensitive to glycolytic inhibitor 3-BrOP. Sensitivity of GSCs to TMZ, BCNU, and 3-BrOP under hypoxic and normoxic conditions. GSC11 or GSC23 cells were incubated with the indicated concentrations of drugs for 72 h, and cell viability was measured by MTS assay.

Combination of 3-BrOP and BCNU shows synergistic effect in killing GSCs, especially under hypoxic conditions

We then tested if a combination of 3-BrOP with BCNU or TMZ can lead to more effective killing of GSCs, based on the postulation that 3-BrOP would deplete the cellular ATP by inhibiting glycolysis and thus impair the ability of cells to repair DNA damage induced by BCNU or TMZ. The results showed that 3-BrOP substantially potentiates the killing effect of BCNU but not TMZ, especially under hypoxic conditions (Figure 31A-C). Treatment with the combination of 10 μM 3-BrOP and 50 μM BCNU inhibited cell growth by 50% in GSC11 cells (Figure 31A) and GSC23 cells (Figure 31B), whereas treatment with either drug alone only slightly inhibited cell growth. We further confirmed the synergistic killing effect of the 3-BrOP and BCNU combination using annexin-V/PI staining. Most GSC11 cells were killed after 24 hours of treatment with 200 μM BCNU in combination with 15 μM 3-BrOP, whereas we did not observe significant cell death with treatment with either drug alone (Figure 31C). Similar results were also observed in GSC23 cells (Figure 33A). The combination index (CI), which was calculated according to various concentrations of 3-BrOP and BCNU treatments (Table 6), was between 0.701~0.979, suggesting a synergistic effect (CI<1) of BCNU and 3-BrOP. The cell-death pattern was primarily necrosis, which suggests that the ATP-dependent apoptosis process was hampered due to ATP depletion induced by 3-BrOP. The synergistic killing effects of BCNU and 3-BrOP were more dramatic in hypoxia than in normoxia, as GSCs were more dependent on glycolysis for ATP generation under hypoxia. This finding suggests that 3-BrOP could be an effective therapeutic agent to target GSCs in hypoxic tissue environments.

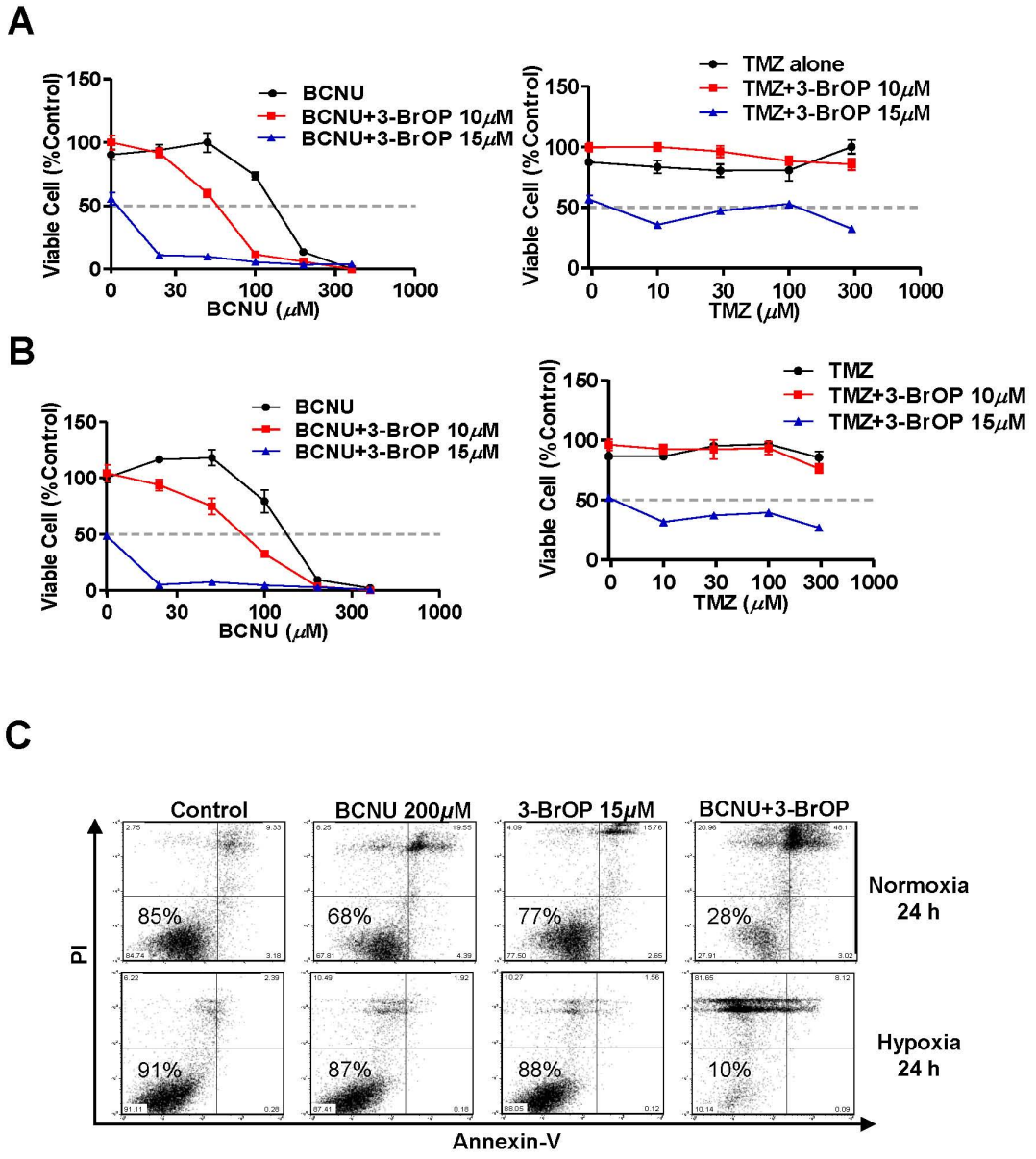

Figure 31. Effective killing of glioblastoma stem cells by combination of 3-BrOP and BCNU. (A) Inhibition of GSC11 cells by BCNU (left panel), TMZ (right panel), or their combination with 3-BrOP (72 h MTS assay under hypoxic conditions). **(B)** Inhibition of GSC23 cells by BCNU (left panel), TMZ (right panel), or their combination with 3-BrOP (72 h MTS assay under hypoxic conditions). **(C)** Induction of cell death in GSC11 cells treated with BCNU, 3-BrOP, or their combination. Cell were incubated with the indicated concentrations of compounds for 24 h under normoxic and hypoxic conditions, and cell viability was measured using annexin-V/PI double staining followed by flow cytometric analysis.

Table 6. 3-BrOP and BCNU have synergistic effect in killing GSCs. CI was calculated using Calcusyn software, according to the results of flow cytometric analysis in GSC11 cells treated with BCNU, 3-BrOP alone or in combination for 24 hours in hypoxic conditions.

Combination Index (CI) of BCNU and 3-BrOP

BCNU(μM)	3-BrOP(μM)	CI
100	10	0.979
100	15	0.780
100	20	0.883
200	10	0.701
200	15	0.710
200	20	0.789

In vitro clonogenicity is considered as an indicator of the tumor-initiating capability of cancer cells in vivo. To assess the drug effect on clonogenicity of GSCs, we treated them with BCNU and 3-BrOP alone or in combination for 3 hours and then evaluated their clonogenicity using a neurosphere-forming assay. The neurosphere-formation ability of GSCs decreased slightly when treated with 50μM BCNU or 15μM 3-BrOP alone. However, combination of both compounds almost completely abolished the ability of GSCs to form neurospheres (Figure 32A). The quantitation of the spheres is shown in Figure 32B. These results indicate that GSCs underwent irreversible loss of ability to form spheres despite a short-term combination treatment (BCNU and 3-BrOP) followed by a period of drug-free incubation to allow for potential recovery.

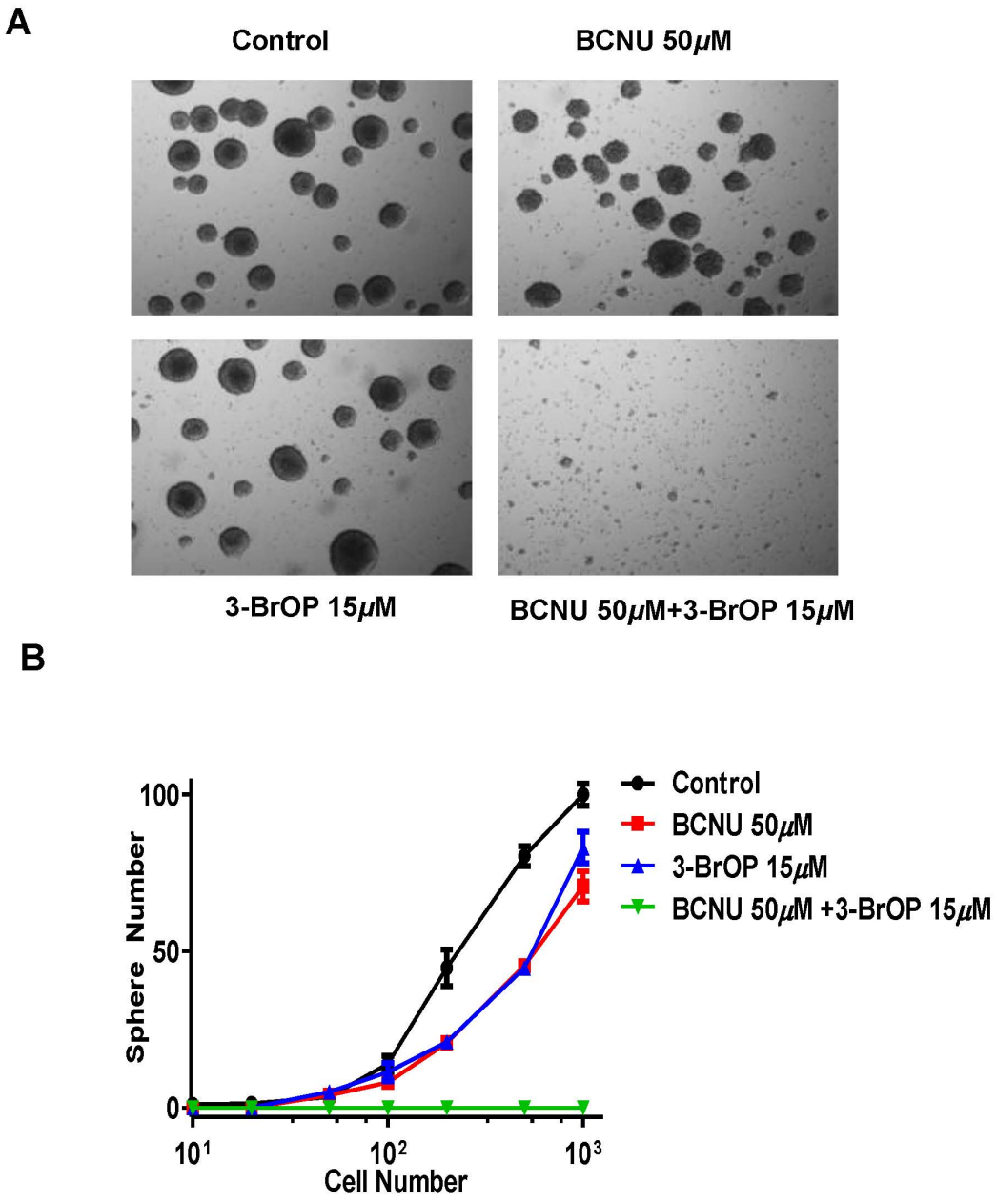

Figure 32. Effect of BCNU, 3-BrOP, or their combination on neurosphere formation in GSCs. Pictures and quantitation of GSC11 neurospheres after incubated with the indicated concentration of drugs for 3 hours, and then cultured in drug-free stem cell medium for 3 weeks.

3-BrOP in combination with BCNU preferentially kills tumor cells with relatively low toxic effect on normal human astrocytes

Since 3-BrOP inhibit the glycolytic pathway, and cancer cells, especially GSCs, are more dependent on this metabolic pathway to generate ATP, we hypothesized that inhibition of glycolysis by 3-BrOP would preferentially deplete ATP in GSCs and other cancer cells, but the non-malignant cells such as normal human astrocytes (NHAs) would be less sensitive to such inhibition. Indeed, as shown in Figure 33, a combination of sub-toxic concentrations of 3-BrOP and BCNU synergistically killed GSC23 cells (Figure 33A), the serum-induced GSC11 cells (Figure 33B), and the human glioma cell line U87 cells which were maintained in serum-containing conditions (Figure 33C). However, this drug combination caused only minimum cytotoxicity in the immortalized NHAs (Figure 33D). These observations suggest that normal human cells are fundamentally different from malignant cells in their energy metabolism and sensitivity to glycolytic inhibitor, and thus provide a therapeutic window for selectivity.

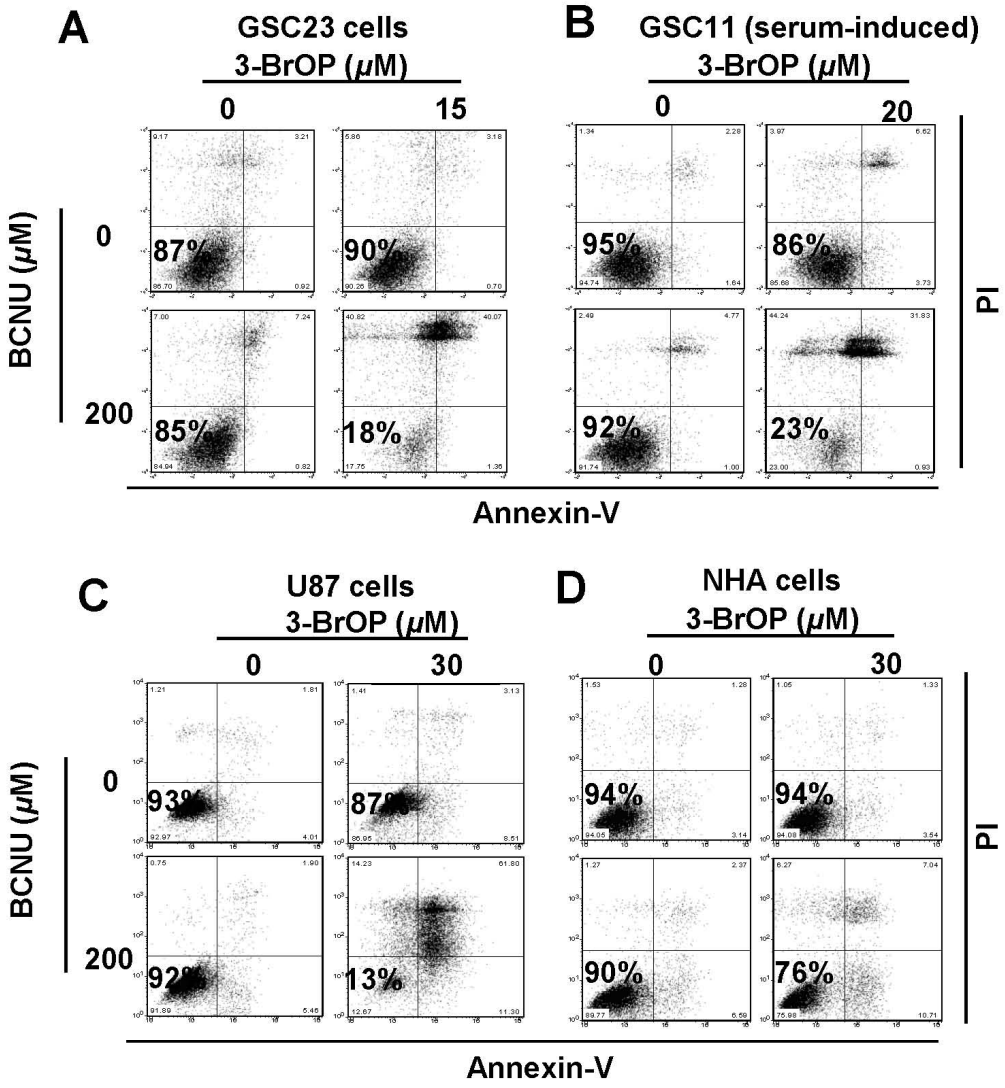

Figure 33. Preferential killing of glioblastoma cells by 3-BrOP and BCNU. The cytotoxic effect of 3-BrOP, BCNU, or their combination was compared in **(A)** GSC23 cells**, (B)** serum-induced GSC11 cells, **(C)** U87 glioma cells, and **(D)** the normal human astrocytes (NHA). Cells were incubated with the indicated drugs for 24 h under hypoxia, and cell viability was measured by annexin-V/PI double staining followed by flow cytometric analysis.

Severe depletion of cellular ATP by 3-BrOP and BCNU in GSCs prior to cell death

Based on the observations that GSCs were highly dependent on glycolysis for ATP generation, we hypothesized that inhibition of glycolysis by 3-BrOP would severely deplete ATP in GSCs. We first tested the effect of 3-BrOP or its combination with BCNU on glycolysis in GSCs, using lactate production as an indicator of glycolytic activity. As shown in Figure 34A, a 3-hour incubation of GSC11 cells with 100-200 μM BCNU or 15-20μM 3-BrOP alone caused only slight inhibition of lactate production, and the combination of these two compounds showed significant inhibition (Figure 34A), leading to a substantial decrease of cellular ATP by more than 50% (Figure 34B). A prolonged incubation with both compounds for 6 hours in hypoxia led to massive depletion of ATP (Figure 34C). It is worth noting that incubation with 200 μM BCNU or 15 μM caused a slight reduction of ATP by 10% and 30%, respectively, while the combination of these two compounds led to more than 90% ATP depletion (Figure 34C). Similar effect of 3-BrOP and BCNU in causing ATP depletion was also observed in GSC23 (Figure 34D). Interestingly, incubation of GSC cells with TMZ did not cause any significant change in ATP, and this compound did not enhance the ability of 3-BrOP to induce ATP depletion (Figure 35). This might explain why treatment of GSCs with 3-BrOP plus TMZ did not show any enhancement of cytotoxicity. Flow cytometric analysis of cell viability showed that GSC cells treated with 3-BrOP plus BCNU remained largely viable at both the 3-hour and 6-hour time points (Figure 34E), suggesting that the observed ATP depletion was an early event and was not a consequence of cell death.

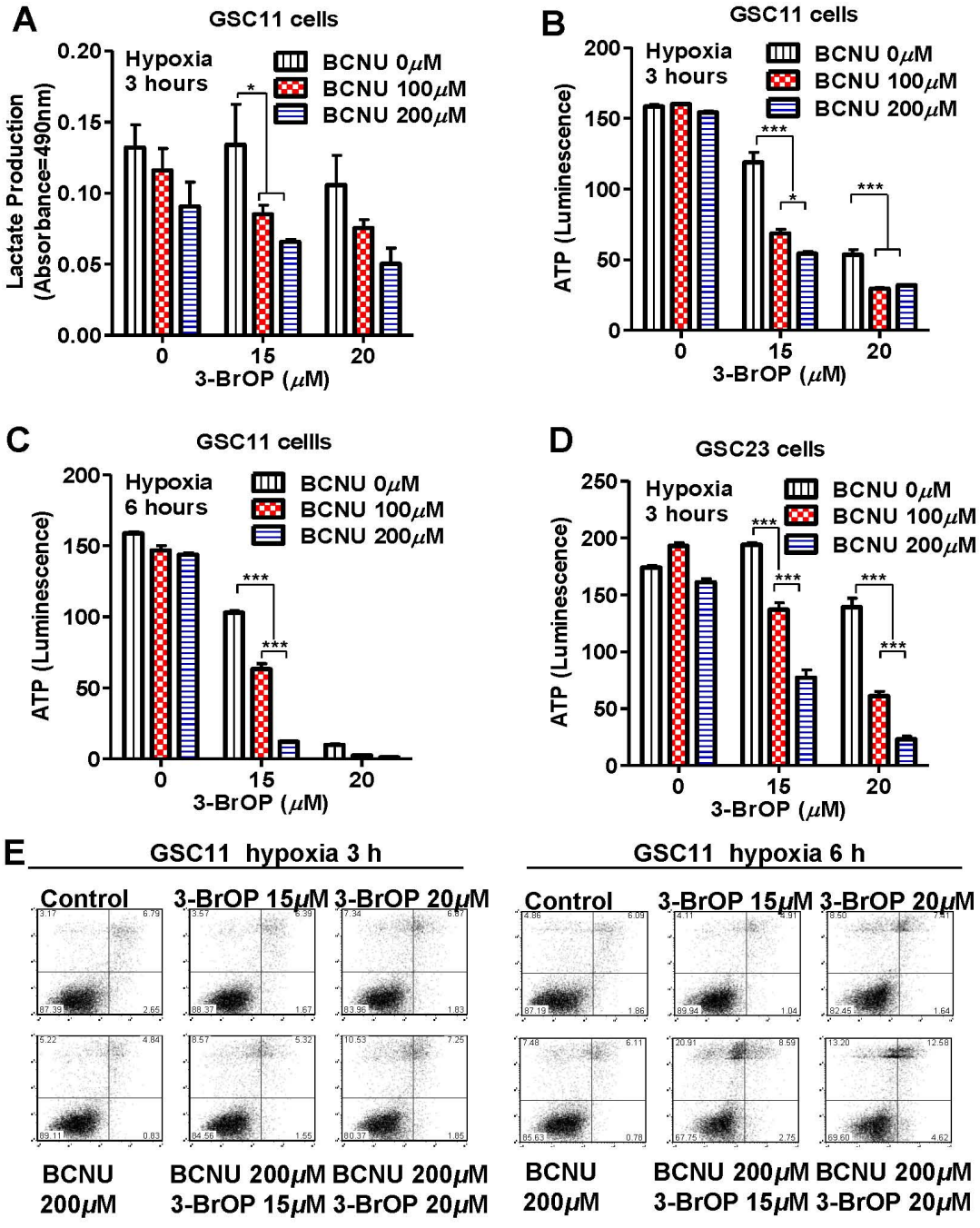
A
GSC11 cells
Hypoxia
3 hours
BCNU 0μM
BCNU 100μM
BCNU 200μM
Lactate Production
(Absorbance=490nm)
0.20
0.15
0.10
0.05
0.00
0
15
20
3-BrOP (μM)
B
GSC11 cells
Hypoxia
3 hours
BCNU 0μM
BCNU 100μM
BCNU 200μM
ATP (Luminescence)
200
150
100
50
0
***
*
***
0
15
20
3-BrOP (μM)
C
GSC11 cellls
Hypoxia
6 hours
BCNU 0μM
BCNU 100μM
BCNU 200μM
ATP (Luminescence)
200
150
100
50
0
***
***
0
15
20
3-BrOP (μM)
D
GSC23 cells
Hypoxia
3 hours
BCNU 0μM
BCNU 100μM
BCNU 200μM
ATP (Luminescence)
250
200
150
100
50
0
***
***
***
***
0
15
20
3-BrOP (μM)
E
GSC11 hypoxia 3 h
Control
3-BrOP 15μM
3-BrOP 20μM
BCNU 200μM
BCNU 200μM
3-BrOP 15μM
BCNU 200μM
3-BrOP 20μM
GSC11 hypoxia 6 h
Control
3-BrOP 15μM
3-BrOP 20μM
BCNU 200μM
BCNU 200μM
3-BrOP 15μM
BCNU 200μM
3-BrOP 20μM

Figure 34. Effect of 3-BrOP and BCNU on energy metabolism in glioblastoma stem cells. **(A)** Inhibition of lactate production in GSC11 cells by the indicated concentrations of BCNU and 3-BrOP (3 h, hypoxia). *, $P<0.05$; ***, $P<0.001$. **(B)** ATP depletion in GSC11 cells by the indicated concentrations of BCNU and 3-BrOP for 3 h under hypoxia. **(C)** ATP depletion in GSC11 cells by the indicated concentrations of BCNU and 3-BrOP for 6 h under hypoxia. **(D)** ATP depletion in GSC23 cells by the indicated concentrations of BCNU and 3-BrOP for 3 h under hypoxia. **(E)** Viability of GSC11 cells after incubation with 3-BrOP and BCNU for 3 h or 6 h under hypoxic conditions. Cell viability was measured by annexin-V/PI double staining followed by flow cytometric analysis.

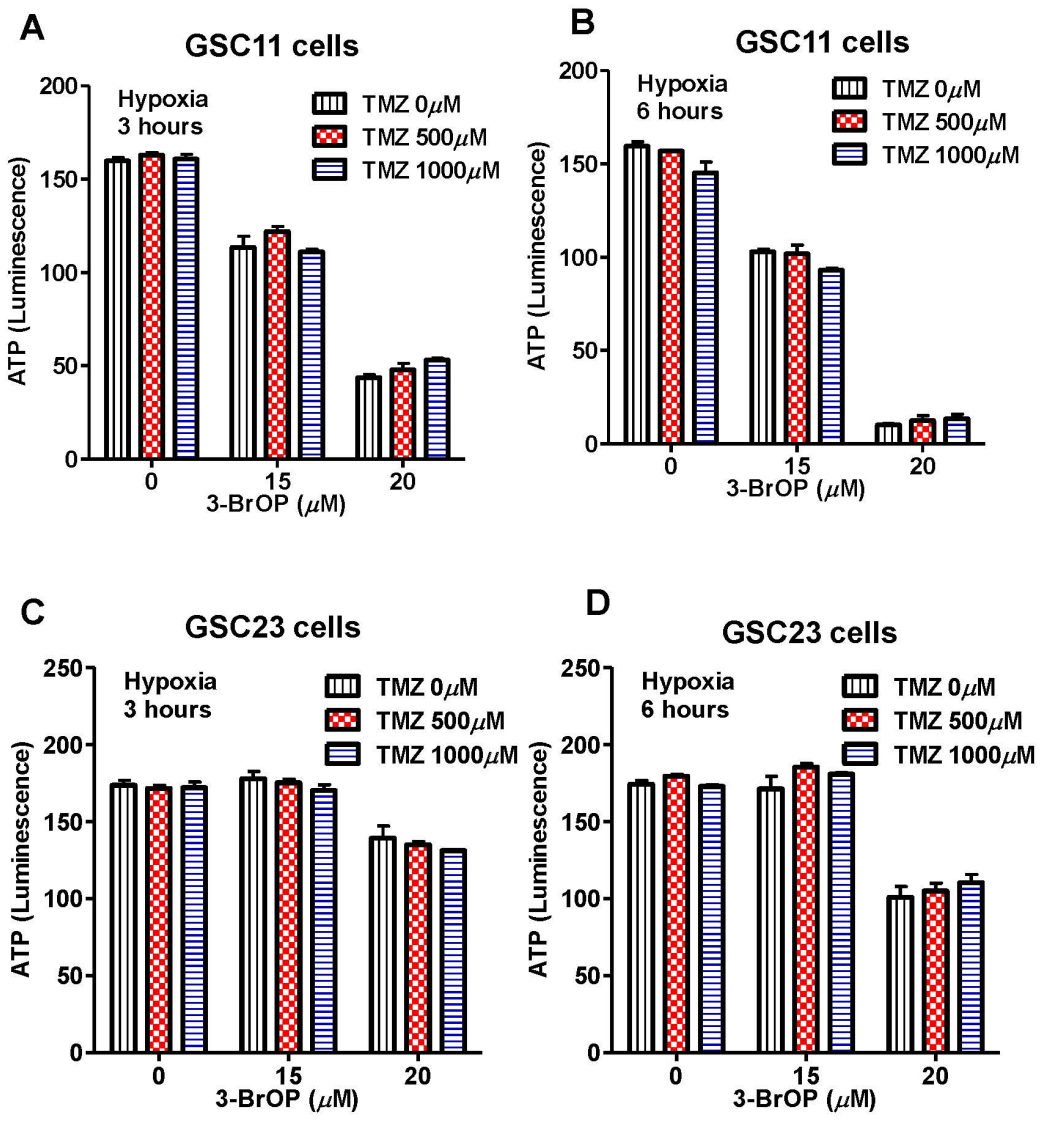

Figure 35. Effect of 3-BrOP and TMZ on ATP generation in glioblastoma stem cells. ATP generation in GSC11 cells by the indicated concentrations of BCNU and TMZ for 3 hours (A) or 6 hours (B) under hypoxia. ATP generation in GSC23 cells by the indicated concentrations of BCNU and TMZ for 3 hours (C) or 6 hours (D) under hypoxia.

Inhibition of GAPDH enzyme activity by BCNU and 3-BrOP

The observation that BCNU but not TMZ was able to potentiate the ability of 3-BrOP to deplete ATP led us to speculate that BCNU might have certain unique mechanism of action different from TMZ. This synergistic killing effect is a unique functional characteristic of BCNU. Since BCNU is known to inhibit glutathione reductase by alkylating its thiolate-active site (189), we speculated that it is possible that this compound might inhibit the glycolytic enzyme GAPDH, which also has potential thiolate-active site for alkylation by BCNU. To test this possibility, we assessed the GAPDH activity of GSCs after treatment with BCNU and 3-BrOP alone and in combination for 30 minutes, and the protein lysates were subjected to the assay for GAPDH activity. Interestingly, treatment with both 3-BrOP and BCNU alone inhibited GAPDH activity by about 60% (Figure 36A), and treatment with the combination of the two inhibited GAPDH activity by almost 80%, which may explain why ATP was depleted dramatically in the combination setting. We further confirmed inhibition of purified GAPDH by BCNU and 3-BrOP at various concentrations using an in vitro enzymatic assay. The concentrations of BCNU and 3-BrOP required to inhibit the purified GAPDH activity by 50% were about 200 μM and 10 μM, respectively (Figure 36B-C). Incubation of purified GAPDH with the combination of BCNU and 3-BrOP in vitro resulted in further inhibition of GAPDH activity (Figure 36D).

Similar to previous studies reported by Pereira da Silva's group(86), we found that hexokinase II is not a prefererd target of 3-BrOP in GSCs. Specifically, we observed that the hexokinase II activity in GSC11 cells treated with 3-BrOP and BCNU at the same concentrations used in our GAPDH activity assay was not effectively inhibited. (Figure 36E).

We performed an in vitro enzymatic assay using purified hexokinase II and confirmed that the same concentrations of 3-BrOP as those used in our GAPDH activity assay could not effectively inhibit hexokinse activity and that concentrations as high as 300μM could inhibit it by only 20% (Figure 36F). We observed no significant differences in the inhibition of purified hexokinase activity in groups of GSCs incubated with BCNU and 3-BrOP alone or in combination at different concentrations in vitro (data not shown).

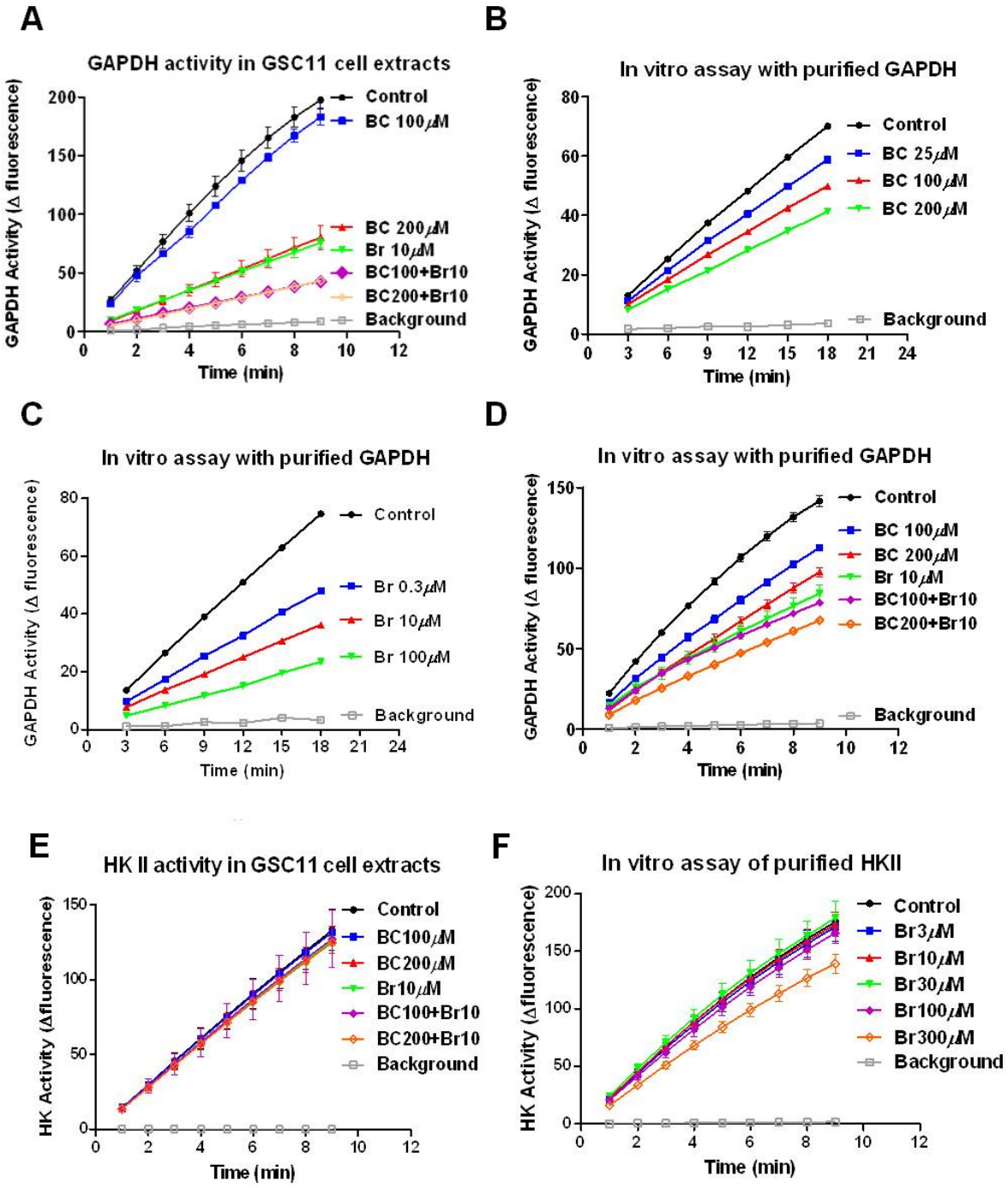
A
GAPDH activity in GSC11 cell extracts
GAPDH Activity (Δ fluorescence)
Time (min)
Control
BC 100μM
BC 200μM
Br 10μM
BC100+Br10
BC200+Br10
Background
B
In vitro assay with purified GAPDH
GAPDH Activity (Δ fluorescence)
Time (min)
Control
BC 25μM
BC 100μM
BC 200μM
Background
C
In vitro assay with purified GAPDH
GAPDH Activity (Δ fluorescence)
Time (min)
Control
Br 0.3μM
Br 10μM
Br 100μM
Background
D
In vitro assay with purified GAPDH
GAPDH Activity (Δ fluorescence)
Time (min)
Control
BC 100μM
BC 200μM
Br 10μM
BC100+Br10
BC200+Br10
Background
E
HK II activity in GSC11 cell extracts
HK Activity (Δfluorescence)
Time (min)
Control
BC100μM
BC200μM
Br10μM
BC100+Br10
BC200+Br10
Background
F
In vitro assay of purified HKII
HK Activity (Δfluorescence)
Time (min)
Control
Br3μM
Br10μM
Br30μM
Br100μM
Br300μM
Background

Figure 36. Inhibition of glyceraldehyde-3-phosphate dehydrogenase (GAPDH) by BCNU and 3-BrOP. (A) Effect of BCNU (BC) and 3-BrOP (Br) on GAPDH enzyme activity in GSC11 cells. Cells were first incubated with the indicated concentrations of BCNU or 3-BrOP for 30 min, and protein extracts were prepared for analysis of GAPDH activity without further addition of the compounds *in vitro*. (B) Inhibition of purified GAPDH enzyme by BCNU *in vitro*. (C) Inhibition of purified GAPDH enzyme by 3-BrOP *in vitro*. (D) Inhibition of purified GAPDH enzyme by combination of BCNU and 3-BrOP *in vitro*. (E) Hexokinase II activity of GSC11 cells after 30min treatment with indicated concentrations of BCNU, 3-BrOP alone and combinations. (F) Enzymatic activity inhibition of purified hexokinase II after 30min in-vitro incubation with serial concentrations of 3-BrOP.

3-BrOP impairs the ability of GSCs to repair BCNU-induced DNA damage

BCNU can cause DNA damage by formation of DNA monoadducts and also cause inter-strand cross-links and double-strand breaks (DSBs) in DNA (190, 191). DSBs are repaired in mammalian cells by nonhomologous end-joining and homologous recombination repair after DNA damage (192), in which γH2AX formation is a rapid, sensitive cellular response to the presence of DSBs (193). Since ATP is required for H2AX phosphorylation and the subsequent complicated DNA repair process, we hypothesized that dramatic depletion of the ATP pool in GSCs could compromise the DNA-repair process, rendering GSCs unable to undergo DNA replication and ultimately leading to cell death. Using a comet assay, we observed that treatment with BCNU alone or combination with 3-BrOP for 6 hours caused severe DNA damage in GSCs, resulting in the appearance of broken DNA as the comet tails after single cell electrophoresis (Figure 37A). In GSCs treated with BCNU alone, the DNA damage could be repaired 3-6 hours after the removal of BCNU, as evidenced by the disappearance or reduction of the DNA tails (Figure 37A-B). However, the GSCs were unable to repair the DNA damage in GSCs treated with the combination of BCNU and 3-BrOP, as the DNA tails persisted after drug removal and the cells were incubated in fresh medium (Figure 37A). In fact, the percentage of DNA in the tails increased from 50% to 60% after 3-hour recovery and to more than 80% after 6-hour recovery in GSCs treated with the drug combination (Figure 37B). Using flow cytometry, we confirmed that the cell death in the combination treatment setting was irreversible even after 18 hours of recovery in fresh medium (Figure 37C).

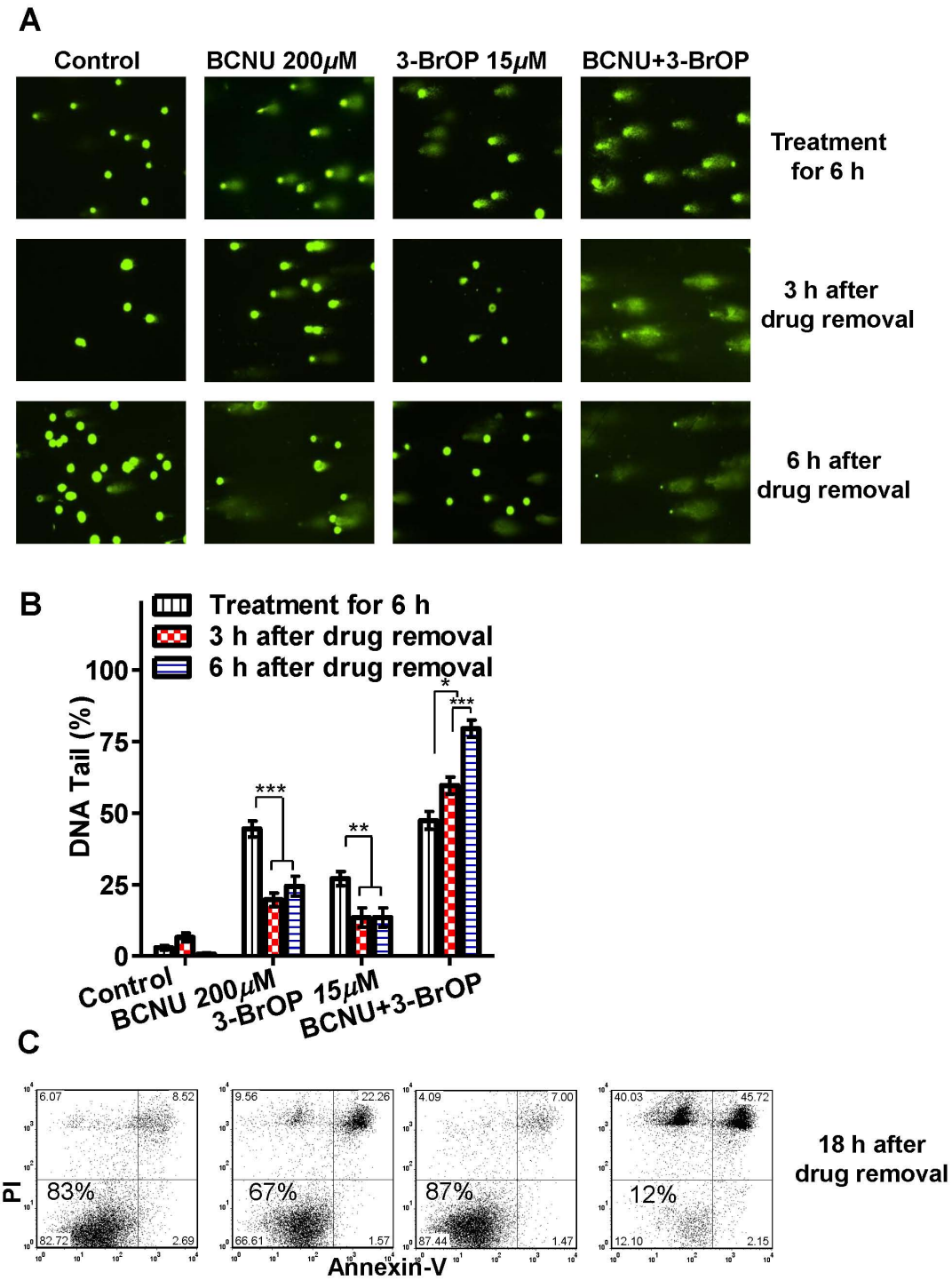
A
Control
BCNU 200μM
3-BrOP 15μM
BCNU+3-BrOP
Treatment for 6 h
3 h after drug removal
6 h after drug removal
B
Treatment for 6 h
3 h after drug removal
6 h after drug removal
DNA Tail (%)
100
75
50
25
0
***
**
*
***
Control
BCNU 200μM
3-BrOP 15μM
BCNU+3-BrOP
C
PI
Annexin-V
6.07
8.52
83%
82.72
2.69
9.56
22.26
67%
66.61
1.57
4.09
7.00
87%
87.44
1.47
40.03
45.72
12%
12.10
2.15
18 h after drug removal

Figure 37. 3-BrOP inhibits the repair of BCNU-induced DNA damage. (A) Comet assay of DNA damage in GSC11 cells treated with BCNU, 3-BrOP, or their combination. Cells were treated with the indicated concentrations of compounds for 6 hours, and then either immediately processed for comet assay or cultured in drug-free medium for additional 3-6 hours for potential DNA repair. The bright green dots represent the positions of cellular nuclei; the "tail" length and intensity and on the right side of each nucleus represent the degree of DNA strand breaks eluted out from the cell during electrophoresis. (B) Quantification of DNA damage in GSC11 cells treated with or without BCNU and 3-BrOp as indicated. At least 30 cells in each sample were quantitatively analyzed for % of DNA tail that eluted from the cellular nuclei. *, $P<0.05$; **, $P<0.01$; ***, $P<0.001$. (C)Flow cytometric analysis (annexin-V/PI staining) was also used to measure cell death at 24 h (18 h after drug removal).

γH2AX is a commonly used marker for DNA DSB repair. Immediately after formation of DSBs, the MRN complex (MRE11, RAD50, and NBS1) binds to broken DNA ends and recruits active ATM, ATR, and/or DNA-PK, resulting in phosphorylation of the subtype of histone H2A, called H2A, in the position of Ser 139 (γH2AX) and initiation of the DNA-repair process (194), and dephosphorylation and removal of γH2AX in the cancer cells has been shown to be a significant step toward turning off the DNA damage response (195). In our study, we observed that when GSCs were incubated with BCNU for 4 hours, both single-agent and combination treatment induced a large increase in γH2AX. When we continuously treated GSCs for 6 hours, we observed that the DNA damage and active repair were ongoing in the BCNU-alone group, whereas it was almost turned off with dephosphorylation of H2AX in the combination group. As shown in Figure 38, the blotting of γH2AX decreased. This was consistent with our results above indicating that maximum ATP pool drainage in GSCs occurred after 6 hours of treatment with the combination of 3-BrOP and BCNU.

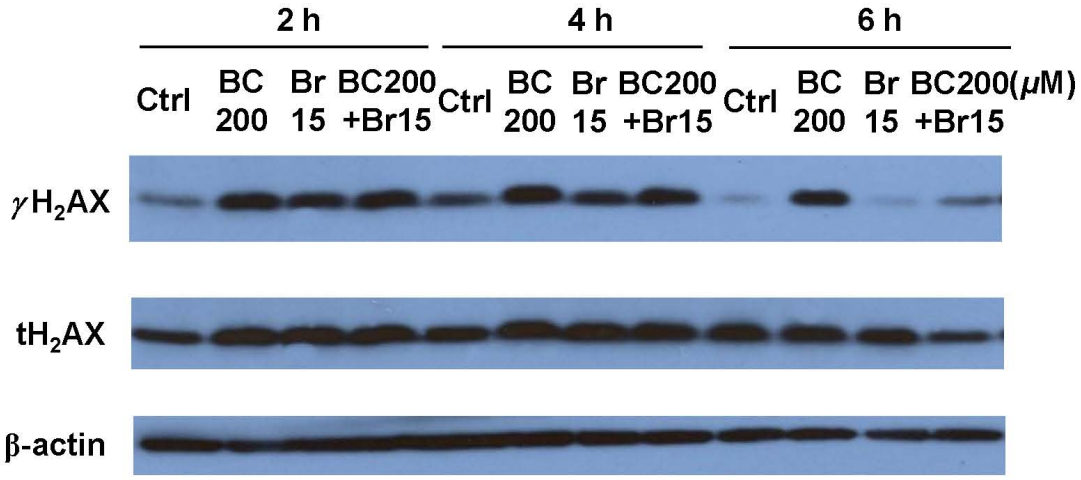

Figure 38. Effect of 3-BrOP and BCNU on H2AX phosphorylation. Western blot analysis of γH_2AX and total H_2AX protein in GSC11 cells treated with the indicated compounds for 2, 4 or 6 hours. BC, BCNU; Br, 3-BrOP.

3-BrOP and BCNU decrease tumorigenicity in vivo.

Since we observed that the combination of 3-BrOP and BCNU completely abolished the ability of GSCs to form neurospheres in vitro, we further tested the effect of 3-BrOP and BCNU on tumorigenicity in vivo by inoculating the cells into mice brain in cooperation with Dr Xiao-nan Li's lab. GSC11 cells were grown in serum-free medium and treated with PBS (control), 20μM of 3-BrOP, 20μM of BCNU and the combination of 3-BrOP and BCNU for 6 hours. The same amount of cells was inoculated into mice brain. All mice in control, 3-BrOP or BCNU group died. But only two out of five mice in the group treated with 20μM 3-BrOP and 20μM BCNU had died (Figure 39). The survival curve showed that the mice in the combination group live significantly longer than the control group (p=0.0027) and the BCNU group (p=0.012).

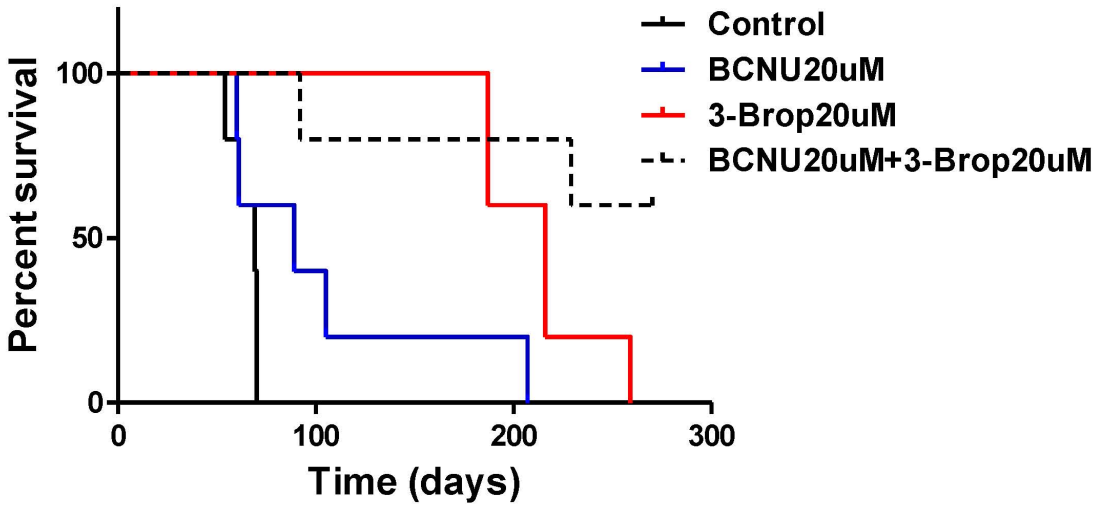

Figure 39. Effect of 3-BrOP and BCNU on mice survival. GSC11 cells were treated with PBS (control), 20μM of 3-BrOP, 20μM of BCNU and the combination of 3-BrOP and BCNU for 6 hours and inoculated orthotopically into mice.

CHAPTER 6

DISSCUSSION

Glioblastoma stem cells are held to be responsible for tumor initiation, progression and recurrence due to resistance to treatments. Therefore, an improved understanding of the mechanisms how GSCs maintain their stemness is crucial for designing new therapeutic strategies for targeting GSCs. This study provided mechanistic and functional evidence that mitochondrial ROS is important in triggering GSCs aberrant differentiation and GSCs rely more on glycolytic metabolism than bulk tumor cells. By treating GSCs with a glycolytic inhibitor 3-BrOP and a standard chemotherapeutic agent, BCNU, we identified a novel therapeutic strategy to kill the GSCs that are resistant to conventional drug.

ROS trigger GSC aberrant differentiation

It has been known for some time that cancer stem cells, similar to normal stem cells, require certain tissue microenvironment to maintain their stemness (76, 196), and exposure of stem cells to serum *in vitro* usually induces differentiation with a loss of self-renewal capacity (94). However, the specific serum factors that induce differentiation and the underlying mechanisms remain unclear. Our study revealed a ROS-mediated mechanism by which serum induces GSC differentiation. We found that exposure of glioblastoma stem cells to serum activated mitochondrial respiration, leading to an increase of oxygen consumption and an increase in generation of mitochondrial O_2^-, which induced the expression of SOD2 to convert O_2^- to H_2O_2. Owing to its relatively long half-life and ability to diffuse across biological membranes, H_2O_2 has been considered as a second messenger that mediates redox-sensitive signaling in cellular response to growth factors (197, 198). The ability of H_2O_2 to cause oxidation of protein thiol via catalytic cysteine can alter the function of the target proteins, and thus provides a mechanism for redox signaling (198).

Since superoxide has an extremely short half-life and cannot pass the mitochondrial membranes, the increased O_2^- within the mitochondria could not directly function as a second messenger to affect the nuclear gene expression. As such, conversion of the mitochondrial O_2^- to H_2O_2 by SOD2 seems important to relay the redox signal from mitochondria to cytosol and nucleus during serum-induced differentiation of GSCs. The upregulation of SOD2 in serum-treated GSCs would facilitate the conversion of O_2^- to H_2O_2.

Previous studies suggest that breast CSCs retain low levels of ROS, which lead to less DNA damage and contribute to their resistance to radiation (46). Drug-tolerant stem-like breast cancer cells show lower levels of ROS and an increase in antioxidant enzymes compared with the parental untreated cells (199). Additionally, tumor sample tissues from patients pre-treated with chemotherapy drugs also show lower levels of ROS and enhanced expression of superoxide dismutase compared with the tumor tissues from patients that don't receive any chemotherapy (199). Our study confirmed that CSCs maintain a low redox status by comparing the GSCs to their aberrant differentiated counterparts. Under serum induction, the GSCs upregulate their mitochondrial ETC function, which triggers the transition of mitochondria from low function into activation and results in an increase of mitochondrial ROS. These results may explain the phenomenon that CSCs have lower ROS than non-stem cancer cells. The correlation between mitochondrial function and the regulation of CSCs has been found in glioma. Inhibition of ETC by a complex I inhibitor rotenone or long-term treatment with low doses of ethidium bromide to deplete mitochondrial DNA (ρ^0 cells) enriched $CD133^+$ cells (83). The ρ^0 cells lacking a functional electron transport chain developed enhanced anchorage-independent growth and increased

invasion phenotypes (83). However, our results showed that the mitochondrial ROS instead of ETC itself is important in triggering serum-induced aberrant differentiation.

Although the ability of ROS to induce stem cell differentiation has been noticed in some experimental systems (200), the exact mechanisms remain unclear. Our study suggests that the down regulation of SOX2, Olig2, and the Notch-related molecules by ROS might be a potential mechanism. Since SOX2, Olig2, and the Notch pathway are involved in promoting neural stem cells function (201, 202), down regulation of these genes would lead to a loss of stemness and promote differentiation. It is possible that the expression of SOX2, Olig2, and the Notch-related molecules are regulated via a redox-sensitive mechanism, with ROS being a negative regulator. The ability of exogenous antioxidant NAC to prevent the decreased expression of these genes and to block the serum-induced differentiation phenotype supports this notion. CSCs may maintain their ROS at a low status through expressing some special molecules. For instance, CD44, a widely used CSC marker, was recently found to contribute to ROS defense by stabilizing a glutamate-cystine transporter, xCT, and promoting the synthesis of GSH (154).

The effects of ROS on the GSC aberrant differentiation are likely mediated by NFκB

NFκB signaling pathway plays a crucial role in cancer development and progression (203). It can either promote or inhibit carcinogenesis, depending on the cell type in which it acts. The NFκB transcription factors are assembled through dimerization of five subunits, namely p65 (RelA), v-rel reticuloendotheliosis viral oncogene homolog B (RelB), c-Rel, p50 (NFκB1) and p52(NFκB2) (204). The five subunits share the same DNA binding domain, Rel homology domain. Prior to cell stimulation, the majority of NFκB subunits are kept in the cytoplasm by a family of proteins called IκBs that prevent NFκB's binding to DNA. Activated IκB kinase (IKK) phosphorylates IκBs and triggers their degradation and the nucleus translocation of NFκB. NFκB signaling pathway is often activated by ROS through IκB or IKK phosphorylation (205). This study found that serum could cause the activation of NFκB which could be blocked by the antioxidant NAC. These results suggest that the activation of NFκB in the serum-induced cells is probably caused by the ROS increase (Figure 40). It's worth noting that deletion of NFκBIA which encodes the NFκB inhibitor IκBα is a frequent oncogenic event in GBM (206). NFκB activation is also involved in the formation of breast cancer stem cells in response to transient activation of Src oncoprotein (207). Our observation that NFκB is activated in glioblastoma-initiating cells after induction of differentiation by FBS was also confirmed by Nogueira et al (208). Since NFκB plays a crucial role not only in neural stem cell differentiation but also in brain cancer stem cells (208, 209), it is probably the signaling pathway which connects serum-induced ROS increase with the aberrant differentiation of glioblastoma stem cells. We have found a selective IKK1 and IKK2 inhibitor BMS-345541 can protect the decrease of a stem cell marker CD133 and prevent the increase of a differentiation marker ANXA1 (210).

However, the underlying mechanism of how NFκB pathway affects GSC differentiation still needs to be further clarified.

Interestingly, although the serum induction caused the aberrant differentiation of GSCs and the decreases of stem cell markers-CD133, SOX2 and Olig2, it led to an increase of tumorigenicity and a reduction of survival in mice. These results seem to jeopardize the conventional theory of cancer stem cells which holds that only CSCs have the ability to form tumor and they will lose the tumorigenicity once going to differentiation. It has been postulated that CSCs preferentially transplant disease and contribute disproportionately to tumor growth compared to more differentiated cells (211). However, a recent study found that tumor cell self-renewal doesn't predict tumor growth potential (211). Glioma cells with low self-renewal capacity were more tumorigenic and generate tumor more rapidly than cells with high self-renewal capacity (211). Our results had similar observations and may provide a mechanistic interpretation of this phenomenon. The role of NFκB pathway in normal stem cell proliferation has been identified. NFκB is stimulated during human embryonic stem cell (hESC) differentiation and inhibition of NFκB leads to a reduction of hESC proliferation and suppression of differentiation toward all primitive extraembryonic and embryonic lineages with the exception of primitive ectoderm and ectodermal lineages (204). Whether the NFκB signaling has a similar role in CSCs still needs to be elucidated.

If NFκB is the crucial pathway in promoting CSCs proliferation and disease progression, targeting NFκB will be effective in eradicating the CSCs. Several studies have shown that targeting NFκB pathway can be effective in killing CSCs (212-214). Inhibition

of NFκB through using compounds including niclosamide and disulfiram can kill AML stem cells and breast CSCs (212, 214).

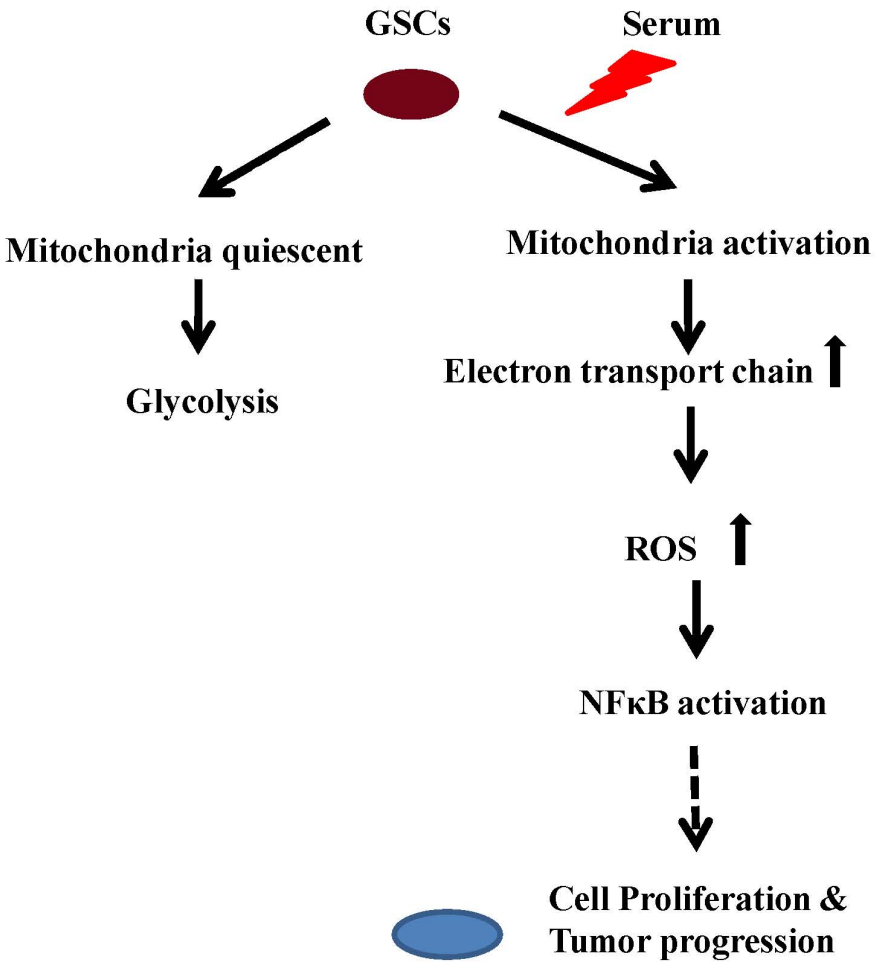

Figure 40. ROS mediates serum-induced aberrant differentiation. GSCs have low mitochondrial function and rely more on glycolysis for energy production. Serum factors trigger the activation of mitochondrial function and electron transport chain, which leads to the ROS increase. The upregulation of ROS causes NFκB activation and results in cell proliferation and tumor progression.

Potential therapeutic importance of inducing differentiation in GSCs

Cancer stem cells or tumor-initiating cells play a major role in drug resistance and disease recurrence owing to their high self-renewal capacity and the ability to repair DNA damage and export cytotoxic compounds (44, 45). The unique biological properties of cancer stem cells render them difficult to be eliminated *in vivo* using conventional therapies. The recognition of the important role of cancer stem cells in drug resistance has prompted recent search for new means to overcome this significant problem in cancer treatment. Because the stemness of cancer cells is critical for cancer development and disease recurrence, induction of cancer stem cell differentiation has been considered as a potential therapeutic strategy (215, 216). For example, all-trans-retinoic acid (ATRA) and arsenic trioxide have been shown to induce differentiation in acute promyelocytic leukemia and turned out to be effective in the treatment of this malignancy (217, 218). ATRA can induce differentiation and reduce tumorigenicity in stem-like glioma cells (219). Thus, identification of the key factors that induce cancer stem cells differentiation and elucidation of the underlying mechanisms could have significant implications in developing novel therapeutic strategies to impact CSCs and to improve the outcomes of cancer treatment. Our study suggests that the cellular redox status may profoundly affect the fates of glioblastoma stem cells, and that modulation of mitochondrial function and ROS generation may be an effective way to impact CSCs. As such, induction of cancer stem cell differentiation by ROS-mediated mechanisms seems to add a new mean to the "radical" therapeutic approaches to cancer therapy (30).

The combination of 3-BrOP and BCNU exhibits a striking synergistic killing effect in GSCs.

In the present study, we observed that GSCs had low mitochondrial respiration. Glycolysis serves as the major energy source for maintenance of CSC metabolism, survival, and self-renewal. An effective agent that targets glycolysis can achieve the goal of eliminating CSCs. A glycolytic inhibitor 3-BrOP shows its efficacy in killing the drug resistant GSCs. We postulated that ATP depletion induced by glycolytic inhibition could cause a severe energy crisis, which could lead to a severe compromise of GSC's ability to repair DNA damage induced by chemotherapeutic agents (Figure 41). However, it seems that it is necessary to deplete ATP to certain level in order to effectively compromise the ability of DNA repair. In GSCs, this severe ATP depletion could be efficiently achieved by combination of 3-BrOP with BCNU, but not with TMZ. This is due to the ability of BCNU and 3-BrOP to inhibit GAPDH activity in a synergistic fashion. This finding raises a potential for use of this drug combination to eliminate GSCs and overcome the resistance of glioblastoma to chemotherapeutic drugs, especially under hypoxic conditions. Almost all GSCs were effectively killed by this combination in 24 hours and a short term exposure to this drug combination that has not shown killing effect in vitro could already reduce GSCs' tumorigenicity and prolong survival in mice.

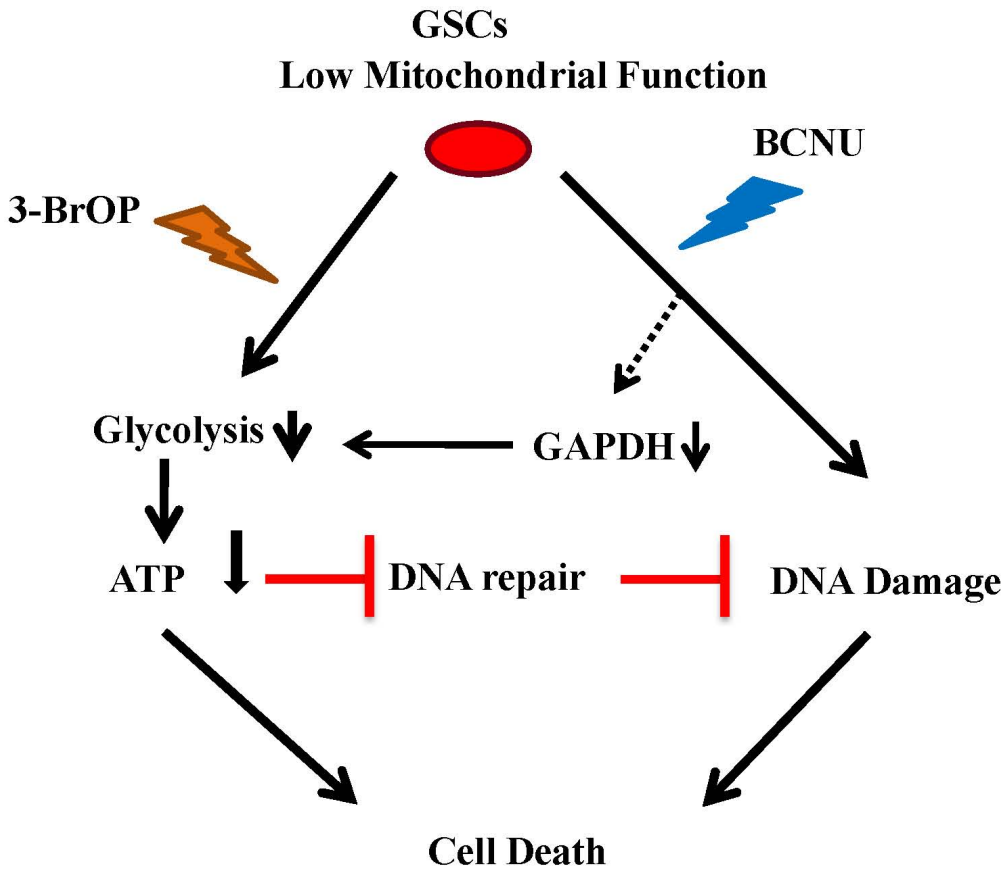

Figure 41. The combination of 3-BrOP and BCNU induces cell death. On one hand, 3-BrOP can cause the decrease of ATP by inhibiting glycolysis and BCNU can induce further decrease of ATP probably through inhibiting GAPDH activity. On the other hand, BCNU causes DNA damage which needs ATP for repairing. While the ATP crisis makes the DNA repair system nonfunctional and results in constant DNA damage and cell death.

Patients with glioblastoma multiforme, the most aggressive primary brain tumor, have poor prognoses, and there have been only limited improvements of therapeutic outcomes and patient overall survival over the past two decades, although multidisciplinary therapies for this cancer are performed (220). GSCs seem to reside in the niches where the cells are in hypoxic microenvironment, which contributes significantly to cancer chemoresistance and radioresistance (221). Although an increase in drug dosage could increase the effective drug concentration in the brain to kill more cancer cells, this may also increase toxic side effect and thus limit its applications. Furthermore, GSCs may adapt quickly to drug treatment by expressing increasing numbers of drug efflux pumps, DNA repair proteins like O^6-methylguanine-DNA methyltransferase, and antiapoptotic proteins. In the case of BCNU, this compound has a very short half-life and the drug become undetectable after 5 minutes of treatment (222). Also, BCNU penetration in the brain tissue occurs over only a very short distance, approximately 2 mm from the ependymal surface (223). Thus, achieving and maintaining effective high concentration of BCNU in the tumor tissue is difficult. For effective and selective killing of cancer cells, especially CSCs, determining the fundamental differences between cancer and normal cells is critically important. For example, the cell energy metabolism pathway has emerged as a potential candidate target for treatment of cancers. Multiple studies have confirmed that nutrient metabolism in cancer cells may be different from that in normal cells. As first proposed by Otto Warburg (157), cancer cells might rely more on glycolysis for metabolism and survival, and the mitochondria in these cells were functionally aberrant.

The observation that BCNU inhibited GAPDH activity is a novel finding of this study, although the primary pharmacological action of BCNU has been traditionally

attributed to its nucleoprotein alkylation and inhibition of DNA synthesis and repair mediated by its active chloroethyl moieties (224). BCNU may covalently inactivate GAPDH activity by S-nitrosylation of cysteine thiols which are important for disulfide formation. Although GAPDH activity can be inhibited by 50% with 200μM BCNU alone, we observed only a moderate depletion of ATP after 6 hours of treatment with BCNU at this concentration. A possible explanation for the small ATP decrease could be that inhibition of glycolysis by BCNU might have been compensated by mitochondrial oxidative phosphorylation. This is in contrast to 3-BrOP, which seems to inhibit both glycolysis and mitochondrial respiration to a certain degree (86, 225, 226). This might explain why 3-BrOP could deplete ATP more efficiently than BCNU when each compound was used alone. Although hexokinase II has been considered a major target of 3-BrPA (174, 227-229), a recent study using HepG2 cells suggested that this compound might inhibit GAPDH activity more effectively (86). It is possible that the synergistic combination effect of 3-BrOP and BCNU observed in the present study might be due, at least in part, to the fact that both compounds inhibit the same glycolytic enzyme GAPDH. The combination of sub-toxic concentrations of 3-BrOP and BCNU seems to be an optimum way to inhibit GAPDH and to achieve effective killing of GSCs with low toxicity to normal cells. This is largely due to the unique mechanisms of action of each compound and the biological properties of GSCs, which are highly dependent on glycolysis and thus sensitive to such metabolic intervention.

Future Perspectives

Many questions regarding the mechanisms of how NFκB pathway leads to serum-induced GSC activation and whether the combination of 3-BrOP and BCNU is effective in vivo remain. We showed that serum could induce the activation of NFκB pathway and NAC was able to inhibit this activation. It is important to test whether the NFκB pathway is crucial for the serum-induced GSC activation. Ideally, key components of NFκB pathway would be knocked down in GSCs and tumorigenicity of the cells would be tested to confirm that the NFκB pathway trigger the GSC activation. Moreover, activators such as interleukin-1 and TNFα would be used to activate the NFκB in GSCs and their effects on tumorigenicity and malignancy would be assayed. Potentially, besides the NFκB activation, the metabolic alteration caused by serum induction is also important in mediating GSC activation. ATP generation and metabolite intermediates as well as cell cycle change promote the malignant transition of GSCs. Alternatively; other pathways like JNK also play some role in GSC activation. These possibilities should be explored in further detail.

Another important question is whether the combination of 3-BrOP and BCNU is effective in vivo. Our results implicate therapeutic potential of the combination treatment. However, whether 3-BrOP can pass the blood brain barrier remains unknown. Implantable pump for drug delivery to the brain would be utilized to study the effect of 3-BrOP and BCNU combination in glioblastoma xenografts. The toxicities of this combination need to be investigated.

Conclusion

My study demonstrates that GSCs have low mitochondrial function and depend on glycolysis for energy production. Activation of mitochondrial by factors like serum causes ROS increase which leads to the induction of differentiation (Figure 42). The transition from glycolysis to oxidative phosphorylation moves GSCs into an intermediate stage and causes tumor proliferation and progression. Targeting the glycolytic metabolism with 3-BrOP and BCNU can achieve a striking killing effect in GSCs.

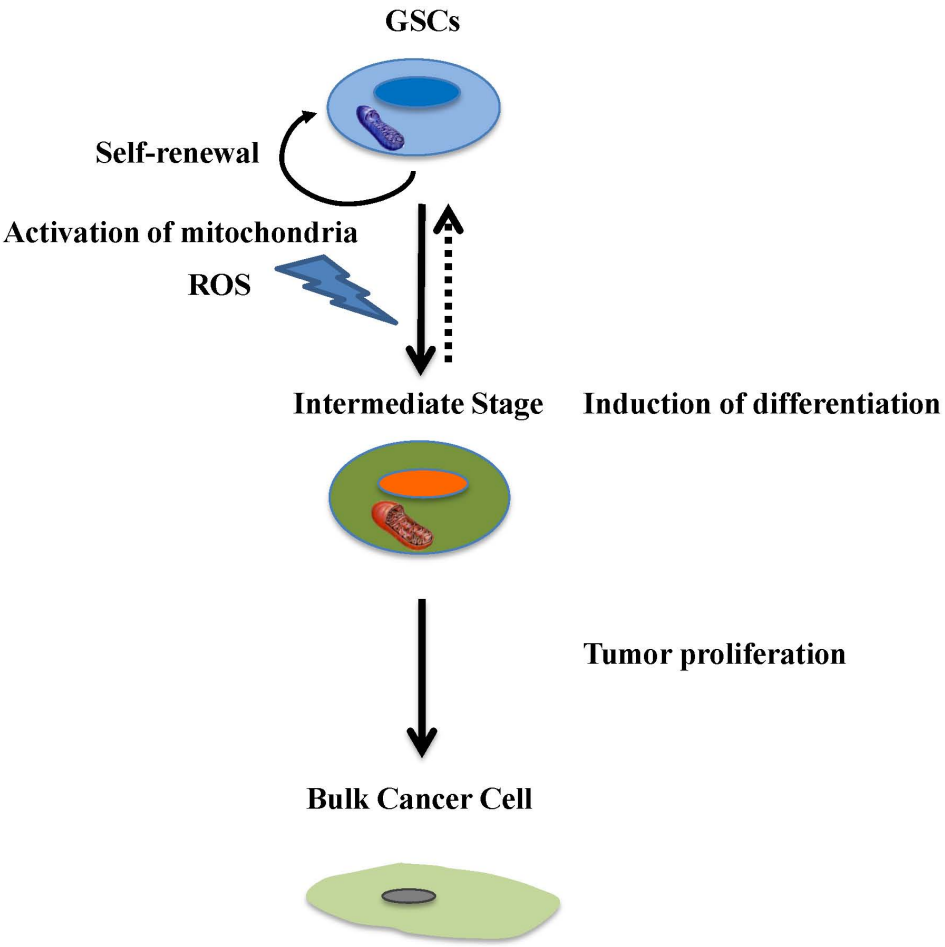

Figure 42. A schematic model representing the role of metabolism change in tumor development.

BIBLIOGRAPHY

1. Reya, T., S. J. Morrison, M. F. Clarke, and I. L. Weissman. 2001. Stem cells, cancer, and cancer stem cells. Nature 414:105-111.
2. Saretzki, G., T. Walter, S. Atkinson, J. F. Passos, B. Bareth, W. N. Keith, R. Stewart, S. Hoare, M. Stojkovic, L. Armstrong, T. von Zglinicki, and M. Lako. 2008. Downregulation of multiple stress defense mechanisms during differentiation of human embryonic stem cells. Stem Cells 26:455-464.
3. Bonnet, D., and J. E. Dick. 1997. Human acute myeloid leukemia is organized as a hierarchy that originates from a primitive hematopoietic cell. Nat Med 3:730-737.
4. Buss, E. C., and A. D. Ho. 2011. Leukemia stem cells. Int J Cancer 129:2328-2336.
5. Lapidot, T., C. Sirard, J. Vormoor, B. Murdoch, T. Hoang, J. Caceres-Cortes, M. Minden, B. Paterson, M. A. Caligiuri, and J. E. Dick. 1994. A cell initiating human acute myeloid leukaemia after transplantation into SCID mice. Nature 367:645-648.
6. Du, X., M. Ho, and I. Pastan. 2007. New immunotoxins targeting CD123, a stem cell antigen on acute myeloid leukemia cells. J Immunother 30:607-613.
7. Moshaver, B., A. van Rhenen, A. Kelder, M. van der Pol, M. Terwijn, C. Bachas, A. H. Westra, G. J. Ossenkoppele, S. Zweegman, and G. J. Schuurhuis. 2008. Identification of a small subpopulation of candidate leukemia-initiating cells in the side population of patients with acute myeloid leukemia. Stem Cells 26:3059-3067.
8. Al-Hajj, M., M. S. Wicha, A. Benito-Hernandez, S. J. Morrison, and M. F. Clarke. 2003. Prospective identification of tumorigenic breast cancer cells. Proc Natl Acad Sci U S A 100:3983-3988.

9. Singh, S. K., I. D. Clarke, M. Terasaki, V. E. Bonn, C. Hawkins, J. Squire, and P. B. Dirks. 2003. Identification of a cancer stem cell in human brain tumors. Cancer Res 63:5821-5828.

10. Pardal, R., M. F. Clarke, and S. J. Morrison. 2003. Applying the principles of stem-cell biology to cancer. Nat Rev Cancer 3:895-902.

11. Visvader, J. E., and G. J. Lindeman. 2008. Cancer stem cells in solid tumours: accumulating evidence and unresolved questions. Nat Rev Cancer 8:755-768.

12. O'Brien, C. A., A. Pollett, S. Gallinger, and J. E. Dick. 2007. A human colon cancer cell capable of initiating tumour growth in immunodeficient mice. Nature 445:106-110.

13. Li, C., D. G. Heidt, P. Dalerba, C. F. Burant, L. Zhang, V. Adsay, M. Wicha, M. F. Clarke, and D. M. Simeone. 2007. Identification of pancreatic cancer stem cells. Cancer Res 67:1030-1037.

14. Patrawala, L., T. Calhoun, R. Schneider-Broussard, H. Li, B. Bhatia, S. Tang, J. G. Reilly, D. Chandra, J. Zhou, K. Claypool, L. Coghlan, and D. G. Tang. 2006. Highly purified CD44+ prostate cancer cells from xenograft human tumors are enriched in tumorigenic and metastatic progenitor cells. Oncogene 25:1696-1708.

15. Ma, S., K. W. Chan, L. Hu, T. K. Lee, J. Y. Wo, I. O. Ng, B. J. Zheng, and X. Y. Guan. 2007. Identification and characterization of tumorigenic liver cancer stem/progenitor cells. Gastroenterology 132:2542-2556.

16. Wicha, M. S., S. Liu, and G. Dontu. 2006. Cancer stem cells: an old idea--a paradigm shift. Cancer Res 66:1883-1890; discussion 1895-1886.

17. Fan, X., W. Matsui, L. Khaki, D. Stearns, J. Chun, Y. M. Li, and C. G. Eberhart. 2006. Notch pathway inhibition depletes stem-like cells and blocks engraftment in embryonal brain tumors. Cancer Res 66:7445-7452.

18. Liu, C. G., Y. Lu, B. B. Wang, Y. J. Zhang, R. S. Zhang, B. Chen, H. Xu, F. Jin, and P. Lu. Clinical implications of stem cell gene Oct-4 expression in breast cancer. Ann Surg 253:1165-1171.

19. Ponti, D., A. Costa, N. Zaffaroni, G. Pratesi, G. Petrangolini, D. Coradini, S. Pilotti, M. A. Pierotti, and M. G. Daidone. 2005. Isolation and in vitro propagation of tumorigenic breast cancer cells with stem/progenitor cell properties. Cancer Res 65:5506-5511.

20. Ginestier, C., M. H. Hur, E. Charafe-Jauffret, F. Monville, J. Dutcher, M. Brown, J. Jacquemier, P. Viens, C. G. Kleer, S. Liu, A. Schott, D. Hayes, D. Birnbaum, M. S. Wicha, and G. Dontu. 2007. ALDH1 is a marker of normal and malignant human mammary stem cells and a predictor of poor clinical outcome. Cell Stem Cell 1:555-567.

21. Matsui, W., C. A. Huff, Q. Wang, M. T. Malehorn, J. Barber, Y. Tanhehco, B. D. Smith, C. I. Civin, and R. J. Jones. 2004. Characterization of clonogenic multiple myeloma cells. Blood 103:2332-2336.

22. Peacock, C. D., Q. Wang, G. S. Gesell, I. M. Corcoran-Schwartz, E. Jones, J. Kim, W. L. Devereux, J. T. Rhodes, C. A. Huff, P. A. Beachy, D. N. Watkins, and W. Matsui. 2007. Hedgehog signaling maintains a tumor stem cell compartment in multiple myeloma. Proc Natl Acad Sci U S A 104:4048-4053.

23. Huang, E. H., M. J. Hynes, T. Zhang, C. Ginestier, G. Dontu, H. Appelman, J. Z. Fields, M. S. Wicha, and B. M. Boman. 2009. Aldehyde dehydrogenase 1 is a marker for normal and malignant human colonic stem cells (SC) and tracks SC overpopulation during colon tumorigenesis. Cancer Res 69:3382-3389.

24. Dalerba, P., S. J. Dylla, I. K. Park, R. Liu, X. Wang, R. W. Cho, T. Hoey, A. Gurney, E. H. Huang, D. M. Simeone, A. A. Shelton, G. Parmiani, C. Castelli, and M. F. Clarke. 2007. Phenotypic characterization of human colorectal cancer stem cells. Proc Natl Acad Sci U S A 104:10158-10163.

25. Lang, S. H., F. M. Frame, and A. T. Collins. 2009. Prostate cancer stem cells. J Pathol 217:299-306.

26. Suetsugu, A., M. Nagaki, H. Aoki, T. Motohashi, T. Kunisada, and H. Moriwaki. 2006. Characterization of CD133+ hepatocellular carcinoma cells as cancer stem/progenitor cells. Biochem Biophys Res Commun 351:820-824.

27. Eramo, A., F. Lotti, G. Sette, E. Pilozzi, M. Biffoni, A. Di Virgilio, C. Conticello, L. Ruco, C. Peschle, and R. De Maria. 2008. Identification and expansion of the tumorigenic lung cancer stem cell population. Cell Death Differ 15:504-514.

28. Ho, M. M., A. V. Ng, S. Lam, and J. Y. Hung. 2007. Side population in human lung cancer cell lines and tumors is enriched with stem-like cancer cells. Cancer Res 67:4827-4833.

29. Prince, M. E., R. Sivanandan, A. Kaczorowski, G. T. Wolf, M. J. Kaplan, P. Dalerba, I. L. Weissman, M. F. Clarke, and L. E. Ailles. 2007. Identification of a subpopulation of cells with cancer stem cell properties in head and neck squamous cell carcinoma. Proc Natl Acad Sci U S A 104:973-978.

30. Hermann, P. C., S. L. Huber, T. Herrler, A. Aicher, J. W. Ellwart, M. Guba, C. J. Bruns, and C. Heeschen. 2007. Distinct populations of cancer stem cells determine tumor growth and metastatic activity in human pancreatic cancer. Cell Stem Cell 1:313-323.

31. Schatton, T., G. F. Murphy, N. Y. Frank, K. Yamaura, A. M. Waaga-Gasser, M. Gasser, Q. Zhan, S. Jordan, L. M. Duncan, C. Weishaupt, R. C. Fuhlbrigge, T. S. Kupper, M. H. Sayegh, and M. H. Frank. 2008. Identification of cells initiating human melanomas. Nature 451:345-349.

32. Zhang, S., C. Balch, M. W. Chan, H. C. Lai, D. Matei, J. M. Schilder, P. S. Yan, T. H. Huang, and K. P. Nephew. 2008. Identification and characterization of ovarian cancer-initiating cells from primary human tumors. Cancer Res 68:4311-4320.

33. Szotek, P. P., R. Pieretti-Vanmarcke, P. T. Masiakos, D. M. Dinulescu, D. Connolly, R. Foster, D. Dombkowski, F. Preffer, D. T. Maclaughlin, and P. K. Donahoe. 2006. Ovarian cancer side population defines cells with stem cell-like characteristics and Mullerian Inhibiting Substance responsiveness. Proc Natl Acad Sci U S A 103:11154-11159.

34. Barker, N., R. A. Ridgway, J. H. van Es, M. van de Wetering, H. Begthel, M. van den Born, E. Danenberg, A. R. Clarke, O. J. Sansom, and H. Clevers. 2009. Crypt stem cells as the cells-of-origin of intestinal cancer. Nature 457:608-611.

35. Kim, C. F., E. L. Jackson, A. E. Woolfenden, S. Lawrence, I. Babar, S. Vogel, D. Crowley, R. T. Bronson, and T. Jacks. 2005. Identification of bronchioalveolar stem cells in normal lung and lung cancer. Cell 121:823-835.

36. Keith, W. N., C. M. Thomson, J. Howcroft, N. J. Maitland, and J. W. Shay. 2007. Seeding drug discovery: integrating telomerase cancer biology and cellular senescence to uncover new therapeutic opportunities in targeting cancer stem cells. Drug Discov Today 12:611-621.

37. Houghton, J., C. Stoicov, S. Nomura, A. B. Rogers, J. Carlson, H. Li, X. Cai, J. G. Fox, J. R. Goldenring, and T. C. Wang. 2004. Gastric cancer originating from bone marrow-derived cells. Science 306:1568-1571.

38. Bachoo, R. M., E. A. Maher, K. L. Ligon, N. E. Sharpless, S. S. Chan, M. J. You, Y. Tang, J. DeFrances, E. Stover, R. Weissleder, D. H. Rowitch, D. N. Louis, and R. A. DePinho. 2002. Epidermal growth factor receptor and Ink4a/Arf: convergent mechanisms governing terminal differentiation and transformation along the neural stem cell to astrocyte axis. Cancer Cell 1:269-277.

39. Bruggeman, S. W., D. Hulsman, E. Tanger, T. Buckle, M. Blom, J. Zevenhoven, O. van Tellingen, and M. van Lohuizen. 2007. Bmi1 controls tumor development in an Ink4a/Arf-independent manner in a mouse model for glioma. Cancer Cell 12:328-341.

40. Joseph, N. M., J. T. Mosher, J. Buchstaller, P. Snider, P. E. McKeever, M. Lim, S. J. Conway, L. F. Parada, Y. Zhu, and S. J. Morrison. 2008. The loss of Nf1 transiently promotes self-renewal but not tumorigenesis by neural crest stem cells. Cancer Cell 13:129-140.

41. Bjerkvig, R., B. B. Tysnes, K. S. Aboody, J. Najbauer, and A. J. Terzis. 2005. Opinion: the origin of the cancer stem cell: current controversies and new insights. Nat Rev Cancer 5:899-904.

42. Visvader, J. E. Cells of origin in cancer. Nature 469:314-322.

43. Eyler, C. E., and J. N. Rich. 2008. Survival of the fittest: cancer stem cells in therapeutic resistance and angiogenesis. J Clin Oncol 26:2839-2845.

44. Morrison, R., S. M. Schleicher, Y. Sun, K. J. Niermann, S. Kim, D. E. Spratt, C. H. Chung, and B. Lu. Targeting the mechanisms of resistance to chemotherapy and radiotherapy with the cancer stem cell hypothesis. J Oncol 2011:941876.

45. Pajonk, F., E. Vlashi, and W. H. McBride. Radiation resistance of cancer stem cells: the 4 R's of radiobiology revisited. Stem Cells 28:639-648.

46. Diehn, M., R. W. Cho, N. A. Lobo, T. Kalisky, M. J. Dorie, A. N. Kulp, D. Qian, J. S. Lam, L. E. Ailles, M. Wong, B. Joshua, M. J. Kaplan, I. Wapnir, F. M. Dirbas, G. Somlo, C. Garberoglio, B. Paz, J. Shen, S. K. Lau, S. R. Quake, J. M. Brown, I. L. Weissman, and M. F. Clarke. 2009. Association of reactive oxygen species levels and radioresistance in cancer stem cells. Nature 458:780-783.

47. Bao, S., Q. Wu, R. E. McLendon, Y. Hao, Q. Shi, A. B. Hjelmeland, M. W. Dewhirst, D. D. Bigner, and J. N. Rich. 2006. Glioma stem cells promote radioresistance by preferential activation of the DNA damage response. Nature 444:756-760.

48. Dean, M., T. Fojo, and S. Bates. 2005. Tumour stem cells and drug resistance. Nat Rev Cancer 5:275-284.

49. Kile, M. L., E. Hoffman, Y. M. Hsueh, S. Afroz, Q. Quamruzzaman, M. Rahman, G. Mahiuddin, L. Ryan, and D. C. Christiani. 2009. Variability in biomarkers of arsenic exposure and metabolism in adults over time. Environ Health Perspect 117:455-460.

50. Stupp, R., W. P. Mason, M. J. van den Bent, M. Weller, B. Fisher, M. J. Taphoorn, K. Belanger, A. A. Brandes, C. Marosi, U. Bogdahn, J. Curschmann, R. C. Janzer, S. K. Ludwin, T. Gorlia, A. Allgeier, D. Lacombe, J. G. Cairncross, E. Eisenhauer, and R. O. Mirimanoff. 2005. Radiotherapy plus concomitant and adjuvant temozolomide for glioblastoma. N Engl J Med 352:987-996.

51. Stupp, R., M. E. Hegi, W. P. Mason, M. J. van den Bent, M. J. Taphoorn, R. C. Janzer, S. K. Ludwin, A. Allgeier, B. Fisher, K. Belanger, P. Hau, A. A. Brandes, J. Gijtenbeek, C. Marosi, C. J. Vecht, K. Mokhtari, P. Wesseling, S. Villa, E. Eisenhauer, T. Gorlia, M. Weller, D. Lacombe, J. G. Cairncross, and R. O. Mirimanoff. 2009. Effects of radiotherapy with concomitant and adjuvant temozolomide versus radiotherapy alone on survival in glioblastoma in a randomised phase III study: 5-year analysis of the EORTC-NCIC trial. Lancet Oncol 10:459-466.

52. Johannessen, T. C., J. Wang, K. O. Skaftnesmo, P. O. Sakariassen, P. O. Enger, K. Petersen, A. M. Oyan, K. H. Kalland, R. Bjerkvig, and B. B. Tysnes. 2009. Highly infiltrative brain tumours show reduced chemosensitivity associated with a stem cell-like phenotype. Neuropathol Appl Neurobiol 35:380-393.

53. Liu, G., X. Yuan, Z. Zeng, P. Tunici, H. Ng, I. R. Abdulkadir, L. Lu, D. Irvin, K. L. Black, and J. S. Yu. 2006. Analysis of gene expression and chemoresistance of CD133+ cancer stem cells in glioblastoma. Mol Cancer 5:67.

54. Chekenya, M., C. Krakstad, A. Svendsen, I. A. Netland, V. Staalesen, B. B. Tysnes, F. Selheim, J. Wang, P. O. Sakariassen, T. Sandal, P. E. Lonning, T. Flatmark, P. O. Enger, R. Bjerkvig, M. Sioud, and W. B. Stallcup. 2008. The progenitor cell marker

NG2/MPG promotes chemoresistance by activation of integrin-dependent PI3K/Akt signaling. Oncogene 27:5182-5194.

55. Neuzil, J., M. Stantic, R. Zobalova, J. Chladova, X. Wang, L. Prochazka, L. Dong, L. Andera, and S. J. Ralph. 2007. Tumour-initiating cells vs. cancer 'stem' cells and CD133: what's in the name? Biochem Biophys Res Commun 355:855-859.

56. Singh, S. K., C. Hawkins, I. D. Clarke, J. A. Squire, J. Bayani, T. Hide, R. M. Henkelman, M. D. Cusimano, and P. B. Dirks. 2004. Identification of human brain tumour initiating cells. Nature 432:396-401.

57. Harris, M. A., H. Yang, B. E. Low, J. Mukherjee, A. Guha, R. T. Bronson, L. D. Shultz, M. A. Israel, and K. Yun. 2008. Cancer stem cells are enriched in the side population cells in a mouse model of glioma. Cancer Res 68:10051-10059.

58. Fukaya, R., S. Ohta, M. Yamaguchi, H. Fujii, Y. Kawakami, T. Kawase, and M. Toda. 2010. Isolation of cancer stem-like cells from a side population of a human glioblastoma cell line, SK-MG-1. Cancer Lett 291:150-157.

59. Guo, C. H., G. S. Hsu, C. J. Chuang, and P. C. Chen. 2009. Aluminum accumulation induced testicular oxidative stress and altered selenium metabolism in mice. Environ Toxicol Pharmacol 27:176-181.

60. Beier, D., P. Hau, M. Proescholdt, A. Lohmeier, J. Wischhusen, P. J. Oefner, L. Aigner, A. Brawanski, U. Bogdahn, and C. P. Beier. 2007. CD133(+) and CD133(-) glioblastoma-derived cancer stem cells show differential growth characteristics and molecular profiles. Cancer Res 67:4010-4015.

61. Joo, K. M., S. Y. Kim, X. Jin, S. Y. Song, D. S. Kong, J. I. Lee, J. W. Jeon, M. H. Kim, B. G. Kang, Y. Jung, J. Jin, S. C. Hong, W. Y. Park, D. S. Lee, H. Kim, and D.

H. Nam. 2008. Clinical and biological implications of CD133-positive and CD133-negative cells in glioblastomas. Lab Invest 88:808-815.

62. Broadley, K. W., M. K. Hunn, K. J. Farrand, K. M. Price, C. Grasso, R. J. Miller, I. F. Hermans, and M. J. McConnell. 2011. Side population is not necessary or sufficient for a cancer stem cell phenotype in glioblastoma multiforme. Stem Cells 29:452-461.

63. Reynolds, B. A., and S. Weiss. 1992. Generation of neurons and astrocytes from isolated cells of the adult mammalian central nervous system. Science 255:1707-1710.

64. Galli, R., E. Binda, U. Orfanelli, B. Cipelletti, A. Gritti, S. De Vitis, R. Fiocco, C. Foroni, F. Dimeco, and A. Vescovi. 2004. Isolation and characterization of tumorigenic, stem-like neural precursors from human glioblastoma. Cancer Res 64:7011-7021.

65. Yuan, X., J. Curtin, Y. Xiong, G. Liu, S. Waschsmann-Hogiu, D. L. Farkas, K. L. Black, and J. S. Yu. 2004. Isolation of cancer stem cells from adult glioblastoma multiforme. Oncogene 23:9392-9400.

66. Yang, M. D., S. Y. Lin, T. H. Chiu, C. C. Lin, M. L. Lin, S. C. Hsu, C. L. Kuo, M. J. Sheu, C. C. Wu, S. S. Lin, and J. G. Chung. 2008. Effects of luteolin on distribution and metabolism of 2-aminofluorene in male Sprague-Dawley rats. In Vivo 22:729-734.

67. McKay, R. 1997. Stem cells in the central nervous system. Science 276:66-71.

68. Gage, F. H., J. Ray, and L. J. Fisher. 1995. Isolation, characterization, and use of stem cells from the CNS. Annu Rev Neurosci 18:159-192.

69. Eramo, A., L. Ricci-Vitiani, A. Zeuner, R. Pallini, F. Lotti, G. Sette, E. Pilozzi, L. M. Larocca, C. Peschle, and R. De Maria. 2006. Chemotherapy resistance of glioblastoma stem cells. Cell Death Differ 13:1238-1241.

70. Bao, S., Q. Wu, S. Sathornsumetee, Y. Hao, Z. Li, A. B. Hjelmeland, Q. Shi, R. E. McLendon, D. D. Bigner, and J. N. Rich. 2006. Stem cell-like glioma cells promote tumor angiogenesis through vascular endothelial growth factor. Cancer Res 66:7843-7848.

71. Pallini, R., L. Ricci-Vitiani, N. Montano, C. Mollinari, M. Biffoni, T. Cenci, F. Pierconti, M. Martini, R. De Maria, and L. M. Larocca. Expression of the stem cell marker CD133 in recurrent glioblastoma and its value for prognosis. Cancer 117:162-174.

72. Lei, Z., B. Li, Z. Yang, H. Fang, G. M. Zhang, Z. H. Feng, and B. Huang. 2009. Regulation of HIF-1alpha and VEGF by miR-20b tunes tumor cells to adapt to the alteration of oxygen concentration. PLoS One 4:e7629.

73. Heddleston, J. M., Z. Li, R. E. McLendon, A. B. Hjelmeland, and J. N. Rich. 2009. The hypoxic microenvironment maintains glioblastoma stem cells and promotes reprogramming towards a cancer stem cell phenotype. Cell Cycle 8:3274-3284.

74. Ganapathy-Kanniappan, S., J. F. Geschwind, R. Kunjithapatham, M. Buijs, J. A. Vossen, I. Tchernyshyov, R. N. Cole, L. H. Syed, P. P. Rao, S. Ota, and M. Vali. 2009. Glyceraldehyde-3-phosphate dehydrogenase (GAPDH) is pyruvylated during 3-bromopyruvate mediated cancer cell death. Anticancer Res 29:4909-4918.

75. Bar, E. E., A. Chaudhry, A. Lin, X. Fan, K. Schreck, W. Matsui, S. Piccirillo, A. L. Vescovi, F. DiMeco, A. Olivi, and C. G. Eberhart. 2007. Cyclopamine-mediated

hedgehog pathway inhibition depletes stem-like cancer cells in glioblastoma. Stem Cells 25:2524-2533.

76. Li, L., and W. B. Neaves. 2006. Normal stem cells and cancer stem cells: the niche matters. Cancer Res 66:4553-4557.

77. Galli, R., A. Gritti, L. Bonfanti, and A. L. Vescovi. 2003. Neural stem cells: an overview. Circ Res 92:598-608.

78. Gilbertson, R. J., and J. N. Rich. 2007. Making a tumour's bed: glioblastoma stem cells and the vascular niche. Nat Rev Cancer 7:733-736.

79. Li, Q., M. C. Ford, E. B. Lavik, and J. A. Madri. 2006. Modeling the neurovascular niche: VEGF- and BDNF-mediated cross-talk between neural stem cells and endothelial cells: an in vitro study. J Neurosci Res 84:1656-1668.

80. Sneddon, J. B., and Z. Werb. 2007. Location, location, location: the cancer stem cell niche. Cell Stem Cell 1:607-611.

81. Borovski, T., E. M. F. De Sousa, L. Vermeulen, and J. P. Medema. 2011. Cancer stem cell niche: the place to be. Cancer Res 71:634-639.

82. Keith, B., and M. C. Simon. 2007. Hypoxia-inducible factors, stem cells, and cancer. Cell 129:465-472.

83. Griguer, C. E., C. R. Oliva, E. Gobin, P. Marcorelles, D. J. Benos, J. R. Lancaster, Jr., and G. Y. Gillespie. 2008. CD133 is a marker of bioenergetic stress in human glioma. PLoS One 3:e3655.

84. Seidel, S., B. K. Garvalov, V. Wirta, L. von Stechow, A. Schanzer, K. Meletis, M. Wolter, D. Sommerlad, A. T. Henze, M. Nister, G. Reifenberger, J. Lundeberg, J.

Frisen, and T. Acker. 2010. A hypoxic niche regulates glioblastoma stem cells through hypoxia inducible factor 2 alpha. Brain 133:983-995.

85. Soeda, A., M. Park, D. Lee, A. Mintz, A. Androutsellis-Theotokis, R. D. McKay, J. Engh, T. Iwama, T. Kunisada, A. B. Kassam, I. F. Pollack, and D. M. Park. 2009. Hypoxia promotes expansion of the CD133-positive glioma stem cells through activation of HIF-1alpha. Oncogene 28:3949-3959.

86. Pereira da Silva, A. P., T. El-Bacha, N. Kyaw, R. S. dos Santos, W. S. da-Silva, F. C. Almeida, A. T. Da Poian, and A. Galina. 2009. Inhibition of energy-producing pathways of HepG2 cells by 3-bromopyruvate. Biochem J 417:717-726.

87. Calabrese, C., H. Poppleton, M. Kocak, T. L. Hogg, C. Fuller, B. Hamner, E. Y. Oh, M. W. Gaber, D. Finklestein, M. Allen, A. Frank, I. T. Bayazitov, S. S. Zakharenko, A. Gajjar, A. Davidoff, and R. J. Gilbertson. 2007. A perivascular niche for brain tumor stem cells. Cancer Cell 11:69-82.

88. Zhu, T. S., M. A. Costello, C. E. Talsma, C. G. Flack, J. G. Crowley, L. L. Hamm, X. He, S. L. Hervey-Jumper, J. A. Heth, K. M. Muraszko, F. DiMeco, A. L. Vescovi, and X. Fan. Endothelial cells create a stem cell niche in glioblastoma by providing NOTCH ligands that nurture self-renewal of cancer stem-like cells. Cancer Res 71:6061-6072.

89. Charles, N., T. Ozawa, M. Squatrito, A. M. Bleau, C. W. Brennan, D. Hambardzumyan, and E. C. Holland. Perivascular nitric oxide activates notch signaling and promotes stem-like character in PDGF-induced glioma cells. Cell Stem Cell 6:141-152.

90. Denysenko, T., L. Gennero, M. A. Roos, A. Melcarne, C. Juenemann, G. Faccani, I. Morra, G. Cavallo, S. Reguzzi, G. Pescarmona, and A. Ponzetto. 2010. Glioblastoma cancer stem cells: heterogeneity, microenvironment and related therapeutic strategies. Cell Biochem Funct 28:343-351.

91. Ricci-Vitiani, L., R. Pallini, M. Biffoni, M. Todaro, G. Invernici, T. Cenci, G. Maira, E. A. Parati, G. Stassi, L. M. Larocca, and R. De Maria. Tumour vascularization via endothelial differentiation of glioblastoma stem-like cells. Nature 468:824-828.

92. Ying, M., S. Wang, Y. Sang, P. Sun, B. Lal, C. R. Goodwin, H. Guerrero-Cazares, A. Quinones-Hinojosa, J. Laterra, and S. Xia. Regulation of glioblastoma stem cells by retinoic acid: role for Notch pathway inhibition. Oncogene 30:3454-3467.

93. He, H., C. L. Nilsson, M. R. Emmett, A. G. Marshall, R. A. Kroes, J. R. Moskal, Y. Ji, H. Colman, W. Priebe, F. F. Lang, and C. A. Conrad. 2010. Glycomic and transcriptomic response of GSC11 glioblastoma stem cells to STAT3 phosphorylation inhibition and serum-induced differentiation. J Proteome Res 9:2098-2108.

94. Lee, J., S. Kotliarova, Y. Kotliarov, A. Li, Q. Su, N. M. Donin, S. Pastorino, B. W. Purow, N. Christopher, W. Zhang, J. K. Park, and H. A. Fine. 2006. Tumor stem cells derived from glioblastomas cultured in bFGF and EGF more closely mirror the phenotype and genotype of primary tumors than do serum-cultured cell lines. Cancer Cell 9:391-403.

95. Campos, B., F. Wan, M. Farhadi, A. Ernst, F. Zeppernick, K. E. Tagscherer, R. Ahmadi, J. Lohr, C. Dictus, G. Gdynia, S. E. Combs, V. Goidts, B. M. Helmke, V. Eckstein, W. Roth, P. Beckhove, P. Lichter, A. Unterberg, B. Radlwimmer, and C.

Herold-Mende. 2010. Differentiation therapy exerts antitumor effects on stem-like glioma cells. Clin Cancer Res 16:2715-2728.

96. Korur, S., R. M. Huber, B. Sivasankaran, M. Petrich, P. Morin, Jr., B. A. Hemmings, A. Merlo, and M. M. Lino. 2009. GSK3beta regulates differentiation and growth arrest in glioblastoma. PLoS One 4:e7443.

97. Waris, G., and H. Ahsan. 2006. Reactive oxygen species: role in the development of cancer and various chronic conditions. J Carcinog 5:14.

98. Bedard, K., and K. H. Krause. 2007. The NOX family of ROS-generating NADPH oxidases: physiology and pathophysiology. Physiol Rev 87:245-313.

99. Liu, Y., G. Fiskum, and D. Schubert. 2002. Generation of reactive oxygen species by the mitochondrial electron transport chain. J Neurochem 80:780-787.

100. Hancock, J. T., R. Desikan, and S. J. Neill. 2001. Role of reactive oxygen species in cell signalling pathways. Biochem Soc Trans 29:345-350.

101. Xia, R., J. A. Webb, L. L. Gnall, K. Cutler, and J. J. Abramson. 2003. Skeletal muscle sarcoplasmic reticulum contains a NADH-dependent oxidase that generates superoxide. Am J Physiol Cell Physiol 285:C215-221.

102. Suh, J. K., L. L. Poulsen, D. M. Ziegler, and J. D. Robertus. 1999. Yeast flavin-containing monooxygenase generates oxidizing equivalents that control protein folding in the endoplasmic reticulum. Proc Natl Acad Sci U S A 96:2687-2691.

103. Puskas, F., L. Braun, M. Csala, T. Kardon, P. Marcolongo, A. Benedetti, J. Mandl, and G. Banhegyi. 1998. Gulonolactone oxidase activity-dependent intravesicular glutathione oxidation in rat liver microsomes. FEBS Lett 430:293-296.

104. Gottlieb, R. A. 2003. Cytochrome P450: major player in reperfusion injury. Arch Biochem Biophys 420:262-267.

105. Lambeth, J. D. 2004. NOX enzymes and the biology of reactive oxygen. Nat Rev Immunol 4:181-189.

106. Boonstra, J., and J. A. Post. 2004. Molecular events associated with reactive oxygen species and cell cycle progression in mammalian cells. Gene 337:1-13.

107. Tsukagoshi, H., W. Busch, and P. N. Benfey. Transcriptional regulation of ROS controls transition from proliferation to differentiation in the root. Cell 143:606-616.

108. Gloire, G., S. Legrand-Poels, and J. Piette. 2006. NF-kappaB activation by reactive oxygen species: fifteen years later. Biochem Pharmacol 72:1493-1505.

109. Sen, C. K., and L. Packer. 1996. Antioxidant and redox regulation of gene transcription. FASEB J 10:709-720.

110. Schreck, R., P. Rieber, and P. A. Baeuerle. 1991. Reactive oxygen intermediates as apparently widely used messengers in the activation of the NF-kappa B transcription factor and HIV-1. EMBO J 10:2247-2258.

111. Ding, M., X. Shi, Y. Lu, C. Huang, S. Leonard, J. Roberts, J. Antonini, V. Castranova, and V. Vallyathan. 2001. Induction of activator protein-1 through reactive oxygen species by crystalline silica in JB6 cells. J Biol Chem 276:9108-9114.

112. Fialkow, L., C. K. Chan, D. Rotin, S. Grinstein, and G. P. Downey. 1994. Activation of the mitogen-activated protein kinase signaling pathway in neutrophils. Role of oxidants. J Biol Chem 269:31234-31242.

113. Simon, A. R., U. Rai, B. L. Fanburg, and B. H. Cochran. 1998. Activation of the JAK-STAT pathway by reactive oxygen species. Am J Physiol 275:C1640-1652.

114. Kroemer, G. 1999. Mitochondrial control of apoptosis: an overview. Biochem Soc Symp 66:1-15.

115. Ames, B. N. 1983. Dietary carcinogens and anticarcinogens. Oxygen radicals and degenerative diseases. Science 221:1256-1264.

116. Higinbotham, K. G., J. M. Rice, B. A. Diwan, K. S. Kasprzak, C. D. Reed, and A. O. Perantoni. 1992. GGT to GTT transversions in codon 12 of the K-ras oncogene in rat renal sarcomas induced with nickel subsulfide or nickel subsulfide/iron are consistent with oxidative damage to DNA. Cancer Res 52:4747-4751.

117. Lunec, J., K. A. Holloway, M. S. Cooke, S. Faux, H. R. Griffiths, and M. D. Evans. 2002. Urinary 8-oxo-2'-deoxyguanosine: redox regulation of DNA repair in vivo? Free Radic Biol Med 33:875-885.

118. Denissenko, M. F., S. Venkatachalam, Y. H. Ma, and A. A. Wani. 1996. Site-specific induction and repair of benzo[a]pyrene diol epoxide DNA damage in human H-ras protooncogene as revealed by restriction cleavage inhibition. Mutat Res 363:27-42.

119. Poulsen, H. E., H. Prieme, and S. Loft. 1998. Role of oxidative DNA damage in cancer initiation and promotion. Eur J Cancer Prev 7:9-16.

120. Wu, W. S. 2006. The signaling mechanism of ROS in tumor progression. Cancer Metastasis Rev 25:695-705.

121. Mori, K., M. Shibanuma, and K. Nose. 2004. Invasive potential induced under long-term oxidative stress in mammary epithelial cells. Cancer Res 64:7464-7472.

122. Kim, M. H., H. S. Cho, M. Jung, M. H. Hong, S. K. Lee, B. A. Shin, B. W. Ahn, and Y. D. Jung. 2005. Extracellular signal-regulated kinase and AP-1 pathways are involved in reactive oxygen species-induced urokinase plasminogen activator receptor expression in human gastric cancer cells. Int J Oncol 26:1669-1674.

123. Szatrowski, T. P., and C. F. Nathan. 1991. Production of large amounts of hydrogen peroxide by human tumor cells. Cancer Res 51:794-798.

124. Kawanishi, S., Y. Hiraku, S. Pinlaor, and N. Ma. 2006. Oxidative and nitrative DNA damage in animals and patients with inflammatory diseases in relation to inflammation-related carcinogenesis. Biol Chem 387:365-372.

125. Toyokuni, S., K. Okamoto, J. Yodoi, and H. Hiai. 1995. Persistent oxidative stress in cancer. FEBS Lett 358:1-3.

126. Irani, K., Y. Xia, J. L. Zweier, S. J. Sollott, C. J. Der, E. R. Fearon, M. Sundaresan, T. Finkel, and P. J. Goldschmidt-Clermont. 1997. Mitogenic signaling mediated by oxidants in Ras-transformed fibroblasts. Science 275:1649-1652.

127. Yang, J. Q., S. Li, F. E. Domann, G. R. Buettner, and L. W. Oberley. 1999. Superoxide generation in v-Ha-ras-transduced human keratinocyte HaCaT cells. Mol Carcinog 26:180-188.

128. Ferraro, D., S. Corso, E. Fasano, E. Panieri, R. Santangelo, S. Borrello, S. Giordano, G. Pani, and T. Galeotti. 2006. Pro-metastatic signaling by c-Met through RAC-1 and reactive oxygen species (ROS). Oncogene 25:3689-3698.

129. Ishikawa, K., K. Takenaga, M. Akimoto, N. Koshikawa, A. Yamaguchi, H. Imanishi, K. Nakada, Y. Honma, and J. Hayashi. 2008. ROS-generating mitochondrial DNA mutations can regulate tumor cell metastasis. Science 320:661-664.

130. Trachootham, D., J. Alexandre, and P. Huang. 2009. Targeting cancer cells by ROS-mediated mechanisms: a radical therapeutic approach? Nat Rev Drug Discov 8:579-591.

131. Griffith, O. W., and A. Meister. 1979. Potent and specific inhibition of glutathione synthesis by buthionine sulfoximine (S-n-butyl homocysteine sulfoximine). J Biol Chem 254:7558-7560.

132. Trachootham, D., H. Zhang, W. Zhang, L. Feng, M. Du, Y. Zhou, Z. Chen, H. Pelicano, W. Plunkett, W. G. Wierda, M. J. Keating, and P. Huang. 2008. Effective elimination of fludarabine-resistant CLL cells by PEITC through a redox-mediated mechanism. Blood 112:1912-1922.

133. Gill, S. S., and N. Tuteja. 2010. Reactive oxygen species and antioxidant machinery in abiotic stress tolerance in crop plants. Plant Physiol Biochem 48:909-930.

134. Zelko, I. N., T. J. Mariani, and R. J. Folz. 2002. Superoxide dismutase multigene family: a comparison of the CuZn-SOD (SOD1), Mn-SOD (SOD2), and EC-SOD (SOD3) gene structures, evolution, and expression. Free Radic Biol Med 33:337-349.

135. Johnson, F., and C. Giulivi. 2005. Superoxide dismutases and their impact upon human health. Mol Aspects Med 26:340-352.

136. Lau, A. T., Y. Wang, and J. F. Chiu. 2008. Reactive oxygen species: current knowledge and applications in cancer research and therapeutic. J Cell Biochem 104:657-667.

137. Rahman, I., F. Antonicelli, and W. MacNee. 1999. Molecular mechanism of the regulation of glutathione synthesis by tumor necrosis factor-alpha and dexamethasone in human alveolar epithelial cells. J Biol Chem 274:5088-5096.

138. Huang, H. C., T. Nguyen, and C. B. Pickett. 2002. Phosphorylation of Nrf2 at Ser-40 by protein kinase C regulates antioxidant response element-mediated transcription. J Biol Chem 277:42769-42774.

139. Li, J., T. Ichikawa, J. S. Janicki, and T. Cui. 2009. Targeting the Nrf2 pathway against cardiovascular disease. Expert Opin Ther Targets 13:785-794.

140. Nguyen, T., P. Nioi, and C. B. Pickett. 2009. The Nrf2-antioxidant response element signaling pathway and its activation by oxidative stress. J Biol Chem 284:13291-13295.

141. Yalcin, S., D. Marinkovic, S. K. Mungamuri, X. Zhang, W. Tong, R. Sellers, and S. Ghaffari. ROS-mediated amplification of AKT/mTOR signalling pathway leads to myeloproliferative syndrome in Foxo3(-/-) mice. EMBO J 29:4118-4131.

142. Essers, M. A., S. Weijzen, A. M. de Vries-Smits, I. Saarloos, N. D. de Ruiter, J. L. Bos, and B. M. Burgering. 2004. FOXO transcription factor activation by oxidative stress mediated by the small GTPase Ral and JNK. EMBO J 23:4802-4812.

143. Pervaiz, S., R. Taneja, and S. Ghaffari. 2009. Oxidative stress regulation of stem and progenitor cells. Antioxid Redox Signal 11:2777-2789.

144. Sauer, H., and M. Wartenberg. 2005. Reactive oxygen species as signaling molecules in cardiovascular differentiation of embryonic stem cells and tumor-induced angiogenesis. Antioxid Redox Signal 7:1423-1434.

145. Ji, A. R., S. Y. Ku, M. S. Cho, Y. Y. Kim, Y. J. Kim, S. K. Oh, S. H. Kim, S. Y. Moon, and Y. M. Choi. Reactive oxygen species enhance differentiation of human embryonic stem cells into mesendodermal lineage. Exp Mol Med 42:175-186.

146. Smith, J., E. Ladi, M. Mayer-Proschel, and M. Noble. 2000. Redox state is a central modulator of the balance between self-renewal and differentiation in a dividing glial precursor cell. Proc Natl Acad Sci U S A 97:10032-10037.

147. Tsatmali, M., E. C. Walcott, and K. L. Crossin. 2005. Newborn neurons acquire high levels of reactive oxygen species and increased mitochondrial proteins upon differentiation from progenitors. Brain Res 1040:137-150.

148. Ito, K., A. Hirao, F. Arai, S. Matsuoka, K. Takubo, I. Hamaguchi, K. Nomiyama, K. Hosokawa, K. Sakurada, N. Nakagata, Y. Ikeda, T. W. Mak, and T. Suda. 2004. Regulation of oxidative stress by ATM is required for self-renewal of haematopoietic stem cells. Nature 431:997-1002.

149. Miyamoto, K., K. Y. Araki, K. Naka, F. Arai, K. Takubo, S. Yamazaki, S. Matsuoka, T. Miyamoto, K. Ito, M. Ohmura, C. Chen, K. Hosokawa, H. Nakauchi, K. Nakayama, K. I. Nakayama, M. Harada, N. Motoyama, T. Suda, and A. Hirao. 2007. Foxo3a is essential for maintenance of the hematopoietic stem cell pool. Cell Stem Cell 1:101-112.

150. Chuikov, S., B. P. Levi, M. L. Smith, and S. J. Morrison. Prdm16 promotes stem cell maintenance in multiple tissues, partly by regulating oxidative stress. Nat Cell Biol 12:999-1006.

151. Juntilla, M. M., V. D. Patil, M. Calamito, R. P. Joshi, M. J. Birnbaum, and G. A. Koretzky. AKT1 and AKT2 maintain hematopoietic stem cell function by regulating reactive oxygen species. Blood 115:4030-4038.

152. Le Belle, J. E., N. M. Orozco, A. A. Paucar, J. P. Saxe, J. Mottahedeh, A. D. Pyle, H. Wu, and H. I. Kornblum. Proliferative neural stem cells have high endogenous ROS

levels that regulate self-renewal and neurogenesis in a PI3K/Akt-dependant manner. Cell Stem Cell 8:59-71.

153. Phillips, T. M., W. H. McBride, and F. Pajonk. 2006. The response of CD24(-/low)/CD44+ breast cancer-initiating cells to radiation. J Natl Cancer Inst 98:1777-1785.

154. Ishimoto, T., O. Nagano, T. Yae, M. Tamada, T. Motohara, H. Oshima, M. Oshima, T. Ikeda, R. Asaba, H. Yagi, T. Masuko, T. Shimizu, T. Ishikawa, K. Kai, E. Takahashi, Y. Imamura, Y. Baba, M. Ohmura, M. Suematsu, H. Baba, and H. Saya. 2011. CD44 variant regulates redox status in cancer cells by stabilizing the xCT subunit of system xc(-) and thereby promotes tumor growth. Cancer Cell 19:387-400.

155. Tamada, M., O. Nagano, S. Tateyama, M. Ohmura, T. Yae, T. Ishimoto, E. Sugihara, N. Onishi, T. Yamamoto, H. Yanagawa, M. Suematsu, and H. Saya. Modulation of glucose metabolism by CD44 contributes to antioxidant status and drug resistance in cancer cells. Cancer Res.

156. Ketola, K., M. Hilvo, T. Hyotylainen, A. Vuoristo, A. L. Ruskeepaa, M. Oresic, O. Kallioniemi, and K. Iljin. Salinomycin inhibits prostate cancer growth and migration via induction of oxidative stress. Br J Cancer 106:99-106.

157. Warburg, O. 1956. On the origin of cancer cells. Science 123:309-314.

158. Hsu, P. P., and D. M. Sabatini. 2008. Cancer cell metabolism: Warburg and beyond. Cell 134:703-707.

159. Warburg, O. 1956. On respiratory impairment in cancer cells. Science 124:269-270.

160. DeBerardinis, R. J., J. J. Lum, G. Hatzivassiliou, and C. B. Thompson. 2008. The biology of cancer: metabolic reprogramming fuels cell growth and proliferation. Cell Metab 7:11-20.

161. Frezza, C., and E. Gottlieb. 2009. Mitochondria in cancer: not just innocent bystanders. Semin Cancer Biol 19:4-11.

162. Cairns, R. A., I. S. Harris, and T. W. Mak. 2011. Regulation of cancer cell metabolism. Nat Rev Cancer 11:85-95.

163. Pfeiffer, T., S. Schuster, and S. Bonhoeffer. 2001. Cooperation and competition in the evolution of ATP-producing pathways. Science 292:504-507.

164. Gatenby, R. A., and R. J. Gillies. 2004. Why do cancers have high aerobic glycolysis? Nat Rev Cancer 4:891-899.

165. Dang, C. V., and G. L. Semenza. 1999. Oncogenic alterations of metabolism. Trends Biochem Sci 24:68-72.

166. Elstrom, R. L., D. E. Bauer, M. Buzzai, R. Karnauskas, M. H. Harris, D. R. Plas, H. Zhuang, R. M. Cinalli, A. Alavi, C. M. Rudin, and C. B. Thompson. 2004. Akt stimulates aerobic glycolysis in cancer cells. Cancer Res 64:3892-3899.

167. Plas, D. R., S. Talapatra, A. L. Edinger, J. C. Rathmell, and C. B. Thompson. 2001. Akt and Bcl-xL promote growth factor-independent survival through distinct effects on mitochondrial physiology. J Biol Chem 276:12041-12048.

168. Semenza, G. L. 2010. HIF-1: upstream and downstream of cancer metabolism. Curr Opin Genet Dev 20:51-56.

169. Papandreou, I., R. A. Cairns, L. Fontana, A. L. Lim, and N. C. Denko. 2006. HIF-1 mediates adaptation to hypoxia by actively downregulating mitochondrial oxygen consumption. Cell Metab 3:187-197.

170. Kim, J. W., I. Tchernyshyov, G. L. Semenza, and C. V. Dang. 2006. HIF-1-mediated expression of pyruvate dehydrogenase kinase: a metabolic switch required for cellular adaptation to hypoxia. Cell Metab 3:177-185.

171. Kim, J. W., P. Gao, Y. C. Liu, G. L. Semenza, and C. V. Dang. 2007. Hypoxia-inducible factor 1 and dysregulated c-Myc cooperatively induce vascular endothelial growth factor and metabolic switches hexokinase 2 and pyruvate dehydrogenase kinase 1. Mol Cell Biol 27:7381-7393.

172. Dang, C. V., J. W. Kim, P. Gao, and J. Yustein. 2008. The interplay between MYC and HIF in cancer. Nat Rev Cancer 8:51-56.

173. Ko, Y. H., P. L. Pedersen, and J. F. Geschwind. 2001. Glucose catabolism in the rabbit VX2 tumor model for liver cancer: characterization and targeting hexokinase. Cancer Lett 173:83-91.

174. Geschwind, J. F., Y. H. Ko, M. S. Torbenson, C. Magee, and P. L. Pedersen. 2002. Novel therapy for liver cancer: direct intraarterial injection of a potent inhibitor of ATP production. Cancer Res 62:3909-3913.

175. Nelson, K. 2002. 3-Bromopyruvate kills cancer cells in animals. Lancet Oncol 3:524.

176. Vander Heiden, M. G. Targeting cancer metabolism: a therapeutic window opens. Nat Rev Drug Discov 10:671-684.

177. Geschwind, J. F., C. S. Georgiades, Y. H. Ko, and P. L. Pedersen. 2004. Recently elucidated energy catabolism pathways provide opportunities for novel treatments in hepatocellular carcinoma. Expert Rev Anticancer Ther 4:449-457.

178. Xu, R. H., H. Pelicano, H. Zhang, F. J. Giles, M. J. Keating, and P. Huang. 2005. Synergistic effect of targeting mTOR by rapamycin and depleting ATP by inhibition of glycolysis in lymphoma and leukemia cells. Leukemia 19:2153-2158.

179. Spoden, G. A., S. Mazurek, D. Morandell, N. Bacher, M. J. Ausserlechner, P. Jansen-Durr, E. Eigenbrodt, and W. Zwerschke. 2008. Isotype-specific inhibitors of the glycolytic key regulator pyruvate kinase subtype M2 moderately decelerate tumor cell proliferation. Int J Cancer 123:312-321.

180. Christofk, H. R., M. G. Vander Heiden, M. H. Harris, A. Ramanathan, R. E. Gerszten, R. Wei, M. D. Fleming, S. L. Schreiber, and L. C. Cantley. 2008. The M2 splice isoform of pyruvate kinase is important for cancer metabolism and tumour growth. Nature 452:230-233.

181. Shu, Q., K. K. Wong, J. M. Su, A. M. Adesina, L. T. Yu, Y. T. Tsang, B. C. Antalffy, P. Baxter, L. Perlaky, J. Yang, R. C. Dauser, M. Chintagumpala, S. M. Blaney, C. C. Lau, and X. N. Li. 2008. Direct orthotopic transplantation of fresh surgical specimen preserves CD133+ tumor cells in clinically relevant mouse models of medulloblastoma and glioma. Stem Cells 26:1414-1424.

182. Simon, R., A. Lam, M. C. Li, M. Ngan, S. Menenzes, and Y. Zhao. 2007. Analysis of gene expression data using BRB-ArrayTools. Cancer Inform 3:11-17.

183. Eisen, M. B., P. T. Spellman, P. O. Brown, and D. Botstein. 1998. Cluster analysis and display of genome-wide expression patterns. Proc Natl Acad Sci U S A 95:14863-14868.

184. He, H., C. L. Nilsson, M. R. Emmett, A. G. Marshall, R. A. Kroes, J. R. Moskal, Y. Ji, H. Colman, W. Priebe, F. F. Lang, and C. A. Conrad. Glycomic and transcriptomic response of GSC11 glioblastoma stem cells to STAT3 phosphorylation inhibition and serum-induced differentiation. J Proteome Res 9:2098-2108.

185. Jiang, H., C. Gomez-Manzano, H. Aoki, M. M. Alonso, S. Kondo, F. McCormick, J. Xu, Y. Kondo, B. N. Bekele, H. Colman, F. F. Lang, and J. Fueyo. 2007. Examination of the therapeutic potential of Delta-24-RGD in brain tumor stem cells: role of autophagic cell death. J Natl Cancer Inst 99:1410-1414.

186. Gaiano, N., and G. Fishell. 2002. The role of notch in promoting glial and neural stem cell fates. Annu Rev Neurosci 25:471-490.

187. Ganapathy-Kanniappan, S., M. Vali, R. Kunjithapatham, M. Buijs, L. H. Syed, P. P. Rao, S. Ota, B. K. Kwak, R. Loffroy, and J. F. Geschwind. 2010. 3-bromopyruvate: a new targeted antiglycolytic agent and a promise for cancer therapy. Curr Pharm Biotechnol 11:510-517.

188. Bhardwaj, V., N. Rizvi, M. B. Lai, J. C. Lai, and A. Bhushan. 2010. Glycolytic enzyme inhibitors affect pancreatic cancer survival by modulating its signaling and energetics. Anticancer Res 30:743-749.

189. Schallreuter, K. U., F. K. Gleason, and J. M. Wood. 1990. The mechanism of action of the nitrosourea anti-tumor drugs on thioredoxin reductase, glutathione reductase and ribonucleotide reductase. Biochim Biophys Acta 1054:14-20.

190. Batista, L. F., W. P. Roos, M. Christmann, C. F. Menck, and B. Kaina. 2007. Differential sensitivity of malignant glioma cells to methylating and chloroethylating anticancer drugs: p53 determines the switch by regulating xpc, ddb2, and DNA double-strand breaks. Cancer Res 67:11886-11895.

191. Cui, B., S. P. Johnson, N. Bullock, F. Ali-Osman, D. D. Bigner, and H. S. Friedman. 2009. Bifunctional DNA alkylator 1,3-bis(2-chloroethyl)-1-nitrosourea activates the ATR-Chk1 pathway independently of the mismatch repair pathway. Mol Pharmacol 75:1356-1363.

192. Drablos, F., E. Feyzi, P. A. Aas, C. B. Vaagbo, B. Kavli, M. S. Bratlie, J. Pena-Diaz, M. Otterlei, G. Slupphaug, and H. E. Krokan. 2004. Alkylation damage in DNA and RNA--repair mechanisms and medical significance. DNA Repair (Amst) 3:1389-1407.

193. Rogakou, E. P., D. R. Pilch, A. H. Orr, V. S. Ivanova, and W. M. Bonner. 1998. DNA double-stranded breaks induce histone H2AX phosphorylation on serine 139. J Biol Chem 273:5858-5868.

194. Ikura, T., S. Tashiro, A. Kakino, H. Shima, N. Jacob, R. Amunugama, K. Yoder, S. Izumi, I. Kuraoka, K. Tanaka, H. Kimura, M. Ikura, S. Nishikubo, T. Ito, A. Muto, K. Miyagawa, S. Takeda, R. Fishel, K. Igarashi, and K. Kamiya. 2007. DNA damage-dependent acetylation and ubiquitination of H2AX enhances chromatin dynamics. Mol Cell Biol 27:7028-7040.

195. Rai, R., G. Peng, K. Li, and S. Y. Lin. 2007. DNA damage response: the players, the network and the role in tumor suppression. Cancer Genomics Proteomics 4:99-106.

196. LaBarge, M. A. The difficulty of targeting cancer stem cell niches. Clin Cancer Res 16:3121-3129.

197. Cuddihy, S. L., C. C. Winterbourn, and M. B. Hampton. Assessment of Redox Changes to Hydrogen Peroxide-Sensitive Proteins During EGF Signaling. Antioxid Redox Signal.

198. Forman, H. J., M. Maiorino, and F. Ursini. Signaling functions of reactive oxygen species. Biochemistry 49:835-842.

199. Achuthan, S., T. R. Santhoshkumar, J. Prabhakar, S. A. Nair, and M. R. Pillai. Drug-induced senescence generates chemoresistant stemlike cells with low reactive oxygen species. J Biol Chem 286:37813-37829.

200. Hernandez-Garcia, D., C. D. Wood, S. Castro-Obregon, and L. Covarrubias. Reactive oxygen species: A radical role in development? Free Radic Biol Med 49:130-143.

201. Gangemi, R. M., F. Griffero, D. Marubbi, M. Perera, M. C. Capra, P. Malatesta, G. L. Ravetti, G. L. Zona, A. Daga, and G. Corte. 2009. SOX2 silencing in glioblastoma tumor-initiating cells causes stop of proliferation and loss of tumorigenicity. Stem Cells 27:40-48.

202. Ligon, K. L., E. Huillard, S. Mehta, S. Kesari, H. Liu, J. A. Alberta, R. M. Bachoo, M. Kane, D. N. Louis, R. A. Depinho, D. J. Anderson, C. D. Stiles, and D. H. Rowitch. 2007. Olig2-regulated lineage-restricted pathway controls replication competence in neural stem cells and malignant glioma. Neuron 53:503-517.

203. Karin, M. 2006. NF-kappaB and cancer: mechanisms and targets. Mol Carcinog 45:355-361.

204. Yang, C., S. P. Atkinson, F. Vilella, M. Lloret, L. Armstrong, D. A. Mann, and M. Lako. Opposing putative roles for canonical and noncanonical NFkappaB signaling on the survival, proliferation, and differentiation potential of human embryonic stem cells. Stem Cells 28:1970-1980.

205. Morgan, M. J., and Z. G. Liu. 2011. Crosstalk of reactive oxygen species and NF-kappaB signaling. Cell Res 21:103-115.

206. Bredel, M., D. M. Scholtens, A. K. Yadav, A. A. Alvarez, J. J. Renfrow, J. P. Chandler, I. L. Yu, M. S. Carro, F. Dai, M. J. Tagge, R. Ferrarese, C. Bredel, H. S. Phillips, P. J. Lukac, P. A. Robe, A. Weyerbrock, H. Vogel, S. Dubner, B. Mobley, X. He, A. C. Scheck, B. I. Sikic, K. D. Aldape, A. Chakravarti, and G. R. t. Harsh. NFKBIA deletion in glioblastomas. N Engl J Med 364:627-637.

207. Iliopoulos, D., H. A. Hirsch, and K. Struhl. 2009. An epigenetic switch involving NF-kappaB, Lin28, Let-7 MicroRNA, and IL6 links inflammation to cell transformation. Cell 139:693-706.

208. Nogueira, L., P. Ruiz-Ontanon, A. Vazquez-Barquero, M. Lafarga, M. T. Berciano, B. Aldaz, L. Grande, I. Casafont, V. Segura, E. F. Robles, D. Suarez, L. F. Garcia, J. A. Martinez-Climent, and J. L. Fernandez-Luna. 2011. Blockade of the NFkappaB pathway drives differentiating glioblastoma-initiating cells into senescence both in vitro and in vivo. Oncogene 30:3537-3548.

209. Widera, D., I. Mikenberg, B. Kaltschmidt, and C. Kaltschmidt. 2006. Potential role of NF-kappaB in adult neural stem cells: the underrated steersman? Int J Dev Neurosci 24:91-102.

210. Burke, J. R., M. A. Pattoli, K. R. Gregor, P. J. Brassil, J. F. MacMaster, K. W. McIntyre, X. Yang, V. S. Iotzova, W. Clarke, J. Strnad, Y. Qiu, and F. C. Zusi. 2003. BMS-345541 is a highly selective inhibitor of I kappa B kinase that binds at an allosteric site of the enzyme and blocks NF-kappa B-dependent transcription in mice. J Biol Chem 278:1450-1456.

211. Barrett, L. E., Z. Granot, C. Coker, A. Iavarone, D. Hambardzumyan, E. C. Holland, H. S. Nam, and R. Benezra. Self-renewal does not predict tumor growth potential in mouse models of high-grade glioma. Cancer Cell 21:11-24.

212. Jin, Y., Z. Lu, K. Ding, J. Li, X. Du, C. Chen, X. Sun, Y. Wu, J. Zhou, and J. Pan. Antineoplastic mechanisms of niclosamide in acute myelogenous leukemia stem cells: inactivation of the NF-kappaB pathway and generation of reactive oxygen species. Cancer Res 70:2516-2527.

213. Nogueira, L., P. Ruiz-Ontanon, A. Vazquez-Barquero, M. Lafarga, M. T. Berciano, B. Aldaz, L. Grande, I. Casafont, V. Segura, E. F. Robles, D. Suarez, L. F. Garcia, J. A. Martinez-Climent, and J. L. Fernandez-Luna. Blockade of the NFkappaB pathway drives differentiating glioblastoma-initiating cells into senescence both in vitro and in vivo. Oncogene 30:3537-3548.

214. Yip, N. C., I. S. Fombon, P. Liu, S. Brown, V. Kannappan, A. L. Armesilla, B. Xu, J. Cassidy, J. L. Darling, and W. Wang. 2011. Disulfiram modulated ROS-MAPK and

NFkappaB pathways and targeted breast cancer cells with cancer stem cell-like properties. Br J Cancer 104:1564-1574.

215. Sell, S. 2006. Cancer stem cells and differentiation therapy. Tumour Biol 27:59-70.

216. Sell, S. 2004. Stem cell origin of cancer and differentiation therapy. Crit Rev Oncol Hematol 51:1-28.

217. Tallman, M. S., J. W. Andersen, C. A. Schiffer, F. R. Appelbaum, J. H. Feusner, A. Ogden, L. Shepherd, C. Willman, C. D. Bloomfield, J. M. Rowe, and P. H. Wiernik. 1997. All-trans-retinoic acid in acute promyelocytic leukemia. N Engl J Med 337:1021-1028.

218. Wang, Z. Y., and Z. Chen. 2008. Acute promyelocytic leukemia: from highly fatal to highly curable. Blood 111:2505-2515.

219. Campos, B., F. Wan, M. Farhadi, A. Ernst, F. Zeppernick, K. E. Tagscherer, R. Ahmadi, J. Lohr, C. Dictus, G. Gdynia, S. E. Combs, V. Goidts, B. M. Helmke, V. Eckstein, W. Roth, P. Beckhove, P. Lichter, A. Unterberg, B. Radlwimmer, and C. Herold-Mende. Differentiation therapy exerts antitumor effects on stem-like glioma cells. Clin Cancer Res 16:2715-2728.

220. Ohgaki, H., and P. Kleihues. 2005. Population-based studies on incidence, survival rates, and genetic alterations in astrocytic and oligodendroglial gliomas. J Neuropathol Exp Neurol 64:479-489.

221. Gilbert, C. A., and A. H. Ross. 2009. Cancer stem cells: cell culture, markers, and targets for new therapies. J Cell Biochem 108:1031-1038.

222. Oliverio, V. T. 1976. Pharmacology of the nitrosoureas: an overview. Cancer Treat Rep 60:703-707.

223. Blasberg, R. G., C. Patlak, and J. D. Fenstermacher. 1975. Intrathecal chemotherapy: brain tissue profiles after ventriculocisternal perfusion. J Pharmacol Exp Ther 195:73-83.

224. Woolley, P. V., R. L. Dion, K. W. Kohn, and V. H. Bono. 1976. Binding of 1-(2-chloroethyl)-3-cyclohexyl-1-nitrosourea to L1210 cell nuclear proteins. Cancer Res 36:1470-1474.

225. Dell'Antone, P. 2009. Targets of 3-bromopyruvate, a new, energy depleting, anticancer agent. Med Chem 5:491-496.

226. Ihrlund, L. S., E. Hernlund, O. Khan, and M. C. Shoshan. 2008. 3-Bromopyruvate as inhibitor of tumour cell energy metabolism and chemopotentiator of platinum drugs. Mol Oncol 2:94-101.

227. Ko, Y. H., B. L. Smith, Y. Wang, M. G. Pomper, D. A. Rini, M. S. Torbenson, J. Hullihen, and P. L. Pedersen. 2004. Advanced cancers: eradication in all cases using 3-bromopyruvate therapy to deplete ATP. Biochem Biophys Res Commun 324:269-275.

228. Xu, R. H., H. Pelicano, Y. Zhou, J. S. Carew, L. Feng, K. N. Bhalla, M. J. Keating, and P. Huang. 2005. Inhibition of glycolysis in cancer cells: a novel strategy to overcome drug resistance associated with mitochondrial respiratory defect and hypoxia. Cancer Res 65:613-621.

229. Chen, Z., H. Zhang, W. Lu, and P. Huang. 2009. Role of mitochondria-associated hexokinase II in cancer cell death induced by 3-bromopyruvate. Biochim Biophys Acta 1787:553-560.

VITA

Feng Wang was born in Gangzhou, Jiang Xi on August 24, 1983. As the single child of Jianguo Wang and Xiaoou Wang, Feng chose to go to a college close to home and was going to fulfill her father's wish, be a doctor in a local hospital. She went to Nanchang to learn about medicine and more importantly about herself at Jiang Xi Medical College. However, Feng began to contemplate her future career the following year when her grandpa was diagnosed as esophagus cancer. After sharing the last two months with him, Feng developed a strong desire to help cancer patients. So after completing her study and obtaining her Doctor of Medicine, Feng decided to attend the master degree program of Medical Oncology at Sun-Yat Sen University Cancer Center, where she found her interest and life time love, Shuqiang. While trained there as a medical oncologist, Feng recognized the need for cancer research and how it would affect cancer patients. In 2008, Feng enrolled in the Graduate School of Biomedical Sciences at the University of Texas Health Sciences Center at Houston and joined the laboratory of Dr Peng Huang in the Department of Molecular Pathology at MD Anderson Cancer Center. During the doctorate study, she was awarded the Rosalie B Hite Fellowship in 2010-2011 and 2011-2012. She was also awarded the Scholarship for Outstanding Oversea Students by the Chinese government in 2011. Feng will go back to China to pursue her career as an oncologist as well as a scientist after graduation.

PUBLICATIONS

1. Lu W, Hu Y, Chen G, Chen Z, Zhang H, **Wang F**, Feng L, Pelicano H, Wang H, Keating M, Liu J, McKeehan W, Wang HM, Luo Y, Huang P. Novel Role of NOX in Supporting Aerobic Glycolysis in Cancer Cells with Mitochondrial Dysfunction and as a Potential Target for Cancer Therapy. *PLoS Biol*. In press.

2. **Wang F**, Yuan SQ, Teng KY, Garcia-Prieto C, Luo HY, Zeng MS, Rao HL, Xia Y, Jiang WQ, Huang HQ, Xia ZJ, Sun XF, Xu RH. High hepatits B virus infection in B-cell lymphoma tissue and its potential clinical relevance. *Eur J Cancer Prev*. 2012; 21(3):261-7.

3. Li ZH, Qiu MZ, Zeng ZL, Luo HY, Wu WJ, **Wang F**, Wang ZQ, Zhang DS, Li YH, Xu RH. Copper-transporting P-type adenosine triphosphatase (ATP7A) is associated with platinum-resistance in non-small cell lung cancer (NSCLC). *J Transl Med*. 2012; 10(1):21.

4. Chen G, **Wang F**, Trachootham D, Huang P. Preferential killing of cancer cells with mitochondrial dysfunction by natural compounds. *Mitochondrion.* 2010; 10 (6): 614-25.

5. **Wang F**, Ogasawara MA, Huang P. Small mitochondria-targeting molecules as anti-cancer agents. *Mol Aspects Med.* 2010; 31(1):75-92.

6. Luo HY, Wei W, Shi YX, Chen XQ, Li YH, **Wang F**, Qiu MZ, Li FH, Yan SL, Zeng MS, Huang P, Xu RH. Cetuximab enhances the effect of oxaliplatin on hypoxic gastric cancer cell lines. *Oncol Rep*. 2010; 23(6): 1735-45.

7. Luo HY, Xu RH, **Wang F**, Qiu MZ, Li YH, Li FH, Zhou ZW, Chen XQ. Phase II trial of XELOX as first-line treatment for patients with advanced gastric cancer. *Chemotherapy*. 2010;56(2):94-100.

8. Chen G, Izzo J, Demizu Y, **Wang F**, Guha S, Wu X, Hung MC, Ajani JA, Huang P. Different redox states in malignant and nonmalignant esophageal epithelial cells and differential cytotoxic responses to bile acid and honokiol. *Antioxid Redox Signal.*2009; 11(5):1083-1095.

9. Li FH, Chen XQ, Luo HY, Li YH, **Wang F**, Qiu MZ, Teng KY, Li ZH, Xu RH. Prognosis of 84 intrahepatic cholangiocarcinoma patients. *Chinese journal of Cancer*.2009;28(5):528-532.

10. **Wang F**, Xu RH, Luo HY, Zhang DS, Jiang WQ, Huang HQ, Sun XF, Xia ZJ, Guan ZZ. Clinical and prognostic analysis of hepatitis B virus infection in diffuse large B-cell lymphoma. *BMC Cancer*. 2008 Apr 23; 8:115.

11. Luo HY, Xu RH, Zhang L, Li YH, Shi YX, Lin TY, Han B, **Wang F**, Qiu MZ, He YJ, Guan ZZ.A pilot study of oxaliplatin, fluorouracil and folinic acid (FOLFOX-6) as first-line chemotherapy in advanced or recurrent gastric cancer. *Chemotherapy*.2008; 54(3):228-235.

12. **Wang F**, Xu RH, Han B, Shi YX, Luo HY, Jiang WQ, Lin TY, Huang HQ, Xia ZJ, Guan ZZ. High incidence of hepatitis B virus infection in B-cell subtype non-Hodgkin lymphoma compared with other cancers. *Cancer*, 2007;109:1360-1364.

13. Shi YX, Xu RH, Jiang WQ, Zhang L, Lin TY, Li YH, Xia ZJ, Luo HY, Han B, **Wang F**, He YJ, Guan ZZ. Efficacy of gemcitabine combined oxaliplatin on advanced pancreatic cancer. Ai Zheng. 2007; 26(12):1381-4.

14. Luo HY, Li YH, Zhang L, Jiang WQ, Shi YX, **Wang F**, He YJ, Xu RH. Efficacy of CPT-11 combined 5-FU/CF (FOLFIRI) regimen on advanced colorectal cancer. *Ai Zheng.*1007; 26:905-908.

15. Qiu MZ, Xu F, Wang SS, Luo HY, **Wang F**, Li FH, Sun XF, Xu GC, Lin TY, Huang HQ, Jiang WQ, Guan ZZ, Xu RH. Responses of 109 adult soft tissue sarcoma patients to chemotherapy. *Ai Zheng.* 2007; 26(12):1344-1349.

16. Han B, Xu RH, Shi YX, Li YH, Luo HY, **Wang F**, Hou JH, Cai MY, Jiang WQ. Expression and clinical significance of hypoxia-inducible factor-1alpha in gastric cancer. *Ai Zheng*. 2006; 25:1439-1442.

CONFERENCES PRESENTATIONS OR ABSTRACTS

1. **Wang F**, Yuan SQ, Chen G, Kim S, Hammodi N, Feng L, Lu WQ, Lee JS, and Huang P. Potential Role of Reactive Oxygen Species in Mediating Glioblastoma Stem Cell Differentiation. The 103rd Annual Meeting of the American Association for Cancer Research, 2012. (Selected for **Oral Presentation**)

2. Hammoudi N, **Wang F**, Huang P. Potential role of mitochondrial respiration in serum-induced tumor stem cell differentiation. The 102nd Annual Meeting of the American Association for Cancer Research, 2011; 3314.

3. **Wang F**, Hammodi N, Yuan SQ, Chen G, Feng L, Kim S, Colman H, Lee JS, Xu RH, and Huang P. Potential role of reactive oxygen species in affecting tumorigenicity of glioblastoma stem cells. The 101st Annual Meeting of the American Association for Cancer Research, 2010; 6692.

4. Yuan SQ, **Wang F**, Zhang W, Huang P. A novel therapeutic strategy to effectively target glioblastoma stem cells using biochemical mechanism-based drug combination. The 101st Annual Meeting of the American Association for Cancer Research, 2010; LB264.

5. Han B, Xu RH, Zhan YQ, Li W, Shi YX, Luo HY, **Wang F**, He YJ. Clinical outcomes and prognostic factors of 137 patients with gastric cancer. *Proceedings of the 4th Chinese Conference on Oncology & 5th Cross-Strait Academic Conference on Oncology,* 2006; 556.